nagra.

Arbeitsbericht NAB 22-02

TBO Stadel-2-1: Data Report

Dossier VII Hydraulic Packer Testing

September 2022

R. Schwarz, R. Beauheim, S.M.L. Hardie & A. Pechstein

National Cooperative
for the Disposal of
Radioactive Waste

Hardstrasse 73
P.O. Box
5430 Wettingen
Switzerland
Tel. +41 56 437 11 11

nagra.ch

nagra.

Arbeitsbericht NAB 22-02

TBO Stadel-2-1: Data Report

Dossier VII Hydraulic Packer Testing

September 2022

R. Schwarz[1], R. Beauheim[2], S.M.L. Hardie[3] & A. Pechstein[4]

[1] CSD Ingenieure AG
[2] INTERA Incorporated
[3] Schwarz Hara Consult
[4] Nagra

Keywords:
STA2-1, Nördlich Lägern, TBO, deep drilling campaign, hydrogeology, hydraulic packer tests, hydraulic conductivity, hydraulic head, fluid logging, gas threshold pressure test equipment

National Cooperative for the Disposal of Radioactive Waste

Hardstrasse 73
P.O. Box
5430 Wettingen
Switzerland
Tel. +41 56 437 11 11

nagra.ch

Nagra Arbeitsberichte ("Working Reports") present the results of work in progress that have not necessarily been subject to a comprehensive review. They are intended to provide rapid dissemination of current information.

This NAB aims at reporting drilling results at an early stage. Additional borehole-specific data will be published elsewhere.

In the event of inconsistencies between dossiers of this NAB, the dossier addressing the specific topic takes priority. In the event of discrepancies between Nagra reports, the chronologically later report is generally considered to be correct. Data sets and interpretations laid out in this NAB may be revised in subsequent reports. The reasoning leading to these revisions will be detailed there.

This report was finalised in June 2023.

This Dossier was prepared by a project team consisting of:
R. Schwarz (QC of test analyses, QC of test reports, writing)
R. Beauheim (performance and analysis of the hydraulic packer tests)
S.M.L. Hardie (writing)
A. Pechstein (project management, conceptualisation, review)

The present report is based on the detailed reports about the performance and analysis of the hydraulic packer tests and fluid logging, as well as on the mobilisation reports about test equipment. These detailed reports, quick look reports and mobilisation reports were written by the testing companies INTERA Inc. for the hydraulic packer tests (R. Beauheim, R. Roberts (HydroResolutions LLC), T. Cavalera, J. Croisé, A. Dausse, M. Hayek, A. Färber, M. Fort (HydroResolutions LLC) and B. Paris, U. Rösli (Solexperts AG) and C. Yu).

Editorial work: P. Blaser and M. Unger

The Dossier has greatly benefitted from technical discussions with, and reviews by, external and internal experts. Their input and work are very much appreciated.

Table of Contents

List of Tables

List of Figures

1 Introduction

1.1 Context

To provide input for site selection and the safety case for deep geological repositories for radioactive waste, Nagra has drilled a series of deep boreholes ("Tiefbohrungen", TBO) in Northern Switzerland. The aim of the drilling campaign is to characterise the deep underground of the three remaining siting regions located at the edge of the Northern Alpine Molasse Basin (Fig. 1-1).

In this report, we present the results from the Stadel-2-1 borehole.

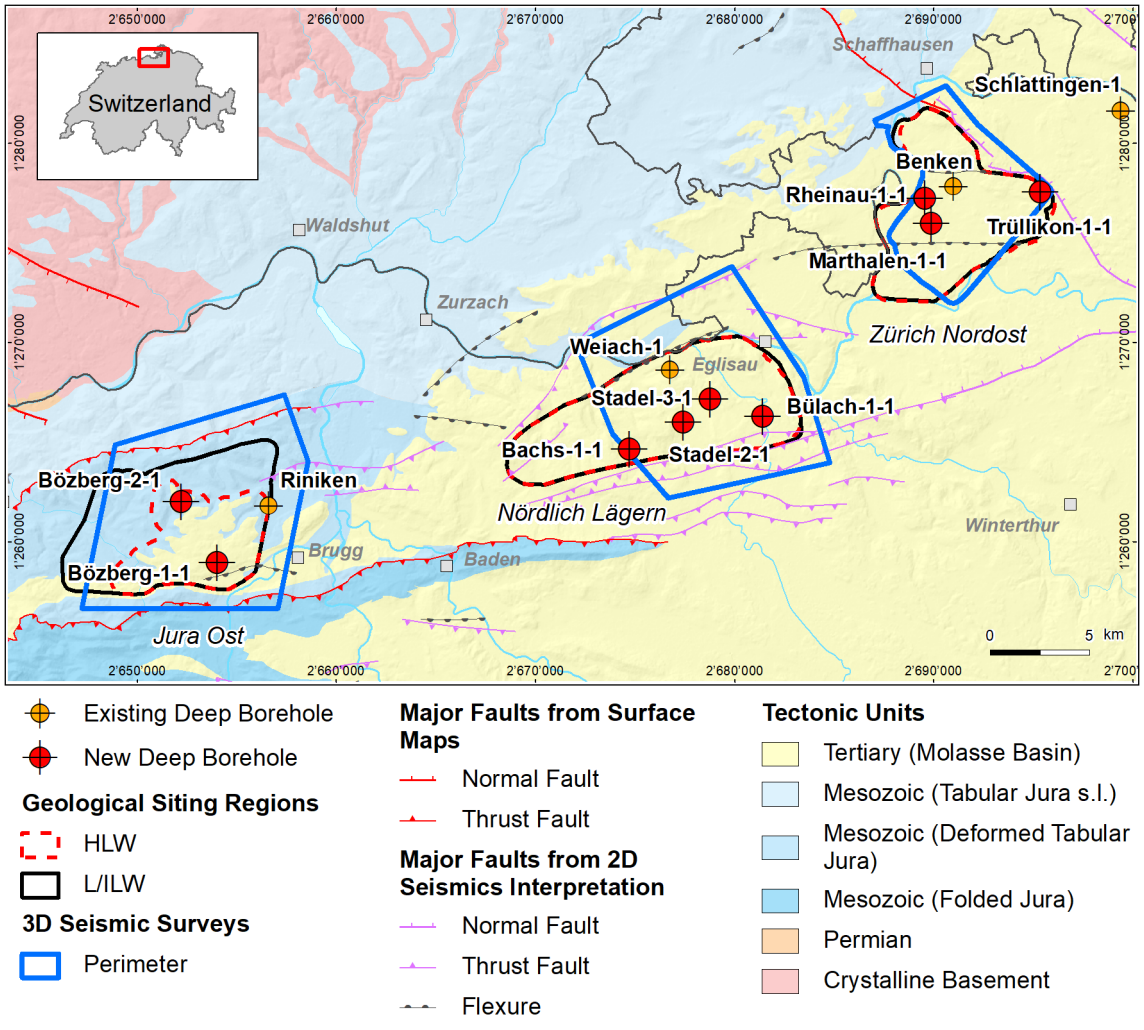

Fig. 1-1: Tectonic overview map with the three siting regions under investigation

1.2 Location and specifications of the borehole

The Stadel-2-1 (STA2-1) exploratory borehole is the seventh borehole drilled within the framework of the TBO project. The drill site is located in the central part of the Nördlich Lägern siting region (Fig. 1-2). The vertical borehole reached a final depth of 1'288.12 m (MD)[1]. The borehole specifications are provided in Tab. 1-1.

Tab. 1-1: General information about the STA2-1 borehole

Siting region	Nördlich Lägern
Municipality	Stadel (Canton Zürich / ZH), Switzerland
Drill site	Stadel-2 (STA2)
Borehole	Stadel-2-1 (STA2-1)
Coordinates	LV95: 2'677'447.617 / 1'265'987.019
Elevation	Ground level = top of rig cellar: 417.977 m above sea level (asl)
Borehole depth	1'288.12 m measured depth (MD) below ground level (bgl)
Drilling period	25th January – 8th July 2021 (spud date to end of rig release)
Drilling company	Daldrup & Söhne AG
Drilling rig	Wirth B 152t
Drilling fluid	Water-based mud with various amounts of different components such as[2]: 0 – 670 m: Bentonite & polymers 670 – 1'051 m: Potassium silicate & polymers 1'051 – 1'117 m: Water & polymers 1'117 – 1'288.12 m: Sodium chloride brine & polymers

The lithostratigraphic profile and the casing scheme are shown in Fig. 1-3. The comparison of the core versus log depth[3] of the main lithostratigraphic boundaries in the STA2-1 borehole is shown in Tab. 1-2.

[1] Measured depth (MD) refers to the position along the borehole trajectory, starting at ground level, which for this borehole is the top of the rig cellar. For a perfectly vertical borehole, MD below ground level (bgl) and true vertical depth (TVD) are the same. In all Dossiers depth refers to MD unless stated otherwise.

[2] For detailed information see Dossier I.

[3] Core depth refers to the depth marked on the drill cores. Log depth results from the depth observed during geophysical wireline logging. Note that the petrophysical logs have not been shifted to core depth, hence log depth differs from core depth.

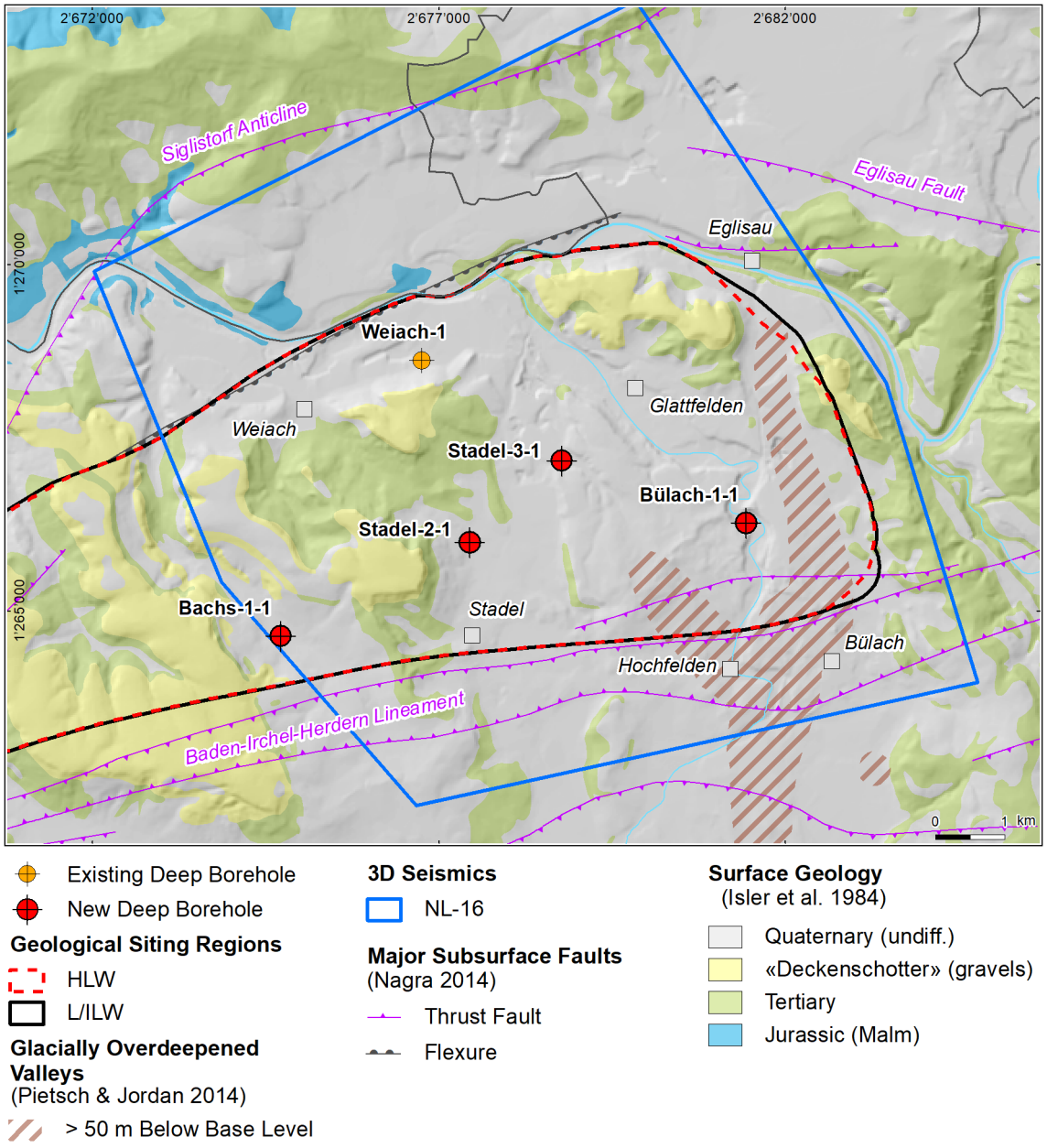

Fig. 1-2: Overview map of the investigation area in the Nördlich Lägern siting region with the location of the STA2-1 borehole in relation to the boreholes Weiach-1, BUL1-1, STA3-1 and BAC1-1

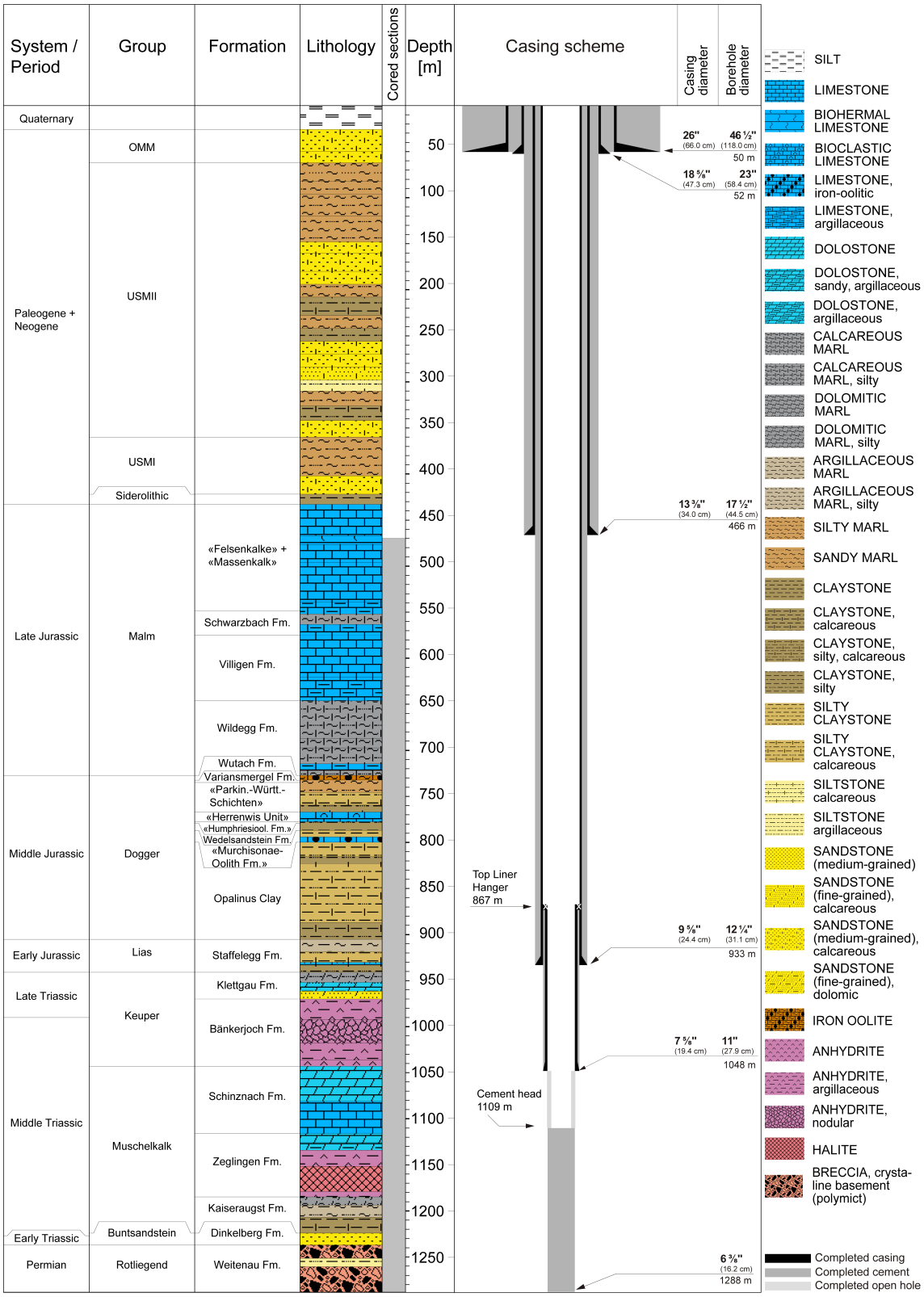

Fig. 1-3: Lithostratigraphic profile and casing scheme for the STA2-1 borehole[4]

[4] For detailed information see Dossier I and III.

Tab. 1-2: Core and log depth for the main lithostratigraphic boundaries in the STA2-1 borehole[5]

System / Period	Group	Formation		Core depth in m (MD)	Log depth in m (MD)	
Quaternary				**26.0**		—
Paleogene + Neogene	OMM			62.0		—
	USM			422.0		—
	Siderolithic			**433.0**		—
Jurassic	Malm	«Felsenkalke» + «Massenkalk»		548.35	548.62	—
		Schwarzbach Formation		575.08	575.45	—
		Villigen Formation		646.23	646.63	—
		Wildegg Formation		727.18	728.20	—
	Dogger	Wutach Formation		732.16	733.25	—
		Variansmergel Formation		734.92	735.95	—
		«Parkinsoni-Württembergica-Schichten»		767.02	768.05	—
		«Herrenwis Unit»		777.54	778.47	—
		«Humphriesioolith Formation»		779.34	780.27	—
		Wedelsandstein Formation		786.85	787.79	—
		«Murchisonae-Oolith Formation»		799.67	800.67	—
		Opalinus Clay		905.20	906.87	—
	Lias	Staffelegg Formation		**940.89**	**941.42**	—
Triassic	Keuper	Klettgau Formation		969.87	970.52	—
		Bänkerjoch Formation		1043.07	1043.62	—
	Muschelkalk	Schinznach Formation		1116.01	1116.69	—
		Zeglingen Formation		1184.72	1185.42	—
		Kaiseraugst Formation		1224.20	1225.07	—
	Buntsandstein	Dinkelberg Formation		**1237.01**	**1237.94**	—
Permian	Rotliegend	Weitenau Formation	final depth	1288.12	1288.87	

[5] For details regarding lithostratigraphic boundaries see Dossier III and IV; for details about depth shifts (core goniometry) see Dossier V.

1.3 Documentation structure for the STA2-1 borehole

NAB 22-02 documents the majority of the investigations carried out in the STA2-1 borehole, including laboratory investigations on core material. The NAB comprises a series of stand-alone dossiers addressing individual topics and a final dossier with a summary composite plot (Tab. 1-3).

This documentation aims at early publication of the data collected in the STA2-1 borehole. It includes most of the data available approximately one year after completion of the borehole. Some analyses are still ongoing (e.g. diffusion experiments, analysis of veins, hydrochemical interpretation of water samples) and results will be published in separate reports.

The current borehole report will provide an important basis for the integration of datasets from different boreholes. The integration and interpretation of the results in the wider geological context will be documented later in separate geoscientific reports.

Tab. 1-3: List of dossiers included in NAB 22-02

Black indicates the dossier at hand.

Dossier	Title	Authors
I	TBO Stadel-2-1: Drilling	P. Hinterholzer-Reisegger
II	TBO Stadel-2-1: Core Photography	D. Kaehr & M. Gysi
III	TBO Stadel-2-1: Lithostratigraphy	P. Jordan, P. Schürch, H. Naef, M. Schwarz, R. Felber, T. Ibele & H.P. Weber
IV	TBO Stadel-2-1: Microfacies, Bio- and Chemostratigraphic Analyses	S. Wohlwend, H.R. Bläsi, S. Feist-Burkhardt, B. Hostettler, U. Menkveld-Gfeller, V. Dietze & G. Deplazes
V	TBO Stadel-2-1: Structural Geology	A. Ebert, S. Cioldi, E. Hägerstedt & H.P. Weber
VI	TBO Stadel-2-1: Wireline Logging, Micro-hydraulic Fracturing and Pressure-meter Testing	J. Gonus, E. Bailey, J. Desroches & R. Garrard
VII	TBO Stadel-2-1: Hydraulic Packer Testing	R. Schwarz, R. Beauheim, S.M.L. Hardie & A. Pechstein
VIII	TBO Stadel-2-1: Rock Properties, Porewater Characterisation and Natural Tracer Profiles	C. Zwahlen, L. Aschwanden, E. Gaucher, T. Gimmi, A. Jenni, M. Kiczka, U. Mäder, M. Mazurek, D. Roos, D. Rufer, H.N. Waber, P. Wersin & D. Traber
IX	TBO Stadel-2-1: Rock-mechanical and Geomechanical Laboratory Testing	E. Crisci, L. Laloui & S. Giger
X	TBO Stadel-2-1: Petrophysical Log Analysis	S. Marnat & J.K. Becker
	TBO Stadel-2-1: Summary Plot	Nagra

1.4 Scope and objectives of this dossier

The dossier at hand aims at providing a summary of the conducted hydrogeological investigations (excluding the detailed analysis of the gas threshold pressure test) and acquired hydrogeological data, including assessments of tests and results, but without interpretation.

Borehole STA2-1 was the fifth borehole in the TBO project in which a gas threshold pressure test (GTPT) was conducted. Because the downhole equipment for the GTPT is part of the packer system used for hydraulic packer testing, a description of the equipment is included in this report. The implementation, data collection and analysis of the GTPT are reported separately.

This report focuses on fluid logging and hydraulic packer testing, and is organised as follows:

- Chapter 2 presents the general strategy for the hydrogeological investigations in the STA2-1 borehole.
- Chapter 3 is dedicated to fluid logging which was performed in the drilled borehole Section II. It discusses all aspects including the test equipment used, general concerns for the analysis, fluid logging test activities, and fluid logging test results in borehole STA2-1.
- Chapter 4 discusses all aspects of the hydraulic packer tests including planning of test strategies, test equipment used, general concerns for the analysis of tests, test activities and hydraulic packer test results in borehole STA2-1. Selected tests and analyses are presented in detail. The results are summarised in tables and plots, and some assessments are made.
- Chapter 5 summarises and discusses the data and results, mainly for the hydraulic packer tests.

Finally, this report includes a set of appendices, which present relevant general project information and further investigation details.

2 Strategy for the hydrogeological investigations

2.1 Hydrogeological objectives of the TBO boreholes

The overall objectives of the hydrogeological investigations are the detailed determination of the hydraulic conductivity and hydraulic head in the aquifers, aquicludes and aquitards on the one hand, and the chemistry and isotopic composition of the deep groundwaters in the aquifers and the porewaters in the aquicludes and aquitards on the other. The results of the hydrogeological investigations in the TBO boreholes form an important dataset for site selection and the safety case. They are mainly needed for the characterisation of:

- Hydraulic and hydrochemical properties of the containment-providing rock zone, which consists of the host rock Opalinus Clay and the confining geological units above and below.
- Hydrogeological conditions in the aquifers providing the hydraulic and hydrochemical boundary conditions for the containment-providing rock zone and providing input for the identification of potential release paths as well as for the planning of future access structures.

2.2 Hydrogeological investigation concept for STA2-1

The hydrogeological investigations for STA2-1 comprised hydraulic packer testing and fluid logging. A fluid logging campaign was performed in the Malm Group and used to define the test interval for the subsequent hydraulic packer test in Section II of the borehole to investigate the zone of main inflow.

Fluid logging was performed, given sufficiently high transmissivities. Water inflow points into the borehole were identified with a series of temperature – electrical conductivity logs.

Hydraulic packer tests were used for the detailed hydraulic characterisation of selected borehole sections to determine transmissivity (T), hydraulic conductivity (K), hydraulic head (h) and to identify the appropriate flow model. Hydraulic packer tests were performed in scheduled testing phases between drilling phases, and also during drilling phases when potentially highly transmissive features or faults were encountered. Depending on the transmissivity of the test interval, different test methods were applied in STA2-1 as follows:

- Pumping tests
- Slug tests
- Pulse tests

These test methods were usually combined, i.e. executed one after the other as a test sequence in a test-specific order.

A gas threshold pressure test (GTPT) was conducted in the STA2-1 borehole and an exchange of drilling mud with synthetic porewater (PEARSON water) was performed in one of the test intervals (Section 4.1). In the siting region Nördlich Lägern a long-term monitoring system will be installed in nearby borehole STA3-1.

The detailed groundwater sampling, subsequent hydrochemical and isotope analyses (including results) are documented in Lorenz & Stopelli (*in prep.*). Further porewater investigations are the subject of Dossier VIII. The laboratory permeability measurements on drill-core sections are discussed in Dossier IX.

3 Flowmeter logging and fluid logging

3.1 Description of equipment

The fluid logging was performed with the equipment introduced below. For the pumping test phase the equipment of the field test contractor for hydraulic packer testing was used (*cf.* Section 4.2).

3.1.1 Borehole logging winch

The winch features a mechanical cable spooling device, an electronic and a mechanical depth measurement and a cable tension measurement. For specifications, see Tab. 3-1. The borehole logging winch is permanently mounted in the logging van and is powered by a motor. As soon as the motor is stopped, a break is automatically engaged in the gearbox. Additionally, there is a manual brake and a clutch.

Tab. 3-1: Specifications of the borehole logging winch

Manufacturer	HEWA Feinwerktechnik Engineering GmbH, Marie-Curie-Str. 2, 79211 Denzlingen, Germany
Type	TT2000, Electrical, 220 V
Cable type	Rochester 3⁄16" 4-conductor cable Type 4-H-181A
Cable breaking strength	14.7 kN
Max. cable length	2'000 m
Logging speed range	0 – 30 m/min
Depth measurement	IVO BAUMER incremental encoder, 2'500 pulse / rotation; 500 mm circumference wheel mounted on the spooling device, mechanical depth counter
Cable tension gauge	External display or input for matrix logger
Safety joint	Cable head is set up to form a weak joint. In the case of a stuck probe, the cable is pulled from the cable head

3.1.2 Matrix logger

The Matrix logger is a logging surface unit that interfaces the probe with the acquisition PC, using the Advanced Logic Technology (ALT) Matrix Logger software (for specifications, see Tab. 3-2). It records the data, depth and logging speed and has a digital interface. The unit supports several communication protocols and can therefore be used to run probes built by different manufacturers (among others electromind, Robertson Geologging, ALT). A browser module connects the acquisition software to an ALT WellCAD document and feeds the data directly into WellCAD. The data of several runs is displayed in one document.

The software used to control the unit and the probes is as follows:

- Heat Pulse: Matrix Heat: V3.3 build 2208 © Advanced Logic Technology, 2005 – 2012
- All other probes: Matrix Logger: V 12.1 build 2388 © Advanced Logic Technology, 1995 – 2018
- Processing: WellCAD 5.2 build 1925 © Advanced Logic Technology, 1993 – 2018

The winch features a mechanical cable spooling.

Tab. 3-2: Specifications of the matrix logger

Manufacturer	Advanced Logic Technology, 30H Rue de Niederpallen, Zoning de Solupla, L-8506 Redange, Luxembourg
Type	Matrix borehole logging system
Data transmission	The data is digitised in the probes and sent to the logging system with a resolution of 15 bit (0 – 32'768 cps resolution per channel) and 16 bit (0 – 65'536 cps resolution per channel), respectively, depending on the probe

3.1.3 Flowmeter-temperature-conductivity-gamma probe

The probe is a combination of a LIM logging / electromind temperature-electrical-conductivity-gamma probe with an Intergeo impeller flowmeter head. For this reason, the actual dimensions of the probe as mentioned below differ from the dimensions on the manufacturer's data sheet. The probe was assembled on the field contractor's request by electromind. The Intergeo flowmeter head combines a larger diameter (88 mm) with jewelled bearings for the impeller instead of ball bearings which provides improved sensitivity compared to the standard electromind impeller head. For specifications, see Tab. 3-3.

This probe measures fluid temperature, electrical fluid conductivity, vertical fluid velocity and natural gamma rays. The electrical conductivity-temperature sensor is mounted on the side of the probe. Fluid can freely flow through it while going down and up. The flowmeter is an impeller type with a cage of 88 mm and is used if relatively higher fluid flow rates are expected. If lower flow rates are anticipated that might be below the detection limit, the performance of the impeller can be improved by using a diverter disc. The diverter disc seals the annulus between the impeller cage and the borehole wall and forces most of the fluid through the sensor. This increases the fluid velocity at the sensor. Different disks are available to adjust to the borehole diameter.

The diverter disc assembly is made from a base plate that is attached to the probe, and a flexible plastic disc that can be changed depending on the borehole diameter. The base plate for the FTC60G probe is made of Nylon and its dimensions are 140 mm outer diameter, 80 mm inner diameter, 42 mm height.

Tab. 3-3: Specifications of the flowmeter-temperature-conductivity-gamma probe

Manufacturer	LIM logging / electromind s.a. 1 Rue de l'Industrie, 4801 Rodange, Grand Duche de Luxembourg + intergeo Haferland AG
Type	FTC60G
Length	1'710 mm
Weight	5.5 kg
Cage diameter	88 mm
Operational temperature range	0 – 70 °C (up to 80 °C for a limited time)
Max. pressure	20 MPa
Borehole diameter range	> 96 mm
Temperature sensor range	0 – 70 °C (up to 80 °C for a limited time)
Temperature sensor accuracy	0.1 °C
Temperature sensor resolution	0.001 °C
Electrical conductivity sensor linear range	0 – 3'000 µS/cm (not on data sheet, information from manufacturer)
Electrical conductivity sensor accuracy	10 µS/cm
Electrical conductivity sensor resolution	1 µS/cm
Flowmeter threshold velocity (static)	1 m/min
Flowmeter impeller sensor resolution (theoretical)	0.003 m/min
Gamma detector	NaI 50 mm × 25 mm crystal

3.1.4 Temperature-conductivity-gamma probe

The probe measures fluid temperature, electrical fluid conductivity and natural gamma rays (for specifications, see Tab. 3-4). The electrical conductivity is referenced to 25 °C and the temperature-electrical conductivity sensor is mounted at the bottom. In the standard setup, the fluid enters the probe through openings at the bottom, flows through the sensor assembly and leaves the probe through openings at the side of the probe a bit further up. This geometry is optimised for logging going down.

Tab. 3-4: Specifications of the temperature-conductivity-gamma probe

Manufacturer	Robertson Geologging Ltd., York Road, Deganwy, Conwy, LL31 9PX, UK
Type	TCG
Length	1'690 mm
Weight	4.5 kg
Tool diameter	38 mm
Operational temperature range	0 – 70 °C (up to 80 °C for a limited time)
Max. pressure	20 MPa
Borehole diameter range	> 50 mm
Temperature sensor range	0 – 70 °C (up to 80 °C for a limited time)
Temperature sensor accuracy	± 0.5 °C (not on data sheet, information from manufacturer)
Temperature sensor resolution	0.04 °C (not on data sheet, information from manufacturer)
Electrical conductivity sensor range	50 – 50'000 µS/cm
Electrical conductivity sensor accuracy	± 2.5% at 500 µS/cm (not on data sheet, information from manufacturer)
Electrical conductivity sensor resolution	4 µS/cm (not on data sheet, information from manufacturer)
Electrical conductivity temperature compensation	25 °C
Gamma detector	NaI 50 mm × 25 mm crystal

3.1.5 High-resolution flowmeter-gamma probe

This probe measures vertical fluid velocity and natural gamma rays (for specifications, see Tab. 3-5). The flowmeter is an impeller type with a cage of 45 mm. This probe is used if relatively higher fluid flow rates are expected. If lower flow rates are anticipated which might be below the detection limit, the performance of the impeller can be improved by using a diverter disk.

The diverter disc assembly is made from a base plate that is attached to the probe, and a flexible plastic disc that can be changed depending on the borehole diameter. The base plate for the probe is made of aluminium. The dimensions are: 90 mm outer diameter, 45 mm inner diameter, 11 mm height.

Tab. 3-5: Specifications of the high-resolution flowmeter-gamma probe

Manufacturer	Robertson Geologging Ltd., York Road, Deganwy, Conwy, LL31 9PX, UK
Type	HRFM
Length	1'530 mm
Weight	4.0 kg
Cage diameter	45 mm
Operational temperature range	0 – 70 °C (up to 80 °C for a limited time)
Max. pressure	20 MPa
Borehole diameter range	> 50 mm
Flowmeter threshold velocity (static)	1 m/min (not on data sheet, information from manufacturer)
Flowmeter sensor resolution (theoretical)	4 pulses per impeller revolution, the time between pulses is measured. Resolution of time measurement 20 ms (not on data sheet, information from manufacturer)
Gamma detector	NaI 50 mm × 25 mm crystal

3.1.6 Gamma sensors

All probes described above are equipped with similar gamma-ray detectors. The detectors are of the scintillation type, set up for total count measurements. They consist of a NaI crystal (50 mm × 25 mm), a photomultiplier tube and a counting circuit. The output is counts per second (cps). No background radiation exists and has to be considered in a borehole.

The range of the sensors is 0 – 65'536 cps (16 bit). In a typical geological context of southern Germany and Switzerland the count rates normally do not exceed 300 – 400 cps with the given sensors.

Remarks on accuracy of a gamma measurement (Richards 1981): There is a statistical noise to the data, because it is possible to predict the rate of emission of gamma rays, but not which individual nuclei will disintegrate or not. It is possible to determine the true mean count rate (cps) for a given source of gamma-rays quite accurately by counting and averaging for a long time. The statistical noise produces a fluctuation of the readings around the true mean count rate. The expected standard deviation is the square root of the true mean count rate n.

The fractional standard deviation expresses the standard deviation as percentage of the true count rate:

fractional std. dev. = (std. dev.)/n*100

e.g. n = 10'000 cps → std. dev.: 100 cps, fractional std. dev.: 1%

n = 100 cps → std. dev.: 10 cps, fractional std. dev.: 10%

This means the precision of the measurement increases as the count rate increases.

3.1.7 Temperature-electrical conductivity meter

The WTW (Wissenschaftlich-technische Werkstätten GmbH) instrument pH/Cond 340i is a hand-held digital instrument to measure fluid pH, electrical conductivity and temperature (for specifications, see Tab. 3-6). This meter is used at the workshop to perform the electrical conductivity calibration of the logging tools, and on-site to check the calibration of electrical conductivity and temperature.

Tab. 3-6: Specifications of the temperature-electrical conductivity meter

Manufacturer	WTW (Wissenschaftlich-technische Werkstätten GmbH), Dr.-Karl-Slevogt-Straße 1, D-82362 Weilheim
Type	pH/Cond 340 i
Temperature sensor range	0 – 105 °C
Temperature sensor accuracy	± 0.1 °C
Electrical conductivity range	0 – 19.99 mS/cm (resolution 0.01), 0 – 199.9 mS/cm (resolution 0.1)
Electrical conductivity accuracy	± 0.5%
Reference temperature	25 °C

3.1.8 Centraliser

When the probes are run in the hole, they are equipped with a set of centraliser blades. The main purpose of the centralisers is to keep the probes off the borehole wall to prevent measurements being influenced by any debris that might be scraped off the borehole wall. For specifications, see Tab. 3-7.

The centralisers are made from brass rings with elastic copper – beryllium blades. The centraliser cage can be set up with different blades to cover different borehole diameter ranges. The blades are fixed to the probe by grub screws.

Tab. 3-7: Specifications of the centraliser

Manufacturer	LIM Logging / electromind s.a.
Type	Bow spring centraliser
Length	420 mm at 165 mm diameter, 530 mm at 215 mm diameter
Weight	Approx. 3 kg
Borehole diameter range	70 – 270 mm

3.1.9 Field analysis IT structure

Logging is performed directly into a WellCAD document to display previous and current measurements. For specifications of the IT structure, see Tab. 3-8.

Tab. 3-8: Specifications of the IT structure for field analysis

Processing software	WellCAD 5.2 build 1925 © Advanced Logic Technology, 1993 – 2018
Logging software	Matrix Logger: V 12.1 build 2388 © Advanced Logic Technology, 1995 – 2018
Logging software (heat pulse flowmeter only)	Matrix Heat: V3.3 build 2208 © Advanced Logic Technology, 2005 – 2012
Uninterrupted power supply	APC Back-UPS Pro 900 BR900-G, 900 VA / 540 Watt
Data back-up	External hard drive
Acquisition computer	Notebook, Windows 10 Pro

3.2 Performance and analysis

Fluid logging was conducted in borehole STA2-1 from 16.02.2021 to 17.02.2021 in the cored borehole Section II after a fluid exchange of drilling mud with tap water was performed. The section comprises calcareous marlstone to limestone within the «Felsenkalke» + «Massenkalk», the Schwarzbach Formation, the Villigen Formation and the Wildegg Formation of the Jurassic Malm Group. The measurements were performed using the temperature-conductivity-gamma probe described in Section 3.1.4. The objectives of the fluid logging analysis were detection of inflow zones and determination of their associated transmissivities. The transmissivity values of the inflow zones were derived from the total transmissivity determined by the analysis of the associated pumping test. The results of the fluid logging analysis were compared with the results from the subsequent hydraulic packer test STA2-1-MAL1 (Section 4.6).

3.2.1 Description of measurements performed

For the execution of the test STA2-1-FL1-MAL, drilling was carried out to a depth of 670 m MD, with the fluid logging being performed to a depth of approximately 665 m MD after the drilling fluid was exchanged with tap water. Tab. 3-9 provides the information on the open borehole section. The pump was installed at a depth of 161.63 m MD, after which, an initial Run (log of the electrical conductivity and the temperature) was performed. The pumping test consisted of two rate withdrawal pumping phases (RW1 and RW2) followed by their recovery phases (RWR1 and RWR2). The first pumping phase RW1 was performed with the highest achievable pumping rate, rapidly reaching the maximum drawdown of around 140 m MD. During this phase, the pressure dropped from 1'573 kPa to 676 kPa (Fig. 3-1). The flow rate decreased from about 120 l/min to about 0.5 l/min. In Figs. 3-1 and 3-2, the flow rate is shown scaled linearly and logarithmically, respectively.

Tab. 3-9: Fluid logging STA2-1-FL1-MAL: Information on the test interval

Test	**Depth**		**Length**	**Configuration**	**Hydraulic testing**		
	from [m MD]	to [m MD]	[m]		Start date	End date	Duration [h]
STA2-1-FL1-MAL	466.00	670.00	204.00	Open borehole	16.02.2021	17.02.2021	15.35

The second pumping phase (RW2) reached approximately stable drawdown conditions (Fig. 3-1) and the formation flow was stabilised between 22:30 on 16.02.2021 until 03:45 on 17.02.2021 (Fig. 3-2). The flow rate was progressively reduced from an initial flow rate of about 220 l/min to 0.7 l/min that stabilised over the last 5 hours (Fig. 3-2). Runs 2 and 3 were performed during the RW1 and RWR1 phases respectively, whereas Runs 4 to 8 were conducted during the RW2 phase. Fig. 3-3 shows the measurement of the electrical conductivity corrected to 25 °C for Runs 4 to 8. The final phase of the test was the second recovery phase (RWR2). During this period, the water pressure increased from 182 kPa to 190 kPa within approximately 2 hours.

In total eight Runs (logs of electrical conductivity and temperature) were carried out. Tab. 3-10 presents an overview.

Tab. 3-10: Fluid logging activities in STA2-1-FL1-MAL

Logging run	**Hydraulic test sequence**	**Date**	**Start time**	**Start depth** [m MD]	**End time**	**End depth** [m MD]
1	History	16.02.2021	06:58	471.91	07:37	664.93
2	RW1	16.02.2021	16:34	474.89	16:57	664.98
3	RWR1	16.02.2021	17:23	474.46	17:54	664.98
4	RW2	16.02.2021	20:11	474.35	20:52	664.97
5		16.02.2021	22:00	474.34	22:32	664.97
6		17.02.2021	00:00	474.32	00:32	664.96
7		17.02.2021	01:30	474.33	02:01	664.96
8		17.02.2021	03:00	474.29	03:31	664.98
-	RWR2	17.02.2021	03:45	-	05:35	-

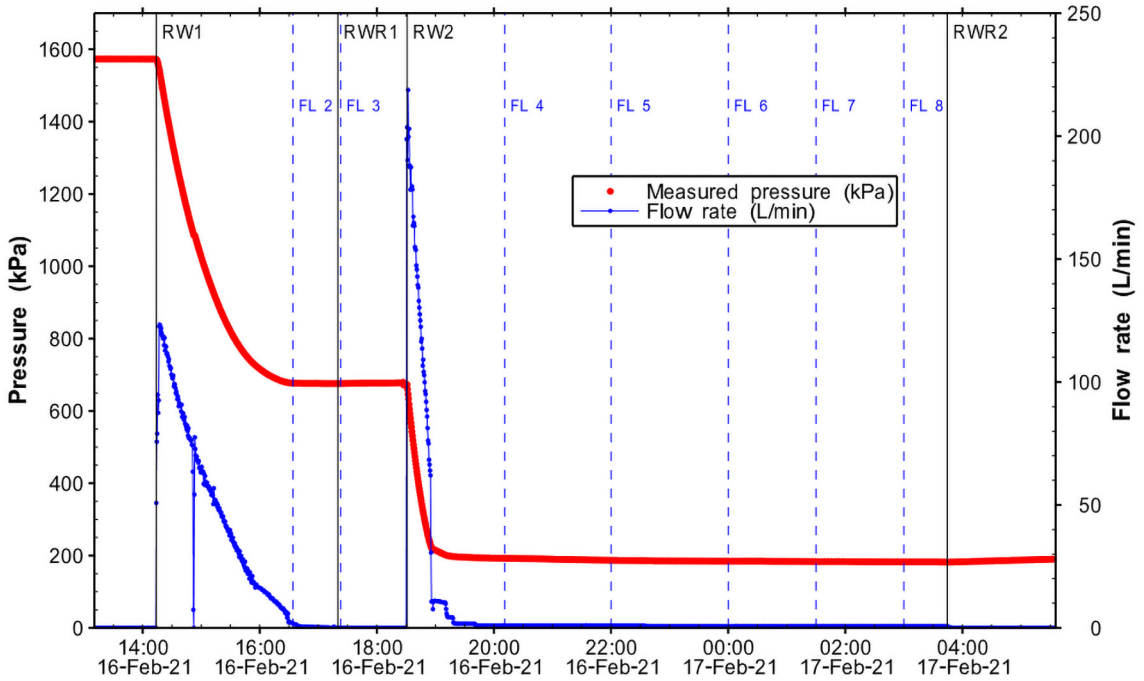

Fig. 3-1: STA2-1-FL1-MAL: Pressure drawdown and the position in time where fluid logging runs were performed

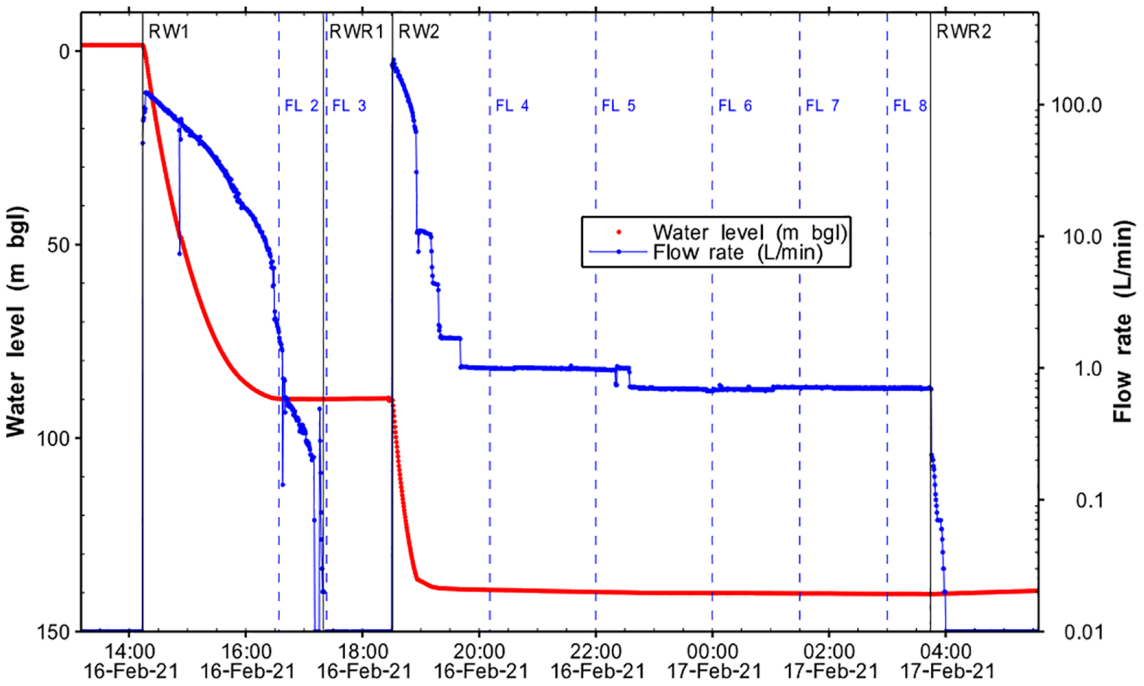

Fig. 3-2: STA2-1-FL1-MAL: Water level drawdown (derived from the pressure drawdown), measured pumping rates and the position in time where fluid logging runs were performed

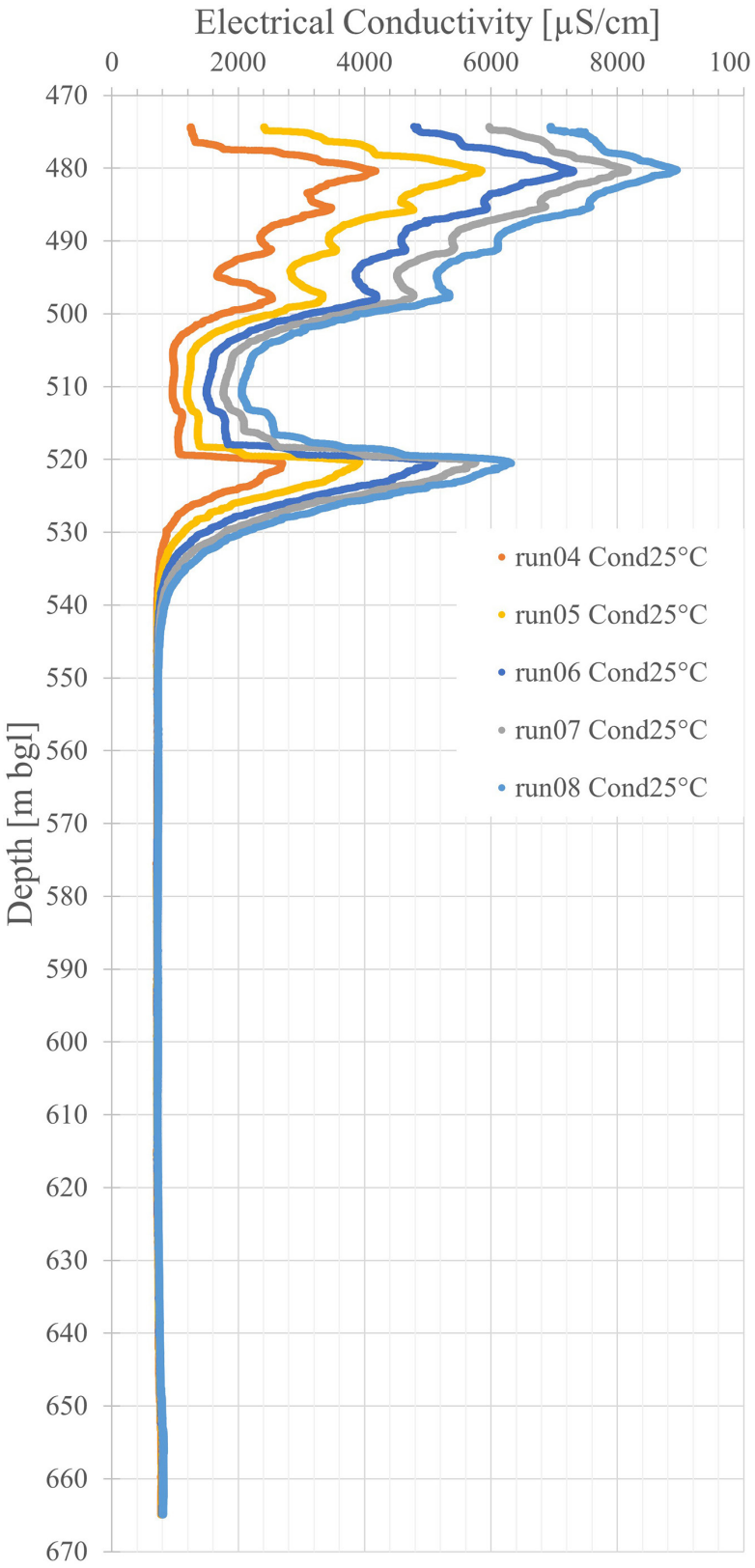

Fig. 3-3: STA2-1-FL1-MAL: Measured electrical conductivity for Runs 4 – 8, calculated for a temperature of 25 °C

Note that the first 3 runs are not shown as they were not included in the visual inspection (due to the fact that they were performed prior to stabilisation of conditions).

3.2.2 Analysis of pumping test data

The pumping test was analysed numerically using the software package nSIGHTS. The pre-test borehole history included the drilling phase, the fluid exchange and the first pumping and recovery phases (RW1 and RWR1). This initial pumping sequence (RW1-RWR1) was considered as a pressure history phase due to the uncertainty related to anomalous pump behaviour. Hence, the analysis focused on pumping phase RW2 and the pressure recovery phase RWR2. The simulation used a radial homogeneous flow model when the formation parameters were optimised in order to estimate the best values and their confidence ranges by means of a perturbation analysis.

The flow rates measured during the RW2 phase and the pressure measured during the RWR2 phase were fitted. The choice of a radial homogeneous model without a skin zone was based on the observed shape of the log-log diagnostic plot of the recovery phase RWR2. The optimised parameters were: the hydraulic transmissivity T, the storage coefficient S and the static formation pressure P_f. A perturbation analysis using 3'000 runs was used for the estimation of the best fit values and the confidence ranges (Tab. 3-11). The presented hydraulic conductivity along with the other formation parameters, assumed a total contributing formation thickness of 41 m (480 – 521 m MD), thus differing from the length of the entire open borehole section (Tab. 3-9). The thickness of 41 m corresponds to the total extent of the inflow region that were determined in the fluid logging analysis (Section 3.2.3).

Tab. 3-11: STA2-1-FL1-MAL: Best estimates of the hydraulic parameters and their confidence ranges derived from the pumping test analysis in the framework of the fluid logging operations

[1)] Considering a contributing formation thickness of 41 m.

Parameter	**Minimum**	**Best Estimate**	**Maximum**
Pumping test phases considered	RW2 + RWR2		
Flow model	Radial homogeneous model		
Hydraulic conductivity (K) [m s^{-1}] [1)]	1.5×10^{-9}	2.2×10^{-9}	2.4×10^{-9}
Total transmissivity (T) [1] [m^2 s^{-1}]	6.0×10^{-8}	8.9×10^{-8}	1.0×10^{-7}
Storativity (S) [-]	4.4×10^{-7}	4.4×10^{-7}	1.8×10^{-4}
Static formation pressure (P_f) [kPa]	912	1'333	1'398

The analysis provides a best estimate for the transmissivity of the open borehole section (204 m) of 8.9×10^{-8} m^2 s^{-1} with 6.0×10^{-8} m^2 s^{-1} as a minimum and 1.0×10^{-7} m^2 s^{-1} as a maximum estimate.

3.2.3 Fluid logging analysis

The fluid logging analysis was based on implementation of a 1D advective-dispersive solute transport equation in a borehole with feed points along the borehole (Tsang & Hufschmied 1988 and Doughty & Tsang 2005).

Five complete runs of electrical conductivity (corrected to 25 °C equivalent conductivity) were considered for the analysis (Runs 4 – 8). Runs 2 and 3 were neglected as they were conducted

during the RW1 and RWR1 phases respectively, and therefore, were possibly affected by the anomalous pump behaviour.

By visual inspection of the electrical conductivity for Runs 4, 5, 6, 7 and 8 (Fig. 3-3), which were carried out during the second pumping period (RW2), two hydraulically active features were identified (Tab. 3-12).

Tab. 3-12: Inflow zones detected qualitatively by STA2-1-FL1-MAL

Depth [m MD]	**Remark**
475.00 – 500.00	Indicated by electrical conductivity
515.00 – 530.00	Indicated by electrical conductivity

Finally, from Runs 4 – 8 only Runs 6, 7 and 8 were conducted under stabilised formation flow rate conditions and, therefore, these three runs were selected for quantitative analysis. Thus, the electrical conductivity logs obtained for Runs 7 and 8 were simulated and matched using the electrical conductivity distribution measured during Run 6, as the initial conditions in the bore-hole. Figs. 3-4 and 3-5 present the best match between both measured and simulated profiles of electrical conductivity. In the quantitative analysis, the mapping of the two qualitatively determined inflows (Tab. 3-12) was simulated and refined.

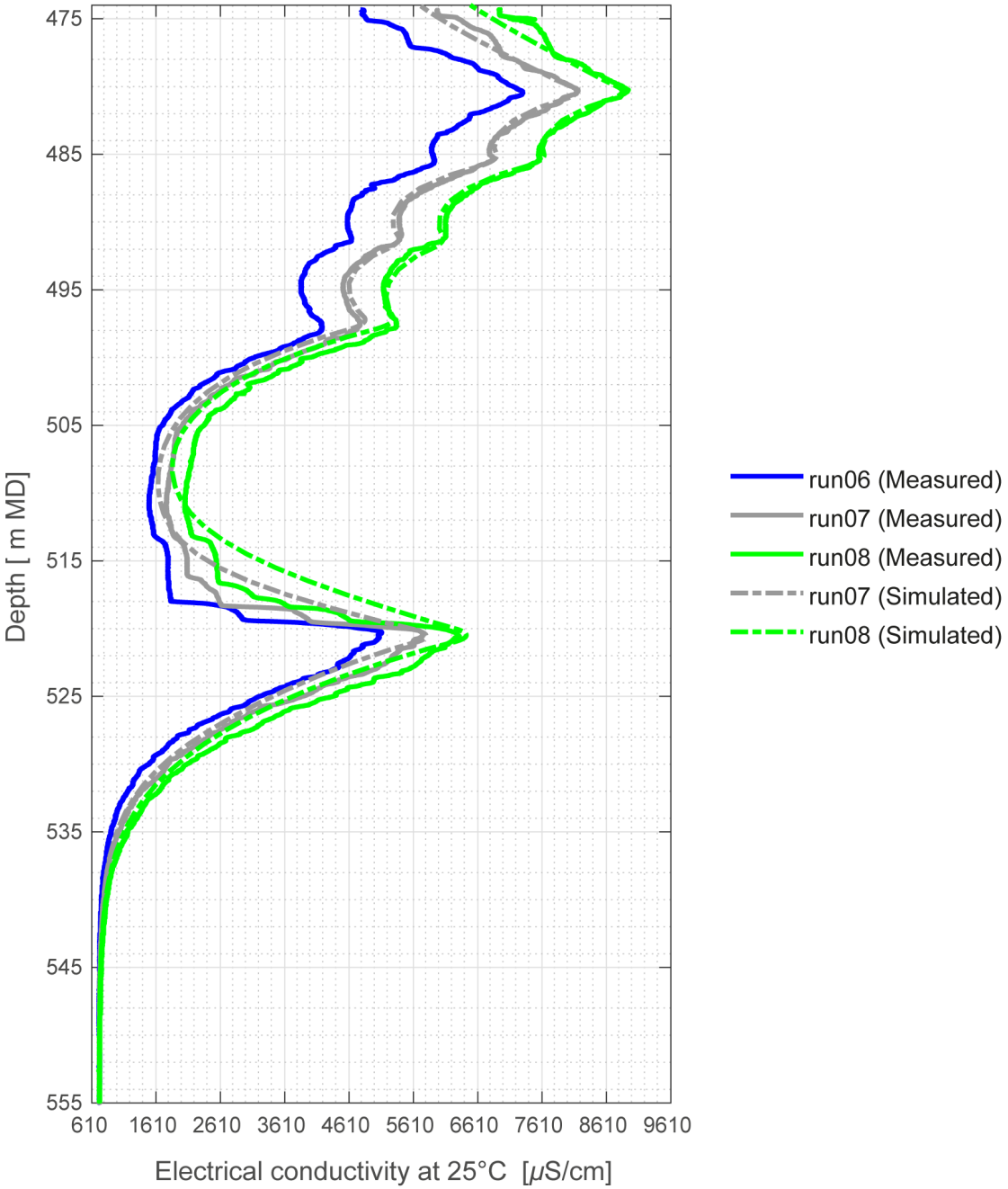

Fig. 3-4: STA2-1-FL1-MAL: Measured and simulated Runs 7 and 8 using the measurement of Run 6 as the initial conditions

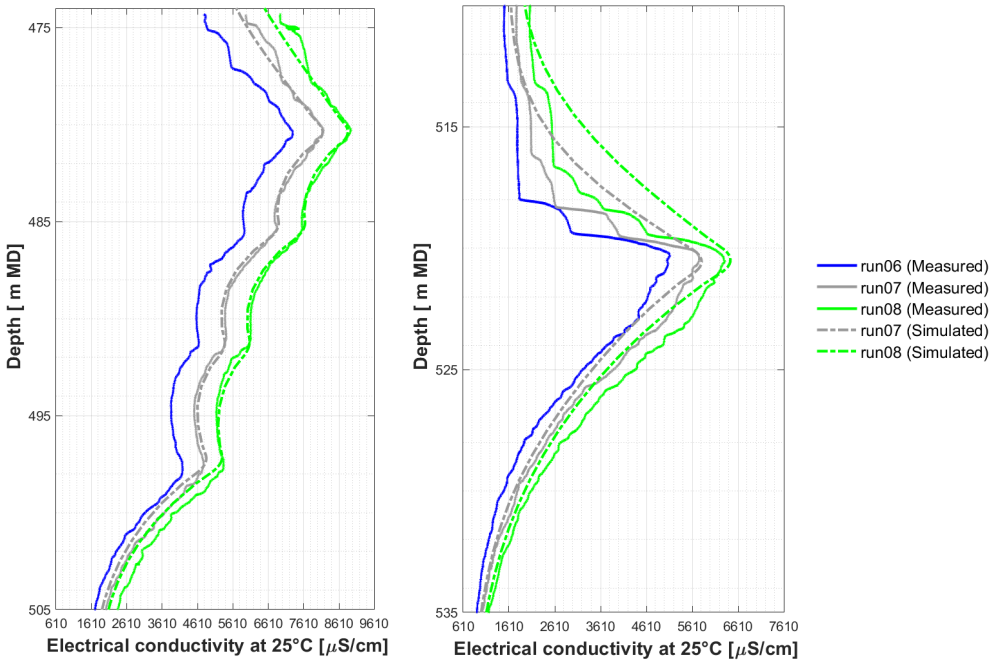

Fig. 3-5: Measured and simulated Runs 7 and 8 using the measurement of Run 6 as the initial conditions (close-ups)

The inflow zones finally identified by means of a quantitative analysis and their related inflow rate q_i, salinity C_i as well as the corresponding electrical conductivity EC_i are provided in Tab. 3-13. The values of the electrical conductivity are within the range of subsequent laboratory measurements of formation water samples (Lorenz & Stopelli *in prep.*) of this inflow zone taken during the following hydraulic packer test (STA2-1-MAL1).

The transmissivity values for the individual inflow zones were computed as the product of the total transmissivity of the logged borehole section obtained in the analysis of the pumping test data (Section 3.2.2) and, the relative contribution of each of the individual inflow zone flow rates, to the total stabilised formation flow rate. Accordingly, the sum of the transmissivities of the inflows corresponds to the total transmissivity, and it was assumed that the main source of uncertainty for the individual inflow zone transmissivity values was based on the total borehole section transmissivity derived from the corresponding pumping test analysis (Section 3.2.2). The reason for this was that the electrical conductivity (and thereby the salinity) was confirmed by formation water samples from the subsequent hydraulic packer test STA2-1-MAL1. Another reason was the attainment of a very good match for the electrical conductivity peak values with the simulation. Hence, the confidence ranges for the transmissivity of the individual inflow zones were computed by propagating the uncertainty in each of the individual inflow zones of the total transmissivity of the whole borehole section provided in Section 3.2.2. Tab. 3-13 provides the results for the inflow zones.

Tab. 3-13: STA2-1-FL1-MAL: Depth and properties of the inflow zones (q_i, C_i, EC_i) and the best estimates and associated confidence ranges for transmissivity

[1] Based on the results presented by the field test contractor in the corresponding report.

Inflow zones	**Top** [m MD]	**Bottom** [m MD]	**q_i** [1] [$m^3\ s^{-1}$]	**C_i** [1] [$g\ l^{-1}$]	**EC_i** [1] [$\mu S\ cm^{-1}$]	**T_i min** [1] [$m^2\ s^{-1}$]	**T_i best** [1] [$m^2\ s^{-1}$]	**T_i max** [1] [$m^2\ s^{-1}$]
1	480.00	481.00	2.1×10^{-6}	14	20'230	1.9×10^{-8}	2.8×10^{-8}	3.2×10^{-8}
2	485.00	486.00	8.3×10^{-7}	24	23'880	6.3×10^{-9}	9.3×10^{-9}	1.1×10^{-8}
3	491.00	492.00	8.3×10^{-7}	17	22'270	6.3×10^{-9}	9.3×10^{-9}	1.1×10^{-8}
4	497.00	498.00	8.3×10^{-7}	22	23'870	6.3×10^{-9}	9.3×10^{-9}	1.1×10^{-8}
5	520.00	521.00	2.5×10^{-6}	12	18'420	2.3×10^{-8}	3.3×10^{-8}	3.8×10^{-8}

3.3 Summary and discussion of fluid logging results

A fluid logging campaign was performed within borehole Section II in order to identify the presence of any inflow zones in the Malm. The analysis of inflow zones was based on the evaluation of the electrical conductivity profiles from Runs 6, 7 and 8, performed during the pumping phase RW2. A visual inspection indicated qualitatively two separate inflow zones in the «Felsenkalke» + «Massenkalk» between depths of 475 – 500 m MD and 515 – 530 m MD. The performed quantitative analysis leads to a more detailed result that showed a total of five inflow zones. Four of these formed the upper inflow zone and the other, the lower inflow zone. The total transmissivity of $8.9 \times 10^{-8}\ m^2\ s^{-1}$ calculated for the entire open borehole section by the analysis of the associated pumping test (Section 3.2.2) resulted from an upper zone hydraulic transmissivity of $5.6 \times 10^{-8}\ m^2\ s^{-1}$ (with a major inflow zone of $2.8 \times 10^{-8}\ m^2\ s^{-1}$ at 480 – 481 m MD) and a lower zone hydraulic transmissivity of $3.3 \times 10^{-8}\ m^2\ s^{-1}$.

The resulting hydraulic properties were based on a perturbation analysis of the corresponding pumping sequence RW2-RWR2 using 3'000 runs. The confidence ranges of the total hydraulic transmissivity estimated by the associated pumping test (Section 3.2.2) ranged from 6.0×10^{-8} to $1.0 \times 10^{-7}\ m^2\ s^{-1}$. This uncertainty range was taken over and used to characterise the uncertainty ranges of the hydraulic transmissivity of the separate inflows.

The entire inflow zone identified within borehole Section II was attributed to limestone interrupted by several intervals containing sponges (*cf.* Dossier III). The hydraulic transmissivity of the upper inflow zone ranged from between $3.8 \times 10^{-8}\ m^2\ s^{-1}$ and $6.5 \times 10^{-8}\ m^2\ s^{-1}$ and is part of the borehole section that shows abundant karst features, mostly filled with claystone. The hydraulic transmissivity of the lower inflow zone ranged from between $2.3 \times 10^{-8}\ m^2\ s^{-1}$ and $3.8 \times 10^{-8}\ m^2\ s^{-1}$, with this section being characterised as limestone with few vugs and pores filled with claystone.

The hydraulic packer test STA2-1-MAL1 (from 473.50 m MD to 542.67 m MD) covered the entire region of possible inflows detected by the fluid logging test STA2-1-FL1-MAL carried out within borehole Section II. The resulting estimate for the hydraulic conductivity of $3 \times 10^{-9}\ m\ s^{-1}$ corresponds well with the results of the analysis of the pumping sequence associated with the fluid logging campaign STA2-1-FL1-MAL of $2.2 \times 10^{-9}\ m\ s^{-1}$. In addition, there is very good agreement in the uncertainty ranges for the result yielded by the hydraulic packer test and that achieved during the pumping sequence associated with the fluid logging campaign. In summary, the fluid logging analyses allowed mapping of the major inflows.

The analysis of the RW2-RWR2 pumping test sequence and the fluid logging data obtained from the STA2-1-FL1-MAL test provided consistent and reliable transmissivity values for the main inflow zones between 480 – 498 m MD (major inflow between 480 and 481 m MD) and 520 – 521 m MD.

4 Hydraulic packer test

4.1 Test strategy

The geological formations examined within the TBO boreholes exhibit a wide range of transmissivities. The host rock, Opalinus Clay, and its confining units are expected to have very low transmissivities, whilst the regional aquifers like the Malm and the Muschelkalk formations are expected to have relatively high transmissivities.

Nagra has long established hydraulic testing strategies (e.g. Nagra 1997) to extract the maximum information in relation to the hydraulic characteristics of the various geological formations. Two testing strategies are preferred (Tabs. 4-1 and 4-2) depending on the transmissivity of the formation (low to very low or medium to high). A typical test sequence is divided into different test phases: test preparation, diagnostic and main phase. The test sequence may be concluded with a pulse test (PW/PI) to check if the total test interval compressibility changed during the test. Modifications to the strategies are made according to the preliminarily available information, the encountered specific test conditions and obtained results while testing. This may lead to the omission of certain test phases, e.g. the diagnostic phase.

The main difference in the two testing strategies is the selection of appropriate test types and phases as well as the duration of the test phases. In a formation with medium to high transmissivity, pressure disturbances due to drilling or temperature effects dissipate relatively quickly. Accordingly, the test preparation phase is short. The main phase delivers results of sufficient accuracy with respect to the hydraulic properties of the formation in a relatively short period.

In the case of formations with low to very low transmissivity, the test types and their duration are different. For the determination of hydraulic head, the borehole pressure history and test duration are important issues. Depending on the pressure difference between the static formation conditions and the pressure induced in the borehole during the pre-test pressure history, the estimates of hydraulic head can be strongly affected by non-static pressure conditions in the surrounding borehole area.

A further aspect of the testing strategy is the use of drilling fluid as a test fluid (see Tab. 1-1). The water-based mud used for drilling contained bentonite and polymers as additives for interval STA2-1-MAL1, polymers as additives for interval STA2-1-MUK1 and potassium silicate and polymers for all other intervals (*cf.* Dossier I). In contrast to previous exploration boreholes drilled by Nagra (e.g. Benken; Nagra 2001), no exchange of drilling fluid in the test intervals was performed within the STA2-1 borehole during hydraulic testing. The main reason for this was maintenance of borehole stability. There were two exceptions to this, however. The first was for interval STA2-1-MAL1 where the hydraulic test followed the fluid logging (STA2-1-FL1-MAL) for which the mud had to be exchanged by tap water. The second was for the interval STA2-1-OPA4 where the drilling fluid was replaced by PEARSON water as test fluid. During the fluid exchange for STA2-1-OPA4, a significant pressure rise was observed and a test induced opening of the formation (probably a hydraulic fracturing) could not be prevented. Thus, the results of STA2-1-OPA4 could not be used to characterise the undisturbed formation conditions.

Finally, the model implementation as a skin in the test analysis is assumed to adequately address any issues linked with drilling fluid properties at the borehole wall.

Tab. 4-1: Preferred test sequence for formations with medium to high transmissivity

[1] For explanation of abbreviations see Tab. A-3.

Test phase	**Phase**[1]	**Aims**
Test preparation phase	COM	Temperature and pressure equilibration in the test interval
	PSR	Pressure static recovery with closed shut-in tool; create pressure conditions for the initiation of the first test, first estimate of formation pressure; recognition of temperature and pressure trends
Diagnostic phase	PW	First estimates of hydraulic conductivity, which are used to plan the following test sequence
Diagnostic / main phase	SW	Estimation of hydraulic conductivity, which is used to plan the following test sequence, especially the pumping rate and drawdown of the RW phase
	SWS	Estimation of an accurate flow model and hydraulic parameters; hydrostatic pressure for subsequent pumping phase
Main phase	RW	Defined signal with a larger radius of influence; allows a representative groundwater sample of the formation to be taken as well as the detection of boundary conditions
	RWS	Estimation of an accurate flow model and hydraulic parameters as well as boundary conditions
Optional	PW/PI	Estimation of the total test interval compressibility at the end of the test

Tab. 4-2: Preferred test sequence for formations with low to very low transmissivity

[1] For an explanation of the abbreviations see Tab. A-3.

Test phase	**Phase**[1]	**Aims**
Test preparation phase	COM	Temperature and pressure equilibration in the test interval
	PSR	Pressure static recovery with closed shut-in tool; create pressure conditions for the initiation of the first test, first estimate of formation pressure; recognition of temperature and pressure trends
Diagnostic phase	PW	First estimates of hydraulic conductivity, which are used to plan the following test sequence
Main phase Version 1	SW	Estimation of hydraulic formation parameters during a flow phase
	SWS	Estimation of an accurate flow model and hydraulic parameters during shut-in conditions
	PW/PI (optional)	Estimation of the total test interval compressibility at the end of the test
Main phase Version 2	PW/PI	Estimation of hydraulic formation parameters (as an alternative to SW/SWS)

4.2 Test equipment

The most relevant components of the field test contractor's equipment have been drawn from the associated mobilisation report and are presented below.

4.2.1 Downhole equipment

The packer system referred to as the heavy-duty double packer system (HDDP) was used for all hydraulic packer tests in open borehole sections. It consisted of a top and bottom inflatable packer (non-inflated outer diameter 114 mm for borehole STA2-1) in order to confine a test interval section of appropriate length for the intended test (Fig. 4-1). Inflow and outflow occurred through a perforated filter segment covered by a filter screen mounted on 2⅞" tubing above the bottom packer.

Four pressure transducers, mounted in a probe carrier shell above the top packer and referred to as the quadruple sub-surface probe or quadruple probe (QSSP), measured the pressures below (P1), within (interval pressure P2) and above the test interval (annulus pressure P3) as well as in the test tubing above the downhole shut-in tool (P4). In addition, the pressure in the test interval was recorded with an autonomous memory gauge at the bottom of the filter screen (P2*).

Temperatures were measured at the level of the QSSP by the temperature sensors associated with each pressure transducer (referred to as T1, T2, T3, T4, respectively) and additionally by the sensor associated with the memory gauge mentioned above (named T2*).

A hydraulically controlled non-displacement downhole shut-in tool (SIT) placed above the probe carrier shell was used to isolate the test zone from the test tubing (2⅞" EUE API CT5 L80). A progressive cavity pump (PCP) or Moyno® type pump or a pump housing with a 4" submersible pump, integrated in the test tubing, was used for production pumping tests.

Additionally, a piston pulse generator (PPG) could be mounted in the test interval. The use of a PPG allowed for reduction of the uncertainty associated with determination of the test zone compressibility on conduction of pulse tests in formations with low transmissivity.

For testing in single packer configuration (Fig. 4-2), the system was set up without the bottom packer but with a prolongation of the interval string and the filter at the bottom. Inflow and outflow occurred through a perforated filter segment covered by a filter screen mounted on a 2⅞" tubing at the bottom of the prolongation.

The quadruple flat-pack consisted of three hydraulic steel tubes of ¼" outer diameter (OD) and one electrical conductor coated in a thermoplastic protective cover. Two steel tubes were used for packer inflation and one for control of the SIT and the pressure release valve (PRV), which was only used when the packers could not be sufficiently deflated by opening the packer lines at the surface.

Certain parts of the downhole equipment are described below in more detail.

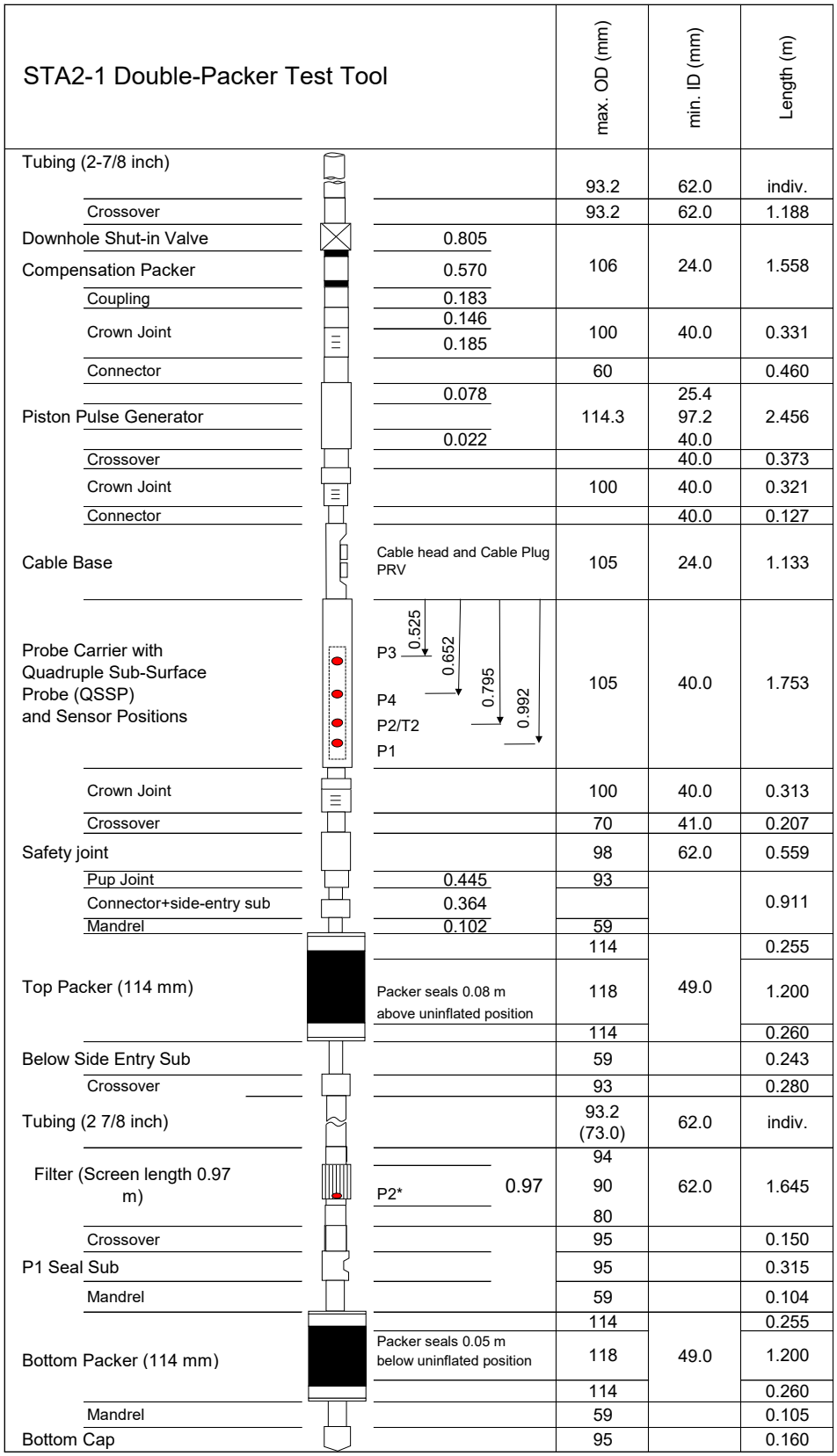

Fig. 4-1: General configuration and specifications of the HDDP in double packer configuration

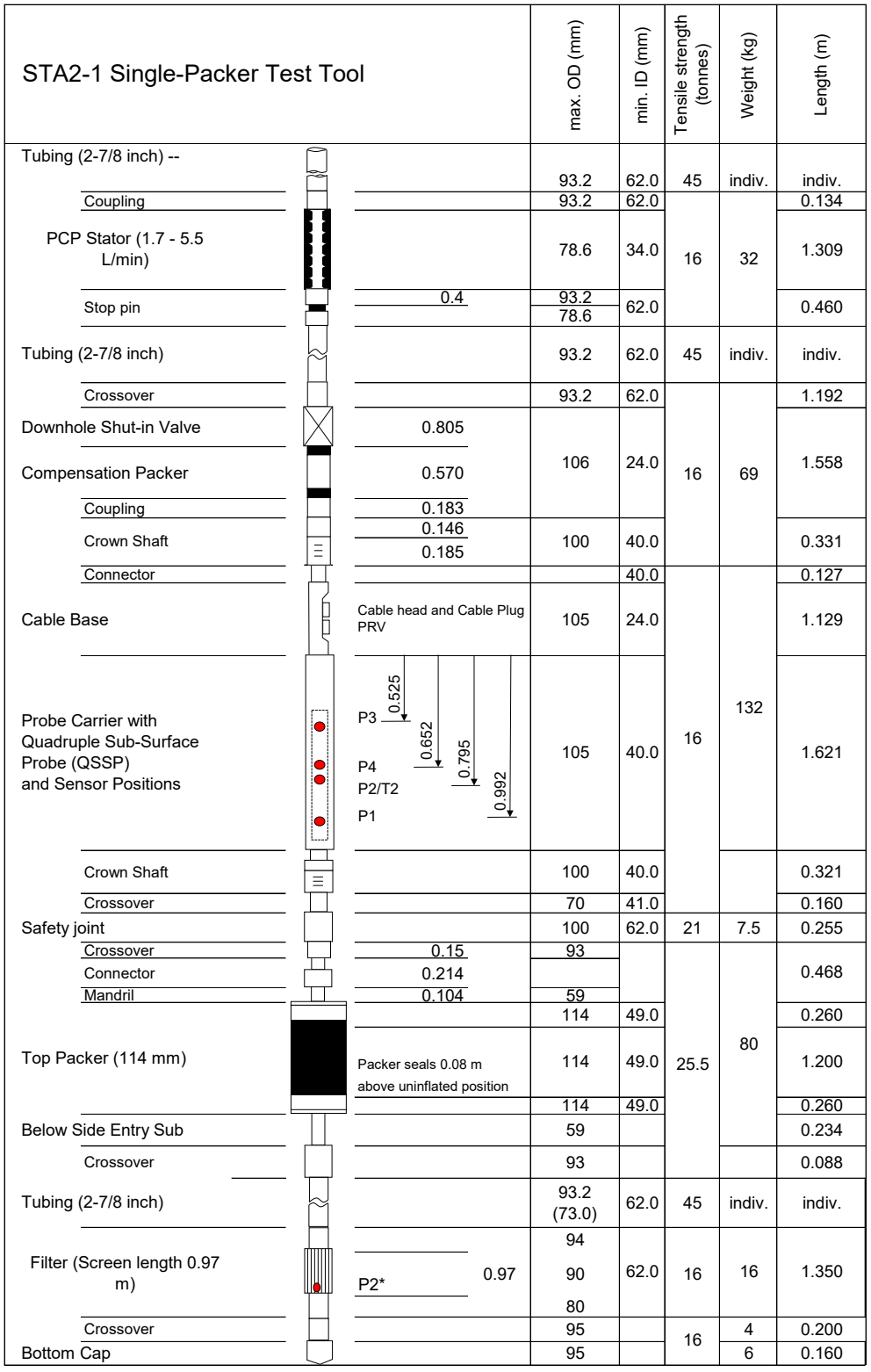

Fig. 4-2: General configuration and specifications of the HDDP in single packer configuration

4.2.1.1 Heavy-duty double packer system

The technical data of the Heavy-duty double packer system (HDDP) are provided in Tab. 4-3. A summary of the downhole equipment with the most important specifications is given in Tab. 4-4.

Tab. 4-3: Specifications for the HDDP

Tool Description	**HDDP**
Packer configuration	Double packer or single packer
Maximum installation depth	1'400 m (vertical); 1'500 m (inclined) along borehole axis
Maximum fluid pressure	20'000 kPa
Maximum differential pressure	114 mm packer system for 162 mm borehole: ~ 12'200 kPa 146 mm packer system for 216 mm borehole: ~ 8'000 kPa
Maximum downhole temperature	80 °C
Range of interval length	3 – 100 m
Probe	QSSP
Shut-in tool (SIT)	Zero-displacement valve
Control lines	4 core encapsulated flat-pack • Hydraulic line – bottom packer (PA1) • Hydraulic line – top packer (PA2) • Hydraulic line – shut-in tool (SIT) and packer pressure release valve (PRV) • ⅛" (3.175 mm) OD tubing encased single conductor cable

Tab. 4-4: Specifications for the HDDP components

Component	**Specifications**	**Minimum inner diameter ID** [mm]
Quadruple flat-pack	3 each ¼" OD × 0.035" WT 316L stainless steel welded and cold drawn annealed tubes 153'339 kPa nominal burst pressure 49'139 kPa maximum test pressure Incorporating 1 each ⅛" OD × 0.022" WT316L stainless steel 16 AWG solid CU conductor /P/N 024440) encapsulated to ¼" OD in TT200 thermoplastic Encapsulated as 33 mm × 11 mm in TT210 thermoplastic, suitable for maximum 98.9 °C brine service	
Tubing	2⅞" EUE API CT5 L80	62
Pup joints	2⅞" EUE API CT5 L80/N80	62
Shut-in tool (SIT)	Duplex 1.4462	24
Pressure release valve (PRV)	Duplex 1.4462	24
Cable base	Duplex 1.4462	
Quadruple sub-surface probe (QSSP)	Duplex 1.4462 4 pressure sensors P1, P2, P3 and P4	3 × Ø19
Coarse thread safety joint	$3^{21}/_{32}$" OD, with $2^{7}/_{16}$" bore with 2⅞" EUE box × pin connections	62
Packers for large borehole diameter	IPI 5¾" (146 mm), steel wire reinforced, duplex, natural rubber Packer 1 Packer 2	 49 49
Packers for normal borehole diameter	IPI 4½" (114 mm), steel wire reinforced, duplex, natural rubber Packer 1 Packer 2	 49 49
Filter	HP well screen: sand free filter screen mounted on 2⅞" tubing L80 Length: 0.50 m Length: 1.00 m	 73 73

4.2.1.2 Packers

Two types of packers were available for use, a 114 mm packer for 162 mm diameter boreholes and a 146 mm packer for 216 mm diameter boreholes (Tab. 4-5). The packers were individually inflated with water through the packer inflation line. The inflation line was integrated in the quadruple flat-pack using a booster pump and anti-freeze was added to the water. Both packer pressure lines were connected to the packer control board at the winch and equipped with pressure sensors (pressure range 0 – 30'000 kPa) for packer pressure monitoring. The packer pressure sensors were connected to the data acquisition system (DAS) for continuous recording. To keep packer pressures constant, the packers were connected to a pressure-maintenance system (see Section 4.2.2.2).

Tab. 4-5: Specifications for the HDDP packers

Manufacturer	Inflatable Packers International, Perth, Australia	
Packer types	IPI 4½" (114 mm)	IPI 5¾" (146 mm)
Material and type	Duplex, natural rubber, sliding end	Duplex, natural rubber, sliding end
Reinforcement type	Steel wire reinforced	Steel wire reinforced
Borehole diameter	162 mm	216 mm
Packer diameters	125 – 230 mm (pressure dependent)	162 – 280 mm (pressure dependent)
Outer diameter, not inflated	114 mm max.	146 mm max.
Inner diameter	49 mm min.	49 mm min.
Overall length: Bottom packer Top packer	 1.93 m 2.08 m	 1.92 m 1.92 m
Rubber sleeve length	1.20 m	1.20 m
Thread connections	2⅞" EUE pin × 2⅞" EUE box	2⅞" EUE pin × 2⅞" EUE box
Max. working temperature for a period > 100 h	+80 °C	+80 °C
Packer inflation lines	Quadruple flat-pack, see Tab. 4-4	Quadruple flat-pack, see Tab. 4-4
Inflation method	Surface controlled	Surface controlled
Inflation fluid	Water and anti-freeze (if necessary)	Water and anti-freeze (if necessary)

4.2.1.3 Downhole sensors in the quadruple sub-surface probe

Four Keller PA-27XW transducers (for transducer types and specifications see Tab. 4-6) were used to monitor fluid pressures in the interval below the bottom packer (P1), within the testing interval (P2), in the annulus between the tubing and borehole wall above the top packer (P3) and in the test string (P4) above the downhole SIT. These four transducers were mounted in the QSSP probe, which was integrated in the probe carrier (see Fig. 4-1). The pressure sensors measured absolute pressure and corrected it to atmospheric pressure; the sensors showed ± 8 kPa at atmospheric pressure conditions on-site.

Each pressure transducer had an associated temperature sensor (referred to as T1, T2, T3 and T4) for full thermal compensation of the pressure measurement (Tab. 4-6). The temperature sensor was mounted inside the pressure transducer housing. Because the temperature measurements were taken at the positions of the pressure transducers, they may not represent the effective temperature of the test interval fluid.

Tab. 4-6: Specifications for the pressure transmitters mounted in the QSSP

[1] FS = full scale

Pressure transducer type	Keller PA-27XW, custom-made
Manufacturer	Keller, Winterthur, Switzerland
Year of commissioning	2018
Pressure range (full scale)	0 – 20'000 kPa (absolute)
Accuracy	-0.004…0.005% FS[1]
Resolution	< 0.0007% FS
Minimum recording rate	1 Hz
Temperature range (FS)	-10 °C to 80 °C
Accuracy (temperature)	1 °C
Resolution (temperature)	0.01 °C
Output signal	RS485 (digital)

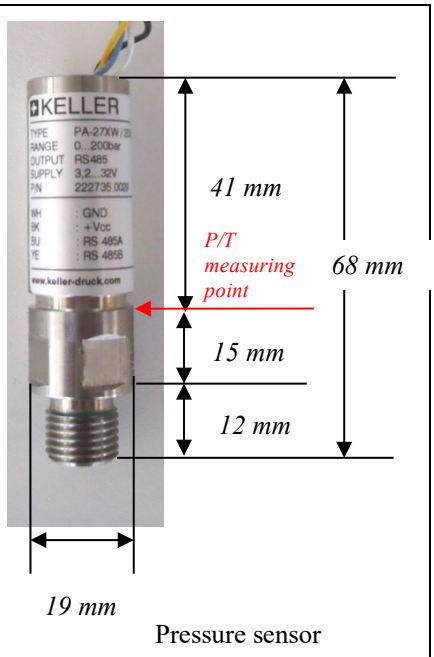

Pressure sensor

4.2.1.4 Autonomous data logger in test interval

Pressures and temperatures were recorded as redundant measurements in the interval at the lower end of the filter screen (referred to as P2* and T2*, respectively) with an autonomous data logger of the type DataCan Memory Pressure Gauges. The specifications are given in Tab. 4-7. The recorded pressure measurement is an absolute measurement.

Tab. 4-7: Specifications for the data logger

[1] FS = full scale

Data logger type	DataCan Memory Pressure Gauge 1.25" Welded Piezo III
Manufacturer	Data Can, Red Deer, Canada
Pressure range (FS[1])	0 – 20'684 kPa (absolute)
Pressure accuracy	0.03% FS
Resolution	0.0003% FS
Temperature range	0 – 150 °C
Temperature accuracy	0.5 °C
Resolution	0.005 °C
Memory capacity	1'000'000 datasets
Minimum recording rate	10 Hz
Year of commissioning	2018

4.2.1.5 Zero-displacement shut-in tool

The downhole SIT controlled the fluid connection between the interior of the test tubing and the test interval. The SIT is a zero-displacement valve that is hydraulically operated via a hydraulic line integrated in the quadruple flat-pack using a booster pump. An axially moveable valve piston opens and closes the valve. The valve piston is moved via the hydraulic (closure) line by applying pressure to close the valve. Releasing the pressure with a pre-stressed spring resets the valve piston and opens the valve (pressure-free opening).

With a pressure compensation element, the pressure at interval depth (annulus pressure) is used to support the spring and to keep the opening/closing pressure constant for the entire borehole depth. The spring force is high enough to ensure a proper functioning of the valve also at low groundwater levels. The specifications are given in Tab. 4-8.

Tab. 4-8: Specifications for the zero-displacement shut-in tool

Zero displacement shut-in tool (SIT)	Manufactured by Solexperts
Maximum water flow rate	Below 40 l/min without friction loss, max. 350 l/min
Pressure loss caused by SIT at a flow rate of 1 l/min and 10 l/min	± 0 kPa
Closing pressure	9'000 – 10'500 kPa

4.2.1.6 Test tubing

API Spec. 5 CT-05 2⅞" tubing was used as test rods. The detailed specifications of the test tubing are summarised in Tab. 4-9.

Tab. 4-9: Specifications for the test tubing

Test tubing type	Seamless steel tubing and pup joints: 2⅞" 6.5 ppf L80 B*P EUE R2 API 5CT
Manufacturer	Normec, Celle, Germany
Steel grade	L80
Inner diameter	62.00 mm
Outer diameter	73.02 mm
Coupling outer diameter	93.20 mm
Thread	API 2⅞" EUE
Weight per meter	9.68 kg
Volume per meter	3.02 l
Individual tubing length	Range 2, ~ 9.5 m
Number of individual tubing lengths	162
Total length of test tubing	Approx. 1'500 m
Lengths of pup joints	Length, quantity 0.5 m, 2 1.0 m, 2 2.0 m, 2 3.0 m, 4 4.5 m, 4

4.2.1.7 Slim tubing

The rate of pressure increase during the flow phase of a slug test depends on the formation transmissivity and the diameter of the test tubing, which mainly defines the wellbore storage of the test system during the slug. To improve the resolution of the pressure change, a slim tubing was used to reduce the diameter of the test tubing for slug tests in formations with low transmissivity. However, the use of the slim tubing in formations with low transmissivity reduces the dominance of the wellbore storage term that is defined by the diameter. In this case, the wellbore storage term that is determined by the compressibility of the test fluid as well as the equipment (defined by determining the test zone compressibility during a shut-in phase) must be taken into account (Black et al. 1987).

The slim tubing consists of a stiff tube, which is installed into the test tubing. A packer at the bottom of the slim tubing with an outer diameter of 56 mm sealed the annulus between the 2⅞" tubing and the slim tubing. The water level in the slim tubing was measured with the P4 sensor from the QSSP. The technical specifications of the slim tubing are summarised in Tab. 4-10.

After lowering the water level in the 2⅞" test tubing for a slug withdrawal test to the specified depth, the slim tubing was installed in the tubing below the water level. Afterwards, the slim tubing packer was inflated, and the test was started by opening the SIT valve. The water level only increased in the tubing. The use of a stiff tube ensured a constant inner diameter independent of the pressure (fluid level). It should be noted, however, that in the numerical analysis the effective diameter of the slim tubing must be used when using a simulator based on Pickens et al. (1987).

Tab. 4-10: Specifications for the slim tubing

[1] FS = full scale

Types	Polyethylene tube	Stainless steel tube	Legris Polyamide Calibre tube
Inner diameter	12 mm	6 mm	4 mm
Outer diameter	16 mm	8 mm	6 mm
Length	300 m	300 m	700 m
Packer specifications	Diameter 56 mm, sealing length 1'000 mm, working pressure 1 – 13.5 MPa		
Packer pressure line	Polyamide OD: 6 mm; ID: 3 mm		
Packer pressure sensor	Keller PA-23SY, 0 – 5'000 kPa, accuracy 0.25% FS[1]		
Installation procedure	Wireline system of the drill rig		

4.2.1.8 Submersible pumps

Frequency driven 3" and 4" Grundfos submersible pumps can be used for pumping tests and during open-hole pumping, e.g. for fluid logging. The specifications are included in Tab. 4-11. The flow rate can be arbitrarily adjusted because of the frequency control of the pump.

Tab. 4-11: Specifications for the submersible pumps

Submersible pump types	4" down-hole pump	3" down-hole pump
Manufacturer	Grundfos, Fällanden, Schweiz	
Type	SP14-27E	SQE1-110
Regulation	Frequency-controlled	Frequency-controlled
Dimensions	101 × 3'040 mm	74 × 852 mm
Pumping rate at 150 m	100 l/min	10 l/min
Range of pumping rates	Max. 300 l/min	Max. 28 l/min
Maximum installation depth	160 m	160 m
Maximum temperature	40 °C	35 °C
Weight	57 kg (pump) 31 kg (motor)	6 kg
Pump housing	Yes	No
Specifications of pump housing	Length: 4.22 m OD max: 180 mm Weight: 130.3 kg	
Purpose	Pumping tests	Pumping tests, fluid logging

4.2.1.9 Progressive cavity pump

For constant rate withdrawal tests (pumping tests) a progressive cavity pump (PCP), a so-called Moyno® type pump, was used. The PCP consisted of a helical rotor and a twin helix in a rubber stator. The stator was integrated into the test tubing string and allowed for pumping, if necessary, but did not preclude any other test methods. For pumping, a suitable rotor had to be installed by means of the so-called sucker rods until the rotor had fully penetrated the stator. The pump specifications are listed in Tab. 4-12.

Tab. 4-12: Specifications for the PCP

Type	Progressive cavity pump (PCP)
Manufacturer	Netzsch
Dimensions	Drive head: L × W × H: 1'375 × 767 × 1'263 mm
Pumping rates	1.7 – 60 l/min Pumping rates of < 1.7 l/min can be reached by closing the valve installed in-line at the wellhead
Maximum installation depth	300 m
Temperature	10 °C to 70 °C
Sucker rods, type	¾" × 7.62 m
Sucker rods, quantity	45
Total length	Approx. 300 m
Available stators	1 for pump rates 10.4 – 60 l/min, Temp. 10 °C to 70 °C 1 for pump rates 1.7 – 5.5 l/min, Temp. 10 °C to 70 °C
Available rotors	3 for pump rates 10.4 – 60 l/min, Temp. 10 °C to 30 °C, 30 °C to 50 °C, 50 °C to 70 °C 3 for pump rates 1.7 – 5.5 l/min, Temp. 10 °C to 30 °C, 30 °C to 50 °C, 50 °C to 70 °C

4.2.1.10 Piston pulse generator

The piston pulse generator (PPG) is an optional downhole tool. It brings a unique and proven technology for conducting pulse tests to the more traditional low-permeability hydraulic testing realm. In an effort to reduce the uncertainty associated with determining the test zone compressibility, a hydraulic piston (i.e. the PPG) of known volume is incorporated into the hydraulic test tool (HTT). This PPG resides within the test zone but not conventionally in between the packers. The PPG is contained within a housing that is located above the top packer and below the downhole SIT.

When deployed in a borehole, the piston is put into the appropriate position (fully extended or fully retracted), the packers are inflated, the SIT is closed, thereby isolating the test zone from the rest of the borehole, and the test zone is allowed to equilibrate for a period of time.

When it has been decided to initiate a pulse with the PPG, fluid from the pressurised fluid reservoir is routed to the appropriate hydraulic line (piston extend or piston retract) through the hydraulic control panel, thereby changing the position of the piston and changing the test zone volume by a known amount in less than two minutes. The resulting test zone pressure change is measured and can be used for the calculation of the interval storage / test zone compressibility. The specifications are listed in Tab. 4-13.

It should be noted that only one piston can be deployed at a time and the piston must be either fully extended or fully retracted. Therefore, only displacement volumes of 50 ml, 250 ml or 500 ml can be achieved once the HTT is deployed.

Tab. 4-13: Specifications for the piston pulse generator

Piston pulse generator type	INTERA-PPG-1
Manufacturer	HydroResolutions
Dimensions of housing	OD: 0.1143 m Length: max. 2.54 m
Piston displacement	50, 250, or 500 ml
Weight	Max. 79 kg
Material	Steel

4.2.2 Surface equipment

The surface equipment consisted of the following equipment:

- Winch for quadruple flat-pack cable
- Flow control system
- Pressure-maintenance system
- Injection and pumping head
- PCP drive head and control unit
- Data acquisition system

Most of the surface equipment parts were installed in a mobile measuring trailer.

4.2.2.1 Flow board

For the control and measuring of pump (and injection) rates, a flow board with two flowmeters of type Yokogawa AXF were available. The flowmeters covered a flow rate range between 0.01 and 100 l/min (Tab. 4-14). The schematic layout of the flow control unit is displayed in Fig. 4-3.

Tab. 4-14: Specifications for the flowmeters

FS = full scale

	Measuring range and accuracy			
	Lower limit		**Upper limit**	
	[l/min]	[% FS]	[l/min]	[% FS]
AXF 010	0.1	1	11.78	0.35
AXF 025	1.0	1	100	0.35

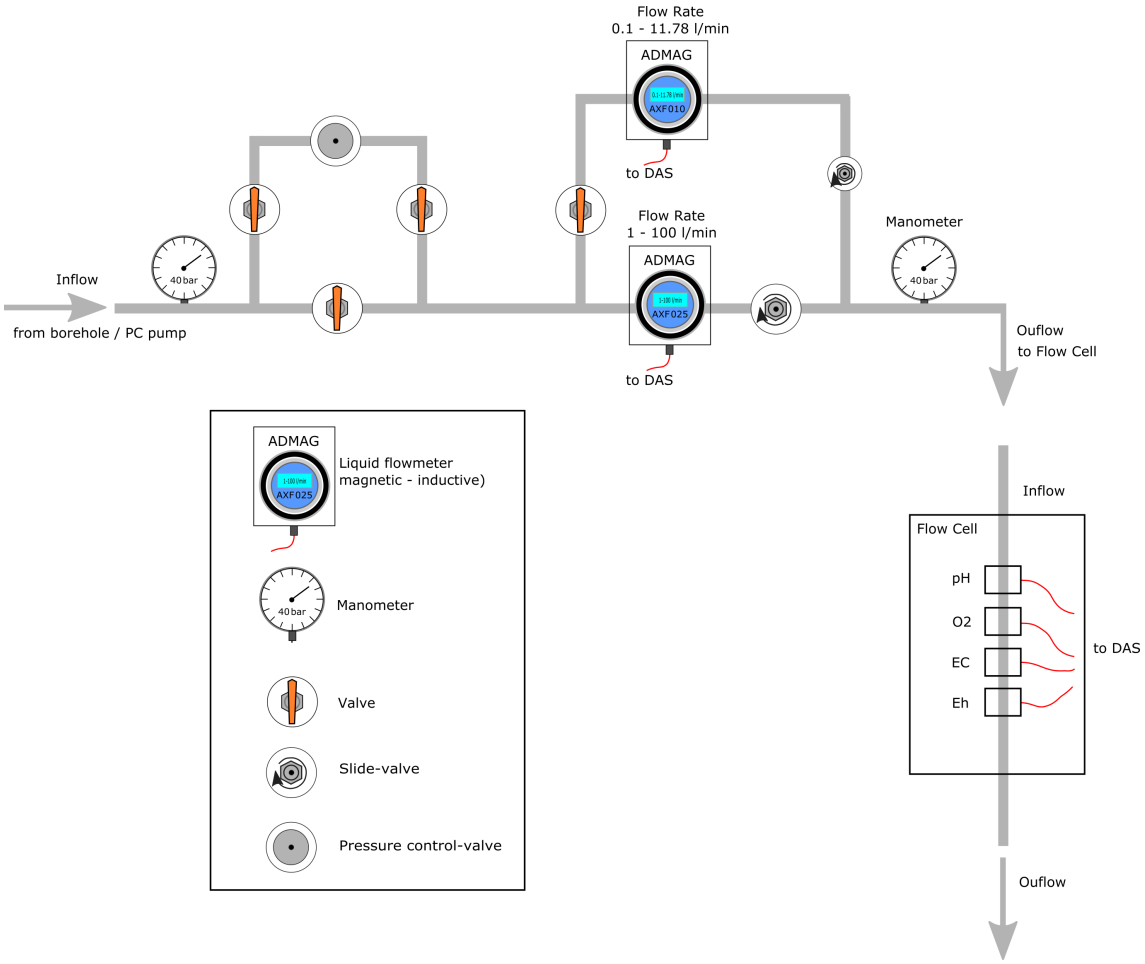

Fig. 4-3: Schematic layout of the flow control unit

4.2.2.2 Packer pressure-maintenance system

The packer pressure-maintenance system had four principal components: a pressurised nitrogen source (bottle) with pressure regulator, an Alicat pressure controller, a high-pressure hydraulic accumulator containing pressurised nitrogen over packer-inflation fluid, and a Mettler digital scale to monitor changes in the fluid volume in the reservoir. The Alicat flow controller was connected to the nitrogen bottle and to the reservoir. The desired packer-inflation pressure ("set" point) was entered into the controller, which had its own pressure sensor, and the controller then added nitrogen to the reservoir if the pressure dropped below the set point, or vented nitrogen from the reservoir if the pressure roses above the set point. The digital scale could be read manually in addition to being connected to the DAS. The packer pressure-maintenance system was installed in the mobile trailer. Fig. 4-4 illustrates a schematic layout of the packer pressure-maintenance system. Additionally, two transducers (type Keller PA-23SY, 30'000 kPa) mounted on the surface inflation control panel were used to monitor the packer inflation pressures.

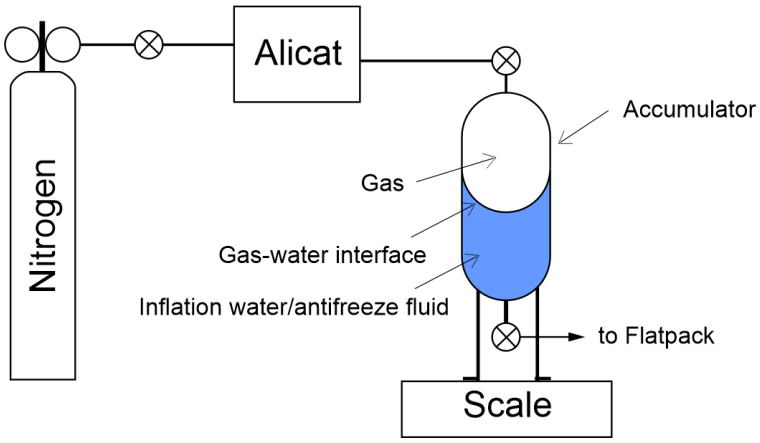

Fig. 4-4: Schematic layout of the packer pressure-maintenance system

4.2.2.3 Additionally recorded measurements at surface

A single pressure transducer (type Keller PAA-33X, 80 – 120 kPa absolute) was mounted outside the monitoring trailer and used to monitor barometric pressure and air temperature (Tab. 4-15).

During pumping tests, the physico-chemical parameters (e.g. pH, EC, Eh, temperature and oxygen concentration) of the extracted fluid were recorded. The specifications of the physico-chemical sensors are given in Tab. 4-16. The sensors were calibrated on-site before each use.

Tab. 4-15: Specifications for the atmospheric pressure sensor
FS = full scale

Temperature sensor type	Keller PAA-33X
Manufacturer	Keller, Winterthur, Switzerland
Pressure range	80 – 120 kPa
Accuracy	0.02% FS
Resolution	0.002% FS

Tab. 4-16: Specifications for the physico-chemical sensors

Sensor type	**EC**	**pH**	**Eh**	**O_2**	**Temperature**
Manufacturer	Xylem analytics, Weilheim, Germany				IST AG
Model	WTW TetraCon 325	WTW SensoLyt DW	WTW SensoLyt PtA/Pt	WTW FDO 700 IQ	Pt 1000
Range	1 µS/cm – 2 S/cm	0 – 14	± 2'000 mV	0 – 20 mg/l	-50 – 650 °C
Accuracy	n/a	n/a	n/a	n/a	± 0.15 °C at 0 °C ± 0.35 °C at 100 °C
Resolution	n/a	n/a	n/a	0.01 mg/l (0.01 ppm)	1.5×10^{-3} °C
Temperature range	0 °C – 100 °C	0 °C – 60 °C	0 °C – 60 °C	-5 °C – 50 °C	-50 °C – 650 °C

4.2.2.4 Data acquisition system

The data acquisition system (DAS) consisted of a Solexperts interface for digital and analogue sensors, an industrial PC, a screen and a keyboard. Data acquisition was performed through the Solexperts GeoMonitor II (GMII) software. The downhole pressures (P1, P2, P3, P4) and temperature measurements (T1, T2, T3, T4) were recorded in real time through the quadruple flat-pack cable assembly. Surface measurements like flowmeter rates, packer pressures, atmospheric pressure and temperature and the physico-chemical parameters were recorded with the same scan rate as the downhole pressures from the QSSP.

The scan rates could be adjusted as required between 1 s (using a reduced number of sensors) and > 30 s.

The measurements were written to a data file on the PC hard drive in real-time with a continuous data collection and database model. From the PC hard drive, the data were transferred to another network PC continuously for 'online' analysis and data back-up. An uninterruptible power supply was utilised to protect the system from short power interruptions.

4.2.3 GTPT equipment

The test equipment for the GTPT was designed in a modular way to be used together with the HDDP system (Section 4.2.1). Additional equipment parts were provided by Nagra. The individual parts were assembled on-site, together with the HDDP system of the field test contractor.

The additional system parts for the downhole equipment were the following:

- X-over 2⅞" to 4½"
- Second shut-in tool (SIT1) with crown shaft below the bottom packer to control the displacement of the interval fluid to the exchange chamber
- 4½" exchange chamber of variable length (API 4½" tubing NU; N80, OD 114.3 mm, ID 100.5 mm, 12.6 lbs/ft = 18.75 kg/m; coupling OD: 132 mm) below the HDDP system / lower SIT1 for the collection of exchanged interval fluid, e.g., drilling mud, sodium hydroxide (NaOH) solution
- Bottom cap / bull nose 4½"
- Dip tube (OD 21.3 mm, wall thickness 2.6 mm) inside the exchange chamber, stainless steel with threads and couplings of variable length, with swivel connection and installation tools
- 3 additional ¼" stainless steel lines (910 m, OD 6.35 mm, inner diameter 4.55 mm) on separate coils (SIT1 line, backflow line from exchange chamber, injection line into the interval equipped with a check valve) besides the standard quadruple flat-pack
- 2 pressure sensors Keller PA-23SY to measure the pressure at the injection and backflow lines
- 2 × 146 mm inflatable packers with a double mandrel including five through-going pieces of ¼" stainless steel lines and fittings

The additional surface equipment encompassed the following components:

- Standard hydrotest equipment
- 1 gas flow controller 0 – 5 ln/min (injection line to interval) (ln = litre normal)
- 2 gas flowmeters 0 – 150 ln/min (one connected to back flow line from exchange chamber and one to injection line for NaOH displacement)
- A flow control board for one gas flow controller and two gas flowmeters with valves and manometers
- Closed tank for NaOH solution, for injection via the (gas-) injection line
- An additional high-pressure injection pump instead of a booster to obtain a higher injection rate and to save time

The flow controller and flowmeters, as well as all other sensors of the GTPT system, were connected to the DAS.

The most relevant system parts are described in detail in the following sections.

A schematic overview of the GTPT system is shown in Fig. 4-5. The four diagrams show the planned test phases of the GTPT:

1. Repeated pressurisation of the (empty) exchange chamber with nitrogen (N_2) to avoid any damage during installation
2. Injection of NaOH solution through the injection line to push the interval fluid to the exchange chamber and simultaneous extraction of N_2 from the exchange chamber to the surface via the extraction line, SIT1 open
3. Injection of N_2 through the injection line to push the NaOH solution from the interval to the exchange chamber and extraction of N_2 from the exchange chamber to the surface via the extraction line, SIT1 open
4. Start of GTPT: Relatively slow injection of N_2 at constant rate into the interval, SIT1 and SIT2[6] closed

[6] In this section, the usual SIT from the HDDP, which controlled the fluid connection between the interior of the test rods and the test interval, is labelled SIT2; in the test string, it was positioned above SIT1, which controlled the fluid connection between the exchange chamber and the test interval during a GTPT.

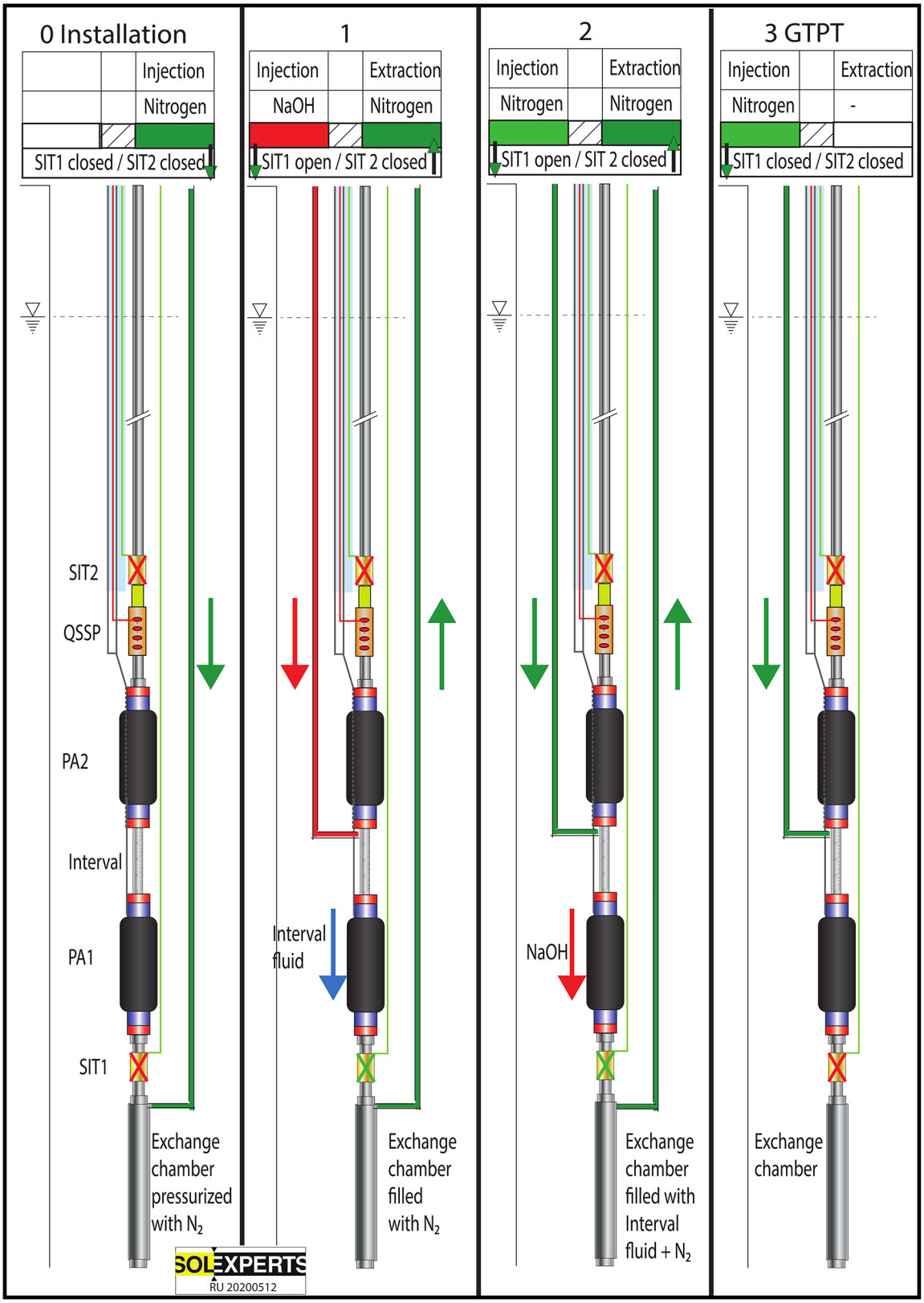

Fig. 4-5: Schematic layout of the modified HDDP system with the four major phases of the GTPT

4.2.3.1 Packers for the GTPT

The system comprised two packers with a diameter of 146 mm and a double mandrel that included five pieces of ¼" stainless steel lines and corresponding fittings.

A detailed description of the packers and the use of the ¼" stainless steel lines is given in Tab. 4-17. Before installation, the packers with the corresponding lines were saturated with water and anti-freeze.

Tab. 4-17: Specifications for the 146 mm packers for the GTPT

Manufacturer	Inflatable Packers International (IPI), Perth, Australia
Packer types	IPI 5¾" (146 mm)
Material and type	Duplex, 316 ss, Nitrile Butadiene Rubber (NBR), sliding end
Mandrel	Double mandrel with 5 through-going pieces of ¼" stainless steel lines
Use of ¼" stainless steel lines	Packer 1 (lower packer): 1. Line to the QSSP sensor P1 2. SIT1 line 3. Not used 4. Backflow line 5. Not used Packer 2 (upper packer) 1. Inflation line packer 1 2. SIT1 line 3. Injection line 4. Backflow line 5. Not used Note: The final allocation of the line ports was defined on-site
Reinforcement type	Steel wire reinforced
Borehole diameter	162 / 216 mm
Packer diameters	162 – 280 mm (pressure dependent)
Outer diameter, not inflated	146 mm max.
Inner diameter	43.7 mm min.
Overall length: Bottom packer Top packer	 2.195 m 2.195 m
Weight	95 kg each
Rubber sleeve length	1.20 m
Thread connections	2⅞" EUE pin × 2⅞" EUE box
Packer inflation lines	Quadruple flat-pack
Inflation method	Surface controlled
Inflation fluid	Water and anti-freeze

4.2.3.2 Stainless steel lines for the GTPT

Three additional ¼" stainless steel lines (OD 6.35 mm, ID 4.55 mm), each with a length of 910 m, were installed together with the downhole equipment and used as follows:

- Activation and de-activation of the SIT1 – SIT1 line; marked with white tape
- Gas/fluid injection into the interval – injection line; marked with green tape
- Backflow line from the exchange chamber – backflow line; marked with red tape.

The lines were connected to the corresponding stainless steel feed-through, through the top and, if required, through the bottom packer double mandrel. At the surface, the lines were coiled up on the corresponding coils. Each stainless steel line was connected to a valve and a 250 bar manometer. Two coils (injection and backflow lines) were additionally equipped with pressure sensors of the type Keller PA-23SY, 0 – 300 bar.

The outlet port for the injection line at the lower end of the top packer was equipped with a check valve which enabled flow into the test interval but no backflow from the test interval into the injection line. The check valve opened at 4 bar injection pressure.

4.2.3.3 Zero-displacement shut-in tool for GTPT

The SIT1 used for the STA2-1 GTPT test was similar to the SIT2 (the HDDP SIT used for hydraulic packer testing) which controlled the fluid connection between the interior of the test rods and the test interval. The SIT1 is a zero-displacement valve which controlled the fluid connection between the exchange chamber and the test interval. The SIT1 was hydraulically operated over a ¼" stainless steel line using the booster pump. The opening and closing were performed via an axially moveable valve piston. The valve piston was moved via the hydraulic (closure) line by application of pressure and the valve was closed. The valve piston was reset at pressure release through a pre-stressed spring, and the valve was opened (pressure-free opening).

With a pressure compensation element, the pressure at interval depth (annulus pressure) was used to support the spring and to keep the opening/closing pressure constant for the entire borehole depth. The spring force was high enough to ensure proper functioning of the valve, even at deep groundwater levels. The specifications are given in Tab. 4-18.

Tab. 4-18: Specifications for the zero-displacement shut-in tool (SIT1) for the GTPT

Manufacturer	Solexperts AG
Maximum water flow rate	Below 40 l/min without friction loss, max. 350 l/min
Pressure loss caused by SIT at a flow rate of 1 to 10 l/min	± 0 kPa
Closing pressure	9'000 – 10'500 kPa

4.2.3.4 Flow control board for GTPT

For the control and measuring of gas injection and extraction rates, the high-pressure gas flow controller and flowmeters were mounted on a flow control board. The flow controller for the control of the injection flow rate had a measuring range of 0.1 – 5 ln/min. The two flowmeters for the flow rate measurements during the displacement of NaOH with gas and during backflow had a measuring range of 3 – 150 ln/min (Tab. 4-19). A schematic drawing of the flow board is included in Fig. 4-6.

In addition to the flow controller and flowmeters, the flow board was equipped with two manometers for 100 bar, two for 160 bar and one for 250 bar maximum pressure. Two needle valves were used to control the flow rates at the injection side and at the backflow side.

Tab. 4-19: Specifications for the gas flow controller / meters for the GTPT

	Gas flow controller (Flow_G_INJ)	**Gas flowmeter (Flow_G_DIS)**	**Gas flowmeter (Flow_G_BCK)**
Manufacturer	Bronkhorst	Bronkhorst	Bronkhorst
Type	IN-FLOW	IN-FLOW	IN-FLOW
Measuring range	0.1 – 5 ln/min	3 – 150 ln/min	3 – 150 ln/min
Accuracy (incl. linearity)	± 0.5% Rd (reading), ± 0.1% FS	± 0.5% Rd (reading), ± 0.1% FS	± 0.5% Rd (reading), ± 0.1% FS
Inlet pressure	50 – 200 bar (calibrated for 125 bar)	70 – 200 bar (calibrated for 135 bar)	50 – 100 bar (calibrated for 75 bar)
Output pressure	1 – 150 bar	–	–
Minimum ΔP	2 bar	–	–
Medium	N_2	N_2	N_2

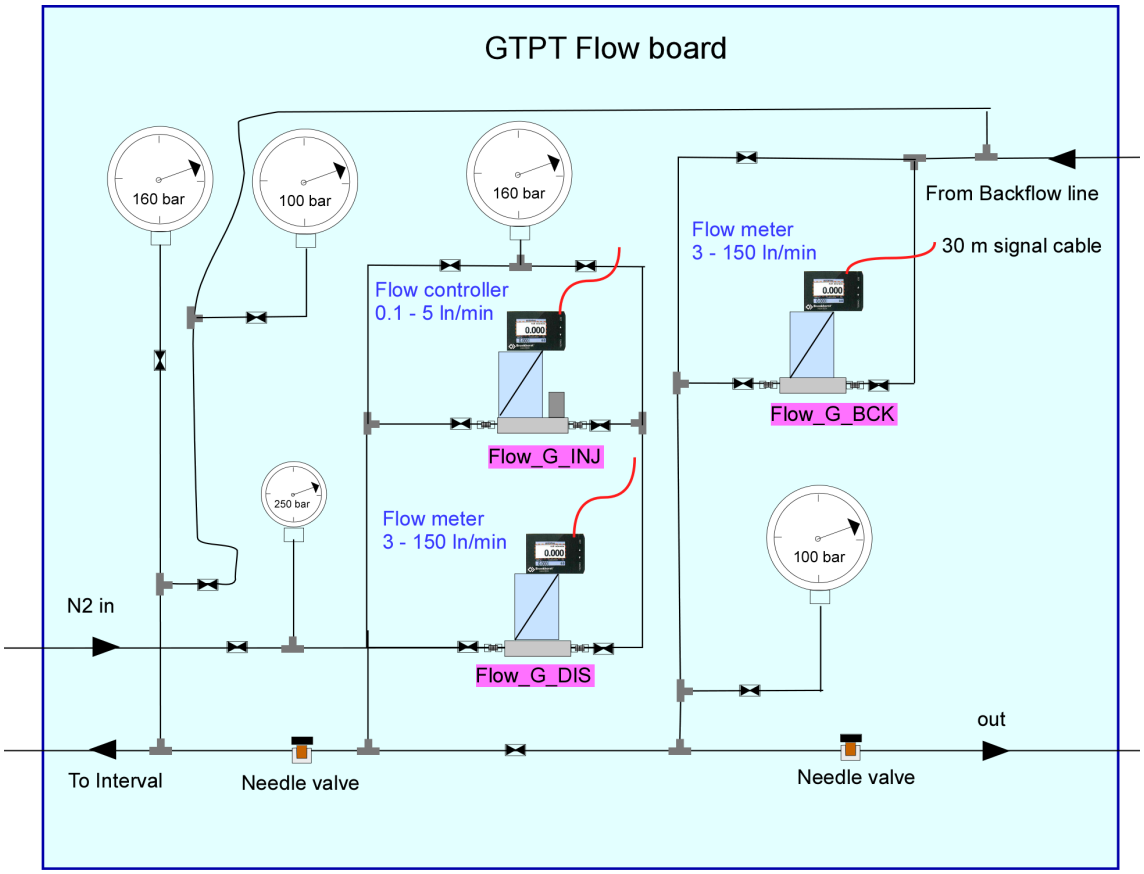

Fig. 4-6: Schematic layout of the flow control unit for the GTPT

4.3 Test analyses

4.3.1 Workflow

For STA2-1, the general on-site analysis approach involved mainly numerical techniques considering the entire borehole pressure history. Analytical solutions were used mainly to present the results and to conduct more detailed consistency checks between measurements and simulations. This ensured a comprehensive evaluation of the recorded data. The numerical solutions were assessed further with a perturbation analysis. Prior to commencement of the hydraulic tests, the representation of the borehole history period and the starting input parameters were defined.

The on-site analysis workflow supported the test design to achieve the quality objectives defined by Nagra:

- Identification of the most appropriate flow model, e.g. by log-log diagnostic plots (Bourdet et al. 1989)
- Numerical simulation of individual test sequences in Cartesian coordinates
- Confirmation of the applied flow model suitability via diagnostic representations of the recorded and simulated pressure data
- Assessment of the suitability of the numerical solution and associated uncertainties through limited perturbation analysis

- Numerical simulation of the entire test sequence in Cartesian coordinates using the optimised parameter set obtained from individual phase analysis
- Confirmation of the consistency of the model applied to the entire dataset
- Consistency check of the test analysis and the estimated parameters by the technical supervisor

The results were used to continuously optimise the test design to achieve the quality objectives within the dedicated time of testing. A general flowchart of the analysis work is provided in Fig. 4-7.

The test data were analysed numerically using the nSIGHTS software (Geofirma Engineering Ltd. & INTERA 2011). For slug and pulse tests, the consistency checks typically involved one or more of the semi-log and log-log plots developed by Ramey et al. (1975). Recovery tests were presented according to Horner (1951). A summary of the applied test analysis methods is presented in Tab. 4-20.

Tab. 4-20: Summary of analytical analysis methods

Test phase	**Analysis method**	**Reference**
Pulse test	Semi-log and log-log representations of the transient pressure change and derivative versus time	Ramey et al. (1975)
Slug test (flow phase SW)	Semi-log and log-log representations of the transient pressure change and derivative versus time	Ramey et al. (1975)
Slug test recovery (pressure recovery after slug flow phase, SWS)	Semi-log and log-log representations of the transient pressure change and derivative versus time	Bourdet et al. (1989)
Pressure recovery after constant rate tests	Log-log representations of the transient pressure change and derivative versus 'superposition time'	Bourdet et al. (1989)
	Diagnostics: Log-log stabilisation of the derivative	Horne (1995)
	Diagnostics: Semi-log representations of the transient pressure change	Horner (1951)

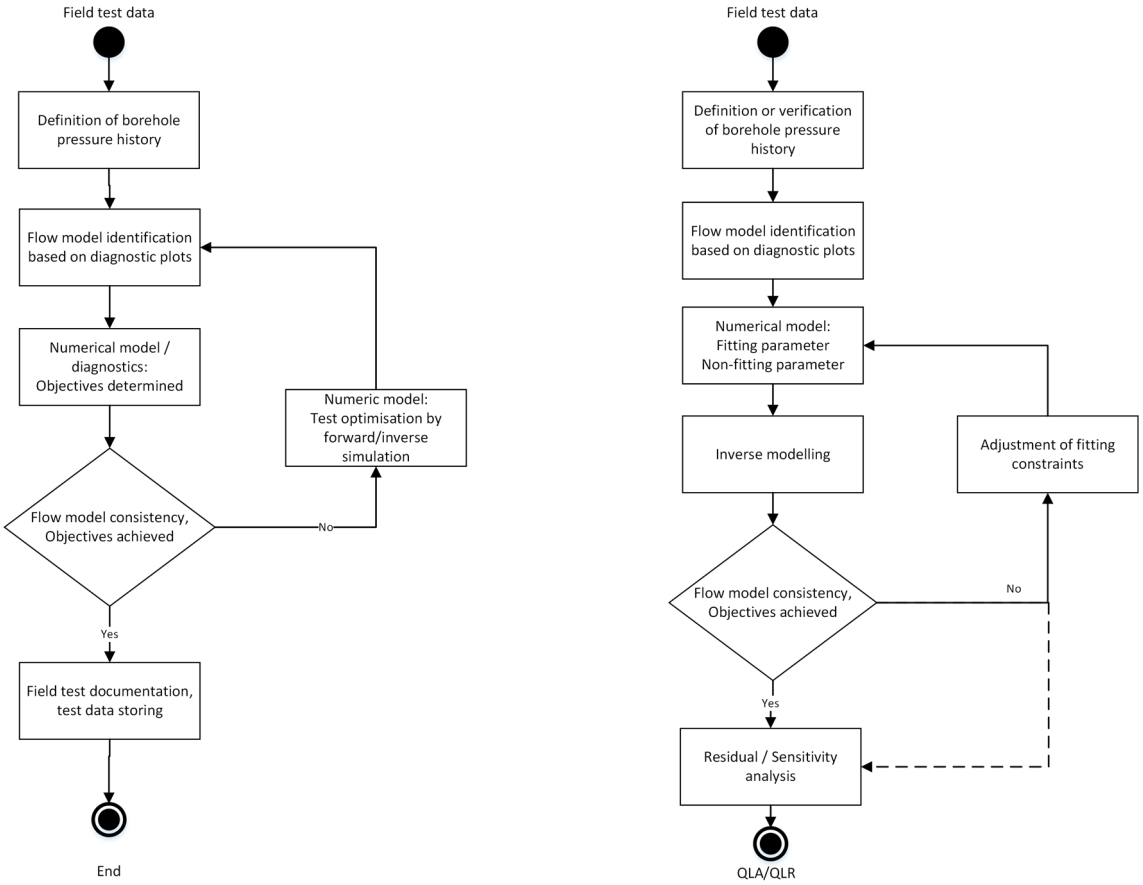

Fig. 4-7: Flowcharts for the on-site hydraulic packer test analysis (left) and Quick Look Analysis (QLA) (right)

The Detailed Analysis (DA) was performed off-site after the test was completed and was based on the Quick Look analysis (QLA) reported in the Quick Look Report (QLR). The QLR was reviewed as part of the Quality Control (QC) programme. During this task, open questions and potential ambiguities of the analysis were defined. Based on the outcome of the QC review, further specifications and, if necessary, further analyses were implemented. Fig. 4-8 provides the general flowchart of the DA, which includes perturbation and non-fitting parameter analyses, to obtain the most reasonable parameter results and ranges of uncertainty. The work is summarised in a Detailed Report (DR), with the QLR included as an Appendix.

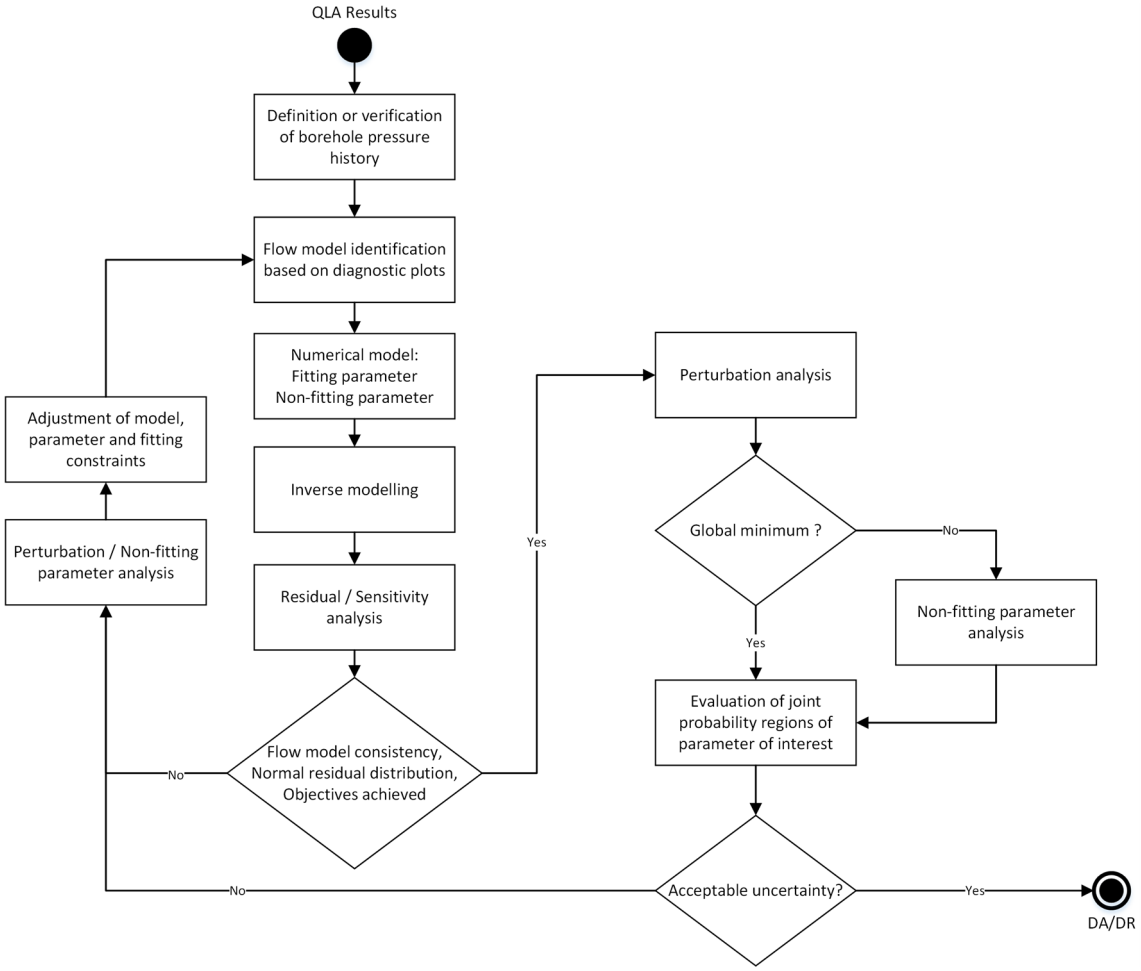

Fig. 4-8: Flowchart for the off-site Detailed Analysis (DA) of a hydraulic packer test

4.3.2 Special effects

The time series measured during hydraulic packer tests were the pressure and temperature inside the test interval. Their development over time was analysed to estimate the hydraulic properties of the formation surrounding the test interval. Various factors affected the recorded time series. All hydraulic tests are affected by factors beyond the test execution and the model used for their analysis (analytical solutions based on assumptions to derive them, numerical models based on the physical processes included in their base equation system). These are referred to as disturbances because they are not considered in the analysis. However, it is possible to describe the development of temperature and pressure signals using the diffusion equation. Disturbances are of short duration in formations with medium to high transmissivity. In formations with low transmissivity, disturbances in the pressure or temperature field can have a significant influence on the pressure signal measured during the test in the test interval (e.g. Nagra 1997, Grauls 1999, Nagra 2001).

Any disturbances of the pressure field during the time before the hydraulic test is started, are summarised under the name 'borehole pressure history'. Disturbances in the pressure and temperature fields can be caused by drilling and other activities before testing. In addition, disturbances can occur even during testing, e.g. mechanical effects (including poroelastic effects) due to

changes in the stress field surrounding the interval, or osmosis due to the chemical interaction of the formation with the drilling fluid. However, results from the experiment 'Deep Borehole Hydraulic Testing Experiment' in the Mont Terri Rock Laboratory showed that osmotic effects have no significant impact on the determination of transmissivity and hydraulic head (Marschall et al. 2003).

As the TBO boreholes are multi-purpose boreholes with many other objectives besides hydraulic packer testing, there is always a trade-off between disciplines regarding optimal test conditions. The hydraulic packer tests were performed without exchange of drilling fluid with testing fluid in order to maintain borehole stability. In addition to this preventative measure, the numerical analysis tool can estimate the effect of these influences, so that plausibility ranges for the parameter estimations can be defined. In the following, possible individual special effects that have previously been identified, e.g. for the Benken borehole (Nagra 2001), are discussed in more detail.

4.3.2.1 Borehole history

All numerical analyses took into account the borehole pressure history. The borehole pressure history was constructed based on activities that took place prior to hydraulic testing. Drilling through the midpoint of the test interval was used as the starting point for the pressure history. The borehole pressure history data were incorporated into the numerical analyses. The following information was used:

- Date and time of drilling through the interval midpoint, from drilling logs
- Drilling fluid density
- Mud level in the borehole prior to testing
- Pressure records of preceding hydraulic testing

The drilling fluid densities were measured four times per day and documented in the drill mud report by the drill mud engineer from AKROS Oilfield Services GmbH. In addition, continuous recordings were available from the mud logging company GEODATA during periods of coring and mud circulation, and mud level measurements in the borehole were performed from time to time.

Most affected by the borehole pressure history is the determination of the static formation pressure or the hydraulic head / hydraulic potential (which are derived from the static formation pressure), which in turn depends on the transmissivity of the formation. In formations with low transmissivity, like the Opalinus Clay, the determination of the static formation pressure can be impossible to carry out in a reasonable time due to the long duration of the pressure history. This was proven by measurements carried out using the Benken long-term monitoring system, which demonstrated that the static formation pressures of the Opalinus Clay determined by hydraulic tests were much higher than those subsequently determined by long-term measurements (e.g. Jäggi & Vogt 2020).

The specific periods of the borehole pressure history taken into account for the analysis of the hydraulic packer tests in borehole STA2-1 are provided in Tab. 4-21.

Tab. 4-21: Specific periods of the pre-test borehole pressure history

Pre-test refers to the period prior to the separation of the test interval from the rest of the borehole through the inflation of the last packer.

Test name	**Drilling through midpoint:** date and time	**Start hydraulic testing:** date and time	**Borehole history duration** [h]
STA2-1-MAL1	07.02.2021 15:02	18.02.2021 19:19	268.28
STA2-1-LIA1	12.03.2021 08:19	21.03.2021 10:23	218.07
STA2-1-BDO1	05.03.2021 01:37	24.03.2021 10:15	464.63
STA2-1-BDO2	03.03.2021 22:11	26.03.2021 14:01	543.83
STA2-1-BDO3	02.03.2021 23:52	27.03.2021 20:31	596.65
STA2-1-OPA1	11.03.2021 01:25	30.03.2021 13:33	468.13
STA2-1-LIA2	13.03.2021 02:44	03.04.2021 21:37	522.88
STA2-1-OPA2	07.03.2021 07:59	07.04.2021 13:14	749.25
STA2-1-OPA3	10.03.2021 04:59	14.04.2021 04:32	839.55
STA2-1-OPA4	07.03.2021 07:59	22.04.2021 03:01	1'099.03
STA2-1-KEU1	14.05.2021 14:27	15.05.2021 22:00	31.55
STA2-1-KEU2	14.05.2021 05:15	20.05.2021 12:50	151.58
STA2-1-MUK1	13.06.2021 10:13	16.06.2021 13:21	75.13

4.3.2.2 Interval temperature changes during testing

All activities inside the open borehole also affect the temperature field in and around the borehole. In formations with low transmissivity, this temperature disturbance affects the pressure field surrounding the borehole due to coupled thermo-hydraulic processes. The analysis of hydraulic tests using the numerical software packages nSIGHTS (version 3.00), Multisim and WellSi can incorporate temperature changes during the hydraulic test that lead to a change in fluid volume and thus pressure within a confined test interval volume. The fluid volume change in the test interval was calculated using the volumetric thermal expansion coefficient of the fluid (water), which itself is temperature-dependent. The pressure change is linearly dependent on the interval fluid volume change using a proportionality factor, the compressibility of the interval.

4.3.2.3 Mechanical effects

The mechanical deformations caused by drilling- and testing-related stress redistribution in the formation can also influence the pressure response during a hydraulic test. Normally, the conceptual model for the description of the storage coefficient used in the underlying hydraulic models assumes a compressible pore volume and an incompressible grain structure. In this model, changes in pore pressure are considered as movement of the fluid into and out of the pore volume. The coupling between fluid volume change and mechanical deformations results in a time-dependent deformation for an elastic medium (Detournay & Cheng 1988). The Opalinus Clay has shown a time-dependent deformation during tunnel excavation in Mont Terri (see Lisjak et al. 2015 for a summary of the observations and for a numerical interpretation of the data). Opalinus

Clay time-dependent behaviour is most likely due to the undrained and drained excavation response, rather than mechanical creep phenomena. In formations with low transmissivity, time-dependent deformations can have an influence on the pressure signal observed in the test interval.

However, there are no data on mechanical deformations available for the tests in borehole STA2-1 that would allow the characterisation of mechanical effects on the tests in formations with low transmissivity. Deformations of the borehole wall can be included in the analysis by all the numerical software packages used, by means of an appropriate parameterisation during the analysis in the same way as for temperature changes inside the interval. The resulting pressure change is caused by volume changes, which can be either linear or quadratic. The proportionality factor between the volume change and the pressure change is the interval compressibility.

4.4 Test activities

A total of thirteen test intervals was investigated in borehole STA2-1 using the HDDP in single and double packer configuration. The most important test specifications are summarised in Tab. 4-22. The hydraulic packer tests were performed in the following geological formations (*cf.* Dossier III):

- Malm Group with a focus on the «Felsenkalke» + «Massenkalk» including zones with abundant karst features, mostly filled with claystone (STA2-1-MAL1) following the realisation of fluid logging (STA2-1-FL1-MAL)
- Dogger Group («Brauner Dogger») with «Parkinsoni-Württembergica-Schichten» (STA2-1-BDO3), «Herrenwis Unit», «Humphriesioolith Formation» (STA2-1-BDO2) and Wedelsandstein Formation and «Murchisonae-Oolith Formation» (STA2-1-BDO1)
- Dogger Group with a focus on Opalinus Clay (STA2-1-OPA1, STA2-1-OPA2, STA2-1-OPA3 and STA2-1-OPA4)
- Lias Group with a focus on the Staffelegg Formation including the Gross Wolf, Rietheim, Grünschholz, Breitenmatt, Rickenbach and Frick Members (STA2-1-LIA1) respectively and also including the Frick, Beggingen and Schambelen Members (STA2-1-LIA2)
- Keuper Group with a focus on the Klettgau Formation including the Gruhalde, Seebi, Gansingen and the top part of the Ergolz Member (STA2-1-KEU2), respectively covering the Seebi, and Gansingen Members, the entire Ergolz Member and the first meters of Bänkerjoch Formation (STA2-1-KEU1)
- Muschelkalk Group with a focus on the Schinznach Formation including Stamberg, Liederswil, Leutschenberg and Kienberg Members (STA2-1-MUK1)

All hydraulic tests (except for STA2-1-MAL1, STA2-1-OPA3 and STA2-1-OPA4) were performed in the cored borehole section with a borehole diameter of 6⅜", with 114 mm (deflated diameter) packers and without any prior fluid exchange, i.e. with the drilling fluid being used as the interval test fluid. For STA2-1-MAL1 and STA2-1-OPA4, the drilling fluid was replaced prior to testing with traced tap water (STA2-1-MAL1 performed after fluid logging STA2-1-FL1-MAL) and PEARSON water (STA2-1-OPA4), respectively. The fluid exchange prior to test STA2-1-OPA4 was performed by replacing the drilling fluid by NaOH and subsequently by PEARSON water over the deflated upper packer. However, during the fluid exchange the pressure inside the test interval increased significantly, so that an artificial opening (probably a hydraulic fracturing) of the formation could not be excluded. For STA2-1-OPA3, which included the GTPT, tests were performed using the 146 mm (deflated diameter) packers.

The density and viscosity of the drilling fluid were reported by the mud engineer in daily mud reports. Sodium-Fluorescein at concentrations of approximately 1 ppm was used to trace the drilling mud. The test tubing was typically filled with traced tap water. Sodium-naphthionate or 1.5-naphthalene disulfonate acid (for the hydraulic tests within the shales) were used as tracers at concentrations of approximately 10 ppm. The SIT was closed during the entire time the HDDP was lowered to the test depth and also during installation. Therefore, in test intervals with low transmissivity, the interval fluid density was not affected by traced water in the test tubing as mainly withdrawal tests were performed and no or only very little fluid flow occurred. If a pressure increase of more than 100 kPa was observed in the test interval during inflation of the top packer, the SIT was opened and the COM phase started. Due to the higher density of the mud in the test interval, for formations with low transmissivity, it was assumed that no flow occurred from the test tubing into the test interval during the COM phase. Flow from the formation into the borehole by means of a longer test phase of pressure reduction in the interval (i.e. a slug or pumping test phase) was created during all tests, except for STA2-1-OPA2.

A swabbing tool was used to create the pressure difference between the test tubing and the test interval. For each of the pumping tests, the PCP was used and the position of the stator of the PCP in the test string was optimised up to the limit of the allowable pumping head. If two tests were performed sequentially without pulling the HDDP out of the borehole between tests, a stator was already installed for the first test (usually the deeper test).

For the tests STA2-1-MAL1, STA2-1-LIA1, STA2-1-KEU1 and STA2-1-MUK1, drilling was stopped for hydraulic testing. For the other tests, a longer section was drilled and then the hydraulic tests were performed. For the tests STA2-1-MAL1 and STA2-1-LIA1, at the end of drilling only a fluid logging campaign, and a petrophysical logging campaign respectively, were performed. The hydraulic tests STA2-1-KEU1 and STA2-MUK1 were performed directly after pulling out of hole (POOH) the coring string without performing logging prior to testing. All the other tests had a longer borehole pressure history. The measured pressures (measured by the downhole sensors in the QSSP) and pumping rates (measured by the flow board at the surface) for all tests conducted in borehole STA2-1 are provided in Figs. 4-9 to 4-21. The figures are taken directly from the reports of the field test contractor.

The temperature increase in the test intervals was included in the analysis of the hydraulic packer tests for formations without a pumping period (low transmissivity). The temperature increase from the start of the initial pressure recovery after closing the shut-in valve (PSR) until the end of the test ranged from 0.14 K to 4.02 K for all tests.

Tab. 4-22: Hydraulic packer testing in borehole STA2-1: test interval and test specifications

[1] For an explanation of the test names and test phases see Tabs. A-2 and A-3, respectively.

[2] FM = flow model, T = transmissivity, h_s = static hydraulic head, WS = water sample.

Test name[1]	**Interval depth** [m MD]	**Interval midpoint** [m MD]	**Packer configuration**	**Test phases**[1]	**Testing period** (duration)	**Geological information** [depth and length values rounded; groups and formations usually named from top down; for details see Dossier III]	**Objectives**[2] [secondary aims in brackets ()]
STA2-1-MAL1	473.50 – 542.67	508.09	Double	INF1, INF2, PSR, SW, SWS, RW, RWS, PI, DEF	18.02. – 23.02.2021 (102.4 h)	Malm Group: Saccharoidal limestone, indicating sponge reef sediments, abundant karst features, mostly filled with claystone. The test was designed to investigate inflow zones detected by the fluid logging.	T, h_s, FM, WS
STA2-1-BDO3	744.68 – 763.00	753.84	Double	INF1, INF2, COM, PSR, SW, SWS, PW, DEF	27.03 – 30.03.2021 (59.9 h)	Dogger Group («Brauner Dogger»): gradual alternation, mostly thin- to medium-bedded silty marl and limestone (silty, argillaceous) in the upper part, silty claystone (calcareous) and silty marl in the middle part, and silty claystone (calcareous) and claystone (silty, calcareous) in the lower part of the «Parkinsoni-Württembergica-Schichten». The hydraulic test was designed for characterisation of the «Parkinsoni-Württembergica-Schichten» with the same interval length to that used in STA2-1-BDO1 and -BDO2.	T, (h_s), FM
STA2-1-BDO2	763.48 – 781.80	772.64	Double	INF1, INF2, PSR, PW1, PW2, SW, SWS, DEF	26.03. – 27.03.2021 (28.0 h)	Dogger Group («Brauner Dogger»): upper part of «Parkinsoni-Württembergica-Schichten», followed by a medium- to thick-bedded sequence of bioclastic limestone of the «Herrenwis Unit» and bioclastic argillaceous marl, silty, bioclastic calcareous marl, limonitic, with iron-ooids of the «Humphriesioolith Formation». The hydraulic test was designed to characterise the «Humphriesioolith Formation» including a fault zone according to the FMI log.	T, (h_s), FM
STA2-1-BDO1	783.10 – 801.42	792.26	Double	INF1, INF2, COM, PSR, SW, SWS, PW, DEF	24.03. – 26.03.2021 (49.8 h)	Dogger Group («Brauner Dogger»): test interval included the lower part of the Wedelsandstein Fm. and consisted of bioclastic limestone, silty claystone (calcareous) and bioclastic calcareous marl, the «Murchisonae-Oolith Formation» of silty claystone and alternation of limestone (iron-oolitic), bioclastic calcareous to argillaceous marl and 1.75 m of Opalinus Clay. Test STA2-1-BDO1 was designed to characterise the «Murchisonae-Oolith Formation».	T, (h_s), FM

Tab. 4-22: continued

[1] For an explanation of the test names and test phases see Tabs. A-2 and A-3, respectively.

[2] FM = flow model, T = transmissivity, h_s = static hydraulic head, WS = water sample.

Test name[1]	**Interval depth** [m MD]	**Interval midpoint** [m MD]	**Packer configuration**	**Test phases**[1]	**Testing period** (duration)	**Geological information** [depth and length values rounded; groups and formations usually named from top down; for details see Dossier III]	**Objectives**[2] [secondary aims in brackets ()]
STA2-1-OPA2	822.00 – 839.11	830.56	Double	INF1, INF2, COM, PSR, PW1, PW2, DEF	07.04. – 10.04.2021 (67.8 h)	Dogger Group: test interval entirely within Opalinus Clay. Test STA2-1-OPA2 was designed to test the upper part of the Opalinus Clay with siltstone to sandstone lenses.	T, h_s, FM
STA2-1-OPA4 (Fluid exchange)	822.00 – 839.13	830.57	Double	INF1, FLUIDEXCHANGE, INF2, COM, PSR, PW, SW, SWS, DEF	22.04. – 25.04.2021 (75.4 h)	Dogger Group: test interval entirely within Opalinus Clay. The STA2-1-OPA4 test interval comprised the STA2-1-OPA2 test interval to test the upper part of the Opalinus Clay with siltstone to sandstone lenses and was conducted with artificial formation water (PEARSON water) as test fluid.	T, h_s, FM
STA2-1-OPA1	881.50 – 899.82	890.66	Double	INF1, INF2, COM, PSR, SW, SWS, PW, DEF	30.03. – 02.04.2021 (61.8 h)	Dogger Group: test interval entirely within Opalinus Clay. Test STA2-1-OPA1 was designed to characterise the lower Opalinus Clay including a fault zone 885.50 – 886.50 m MD also targeted by test STA2-1-OPA3 (see test STA2-1-OPA3 for more information).	T, (h_s), FM
STA2-1-OPA3	882.30 – 888.55	885.43	Double	INF1, INF2, COM, PSR, PW	14.04. – 20.04.2021 (151.4 h)	Dogger Group: test interval entirely within Opalinus Clay. This test was designed to investigate one open steep structure with numerous veins that indicated a typical subseismic fault. It preceded a GTPT.	T, (h_s), FM
STA2-1-LIA1	904.00 – 922.32	913.16	Double	INF1, INF2, COM, PSR, SW, SWS, PW, DEF	21.03. – 24.03.2021 (66.4 h)	Lias Group: test interval covered the lower 1.20 m of Opalinus Clay and mainly the Staffelegg Formation a claystone (silty, micaceous) that dipped from clayey to calcareous marl at the upper end. The test was designed to characterise the upper Staffelegg Formation from Gross Wolf to Frick Members.	T, (h_s), FM
STA2-1-LIA2	924.40 – 936.00	930.20	Single	INF, COM, PSR, PI, PW1, SW, SWS, PW2, DEF	03.04. – 06.04.2021 (55.3 h)	Lias Group: test interval covered the Frick, Beggingen and Schambelen Members of the Staffelegg Formation, consisting of silty to sandy claystone (calcareous), bioclastic calcareous marl and limestone. The test was designed to characterise the Beggingen and Schambellen Members.	T, (h_s), FM

Tab. 4-22: continued

[1] For an explanation of the test names and test phases see Tabs. A-2 and A-3, respectively.

[2] FM = flow model, T = transmissivity, h_s = static hydraulic head, WS = water sample.

Test name[1]	**Interval depth** [m MD]	**Interval midpoint** [m MD]	**Packer configuration**	**Test phases**[1]	**Testing period** (duration)	**Geological information** [depth and length values rounded; groups and formations usually named from top down; for details see Dossier III]	**Objectives**[2] [secondary aims in brackets ()]
STA2-1-KEU2	941.50 – 962.04	951.77	Double	INF1, INF2, COM, PSR, SW, SWS, PW, PI, DEF	20.05. – 22.05.2021 (43.2 h)	Keuper Group: the test interval covered the Klettgau Formation including the Gruhalde Member characterised by variegated dolomitic marl (partly sandy), the Seebi Member showed dolomitic marl (sandy) to dolostone (sandy to silty, argillaceous), the Gansingen Member consisted exclusively of dolostone and the upper part of the Ergolz Member argillaceous marl (silty, dolomitic). The test was designed to clarify if the hydraulic behaviour in STA2-1-KEU1 was dominated by the Ergolz Member as well as to the distinct hydraulic properties of the Klettgau Formation.	T, h_s, (FM)
STA2-1-KEU1	951.00 – 973.00	962.00	Single	INF, COM, PSR, SW, SWS, RW, RWS, PW, PI, DEF	15.05. – 18.05.2021 (67.4 h)	Keuper Group: the test interval covered the Klettgau Formation including the Gruhalde Member characterised by variegated dolomitic marl (partly sandy), the Seebi Member showed dolomitic marl (sandy) to dolostone (sandy to silty, argillaceous), the Gansingen Member consisted exclusively of dolostone and total Ergolz Member represented by fluvial overspill facies composed of variegated argillaceous marl (silty, dolomitic) with nodular dolomitic horizons documenting paleosoils as well as a small part of the Bänkerjoch Formation of claystone with anhydrite nodules. The aim of this test was to target possible transmissive zones in the Klettgau Formation and to provide an overview of the hydraulic properties.	T, h_s, (FM), WS
STA2-1-MUK1	1’058.80 – 1’117.00	1’087.90	Single	INF, PSR, SW, SWS, RW, RWS, PI, DEF	16.06. – 19.06.2021 (75.4 h)	Muschelkalk Group: approx. 57.21 m of the Schinznach Formation (approx. 22.20 m of Stamberg Member, 9.78 m of Liedertswil Member and 25.23 m of Leutschenberg and Kienberg Members) and approx. 0.99 m of Zeglingen Formation, "Dolomitzone". Rocks within the test interval mainly consisted of dolostones and limestones interspersed with anhydrites. The overview test was designed to study the water conducting features of the Schinznach Formation obvious in the cores.	T, h_s, (FM), WS

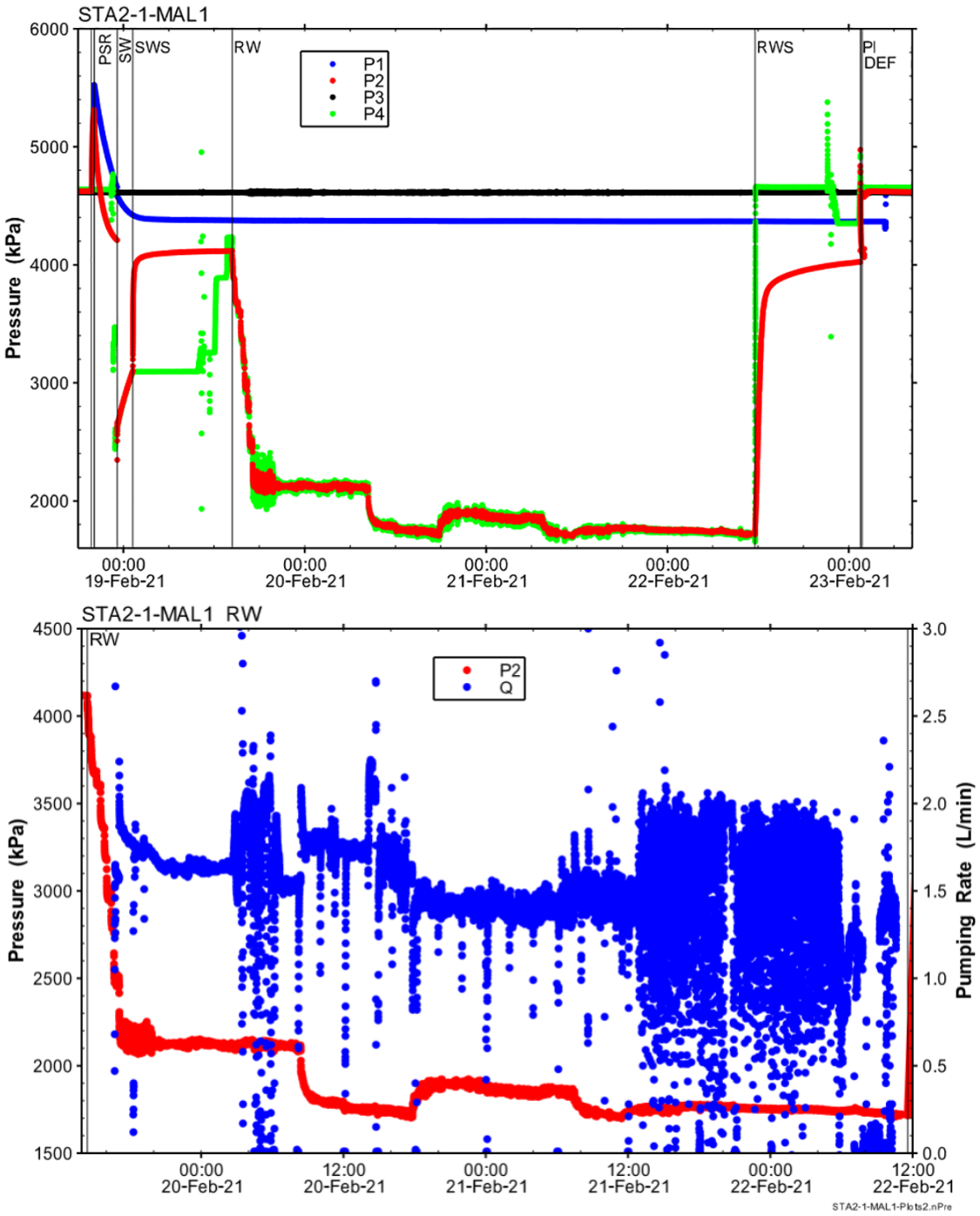

Fig. 4-9: Hydraulic packer test STA2-1-MAL1: Overview plot of pressure (top) and interval pressure (P2) and rate (Q) during the RW (bottom) vs. time and date

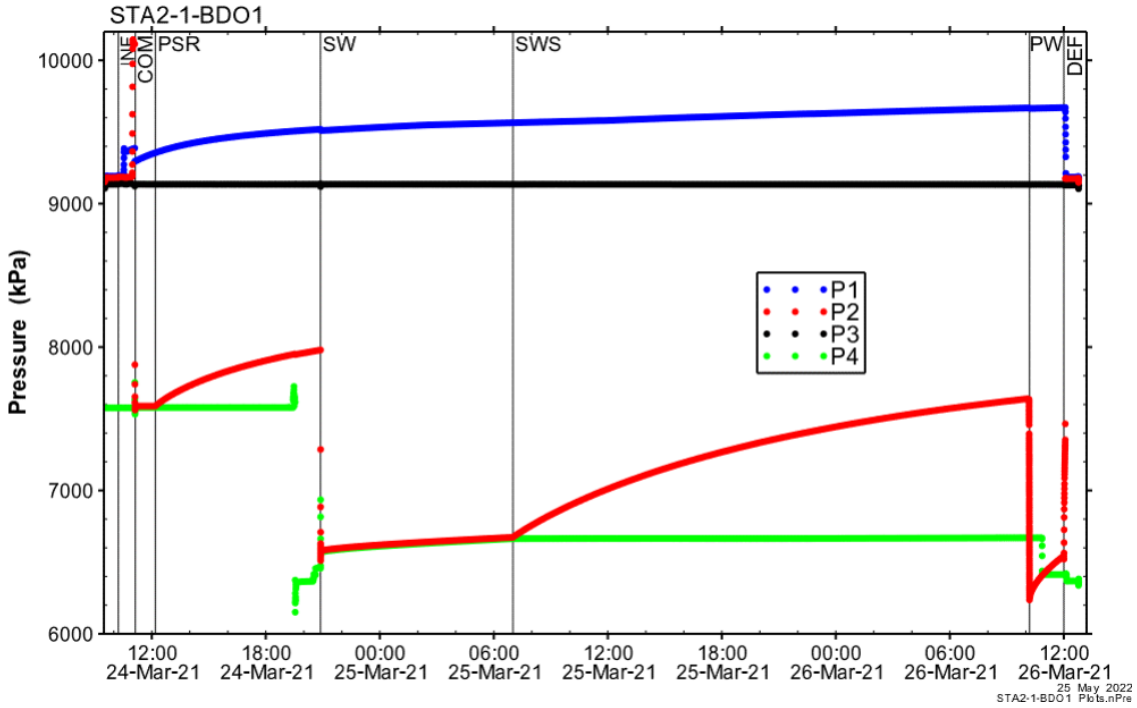

Fig. 4-10: Hydraulic packer test STA2-1-BDO1: Overview plot of pressure vs. time and date

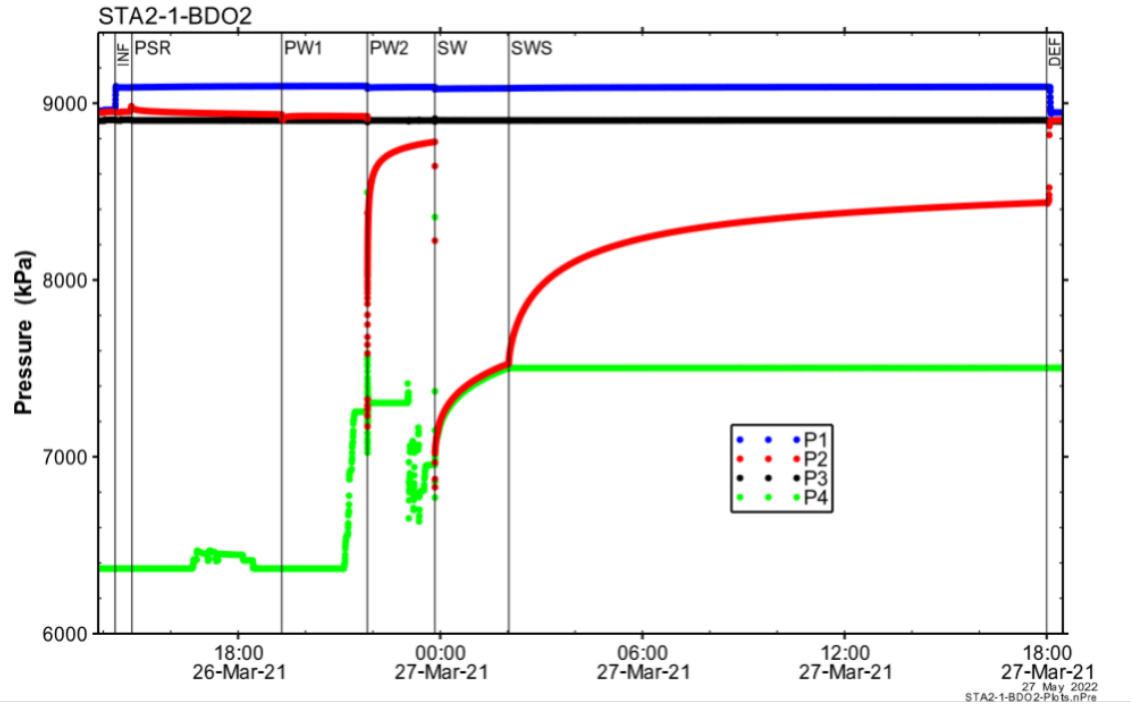

Fig. 4-11: Hydraulic packer test STA2-1-BDO2: Overview plot of pressure vs. time and date

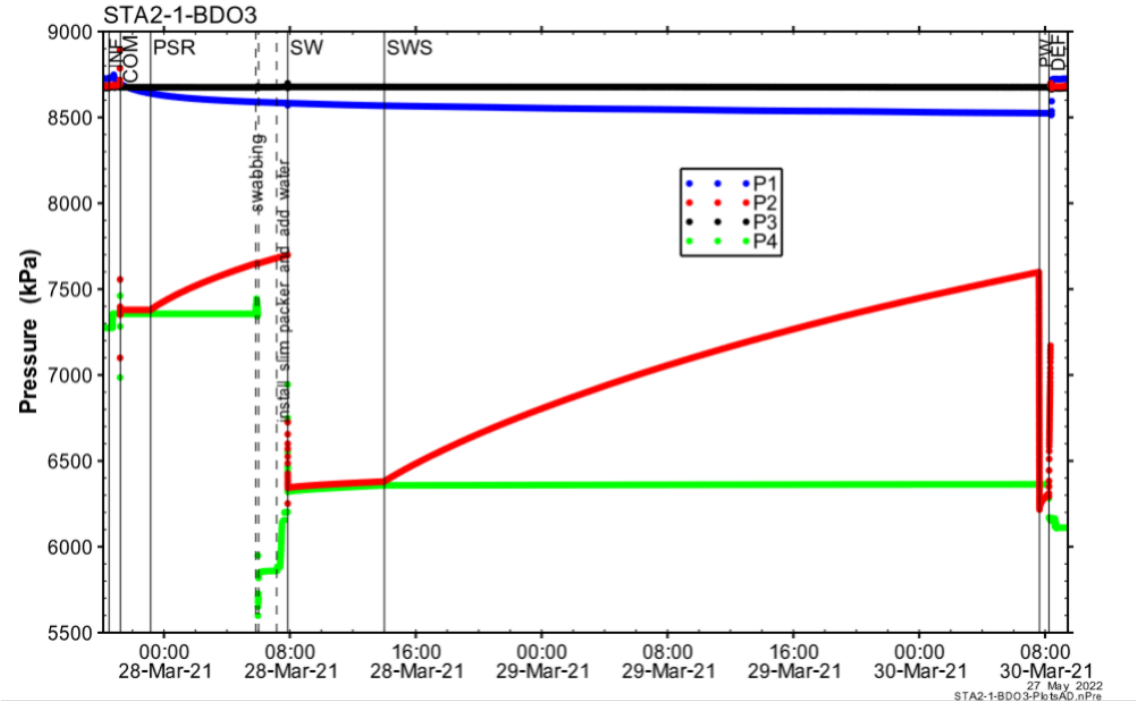

Fig. 4-12: Hydraulic packer test STA2-1-BDO3: Overview plot of pressure vs. time and date

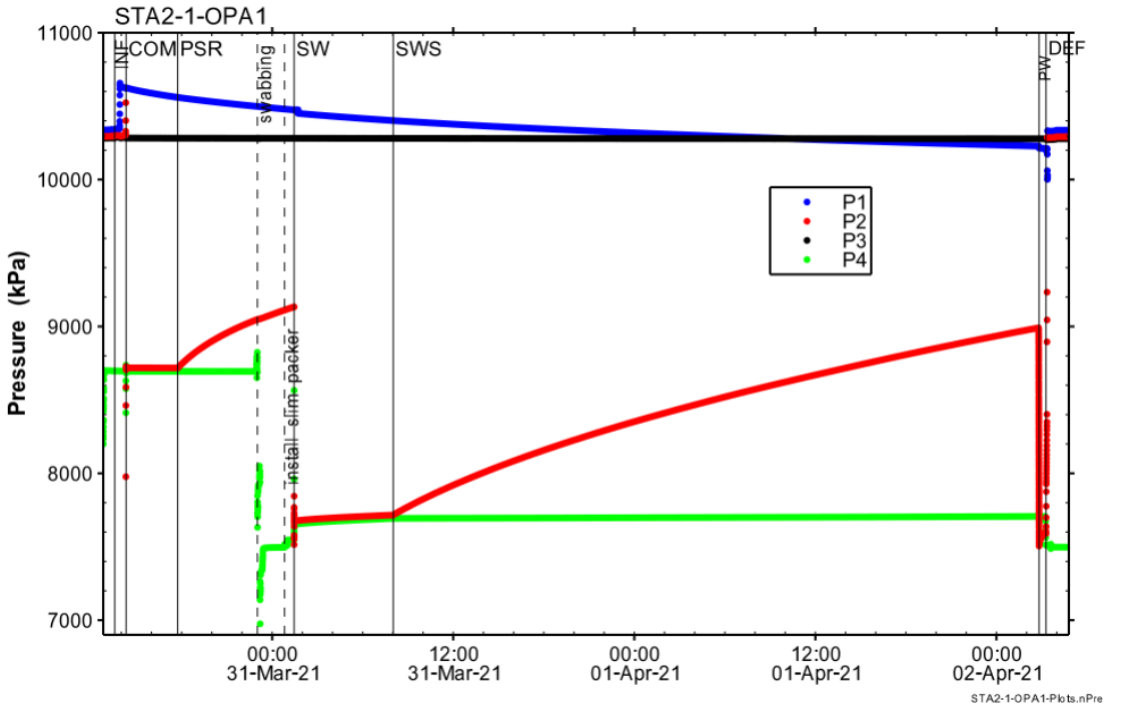

Fig. 4-13: Hydraulic packer test STA2-1-OPA1: Overview plot of pressure vs. time and date

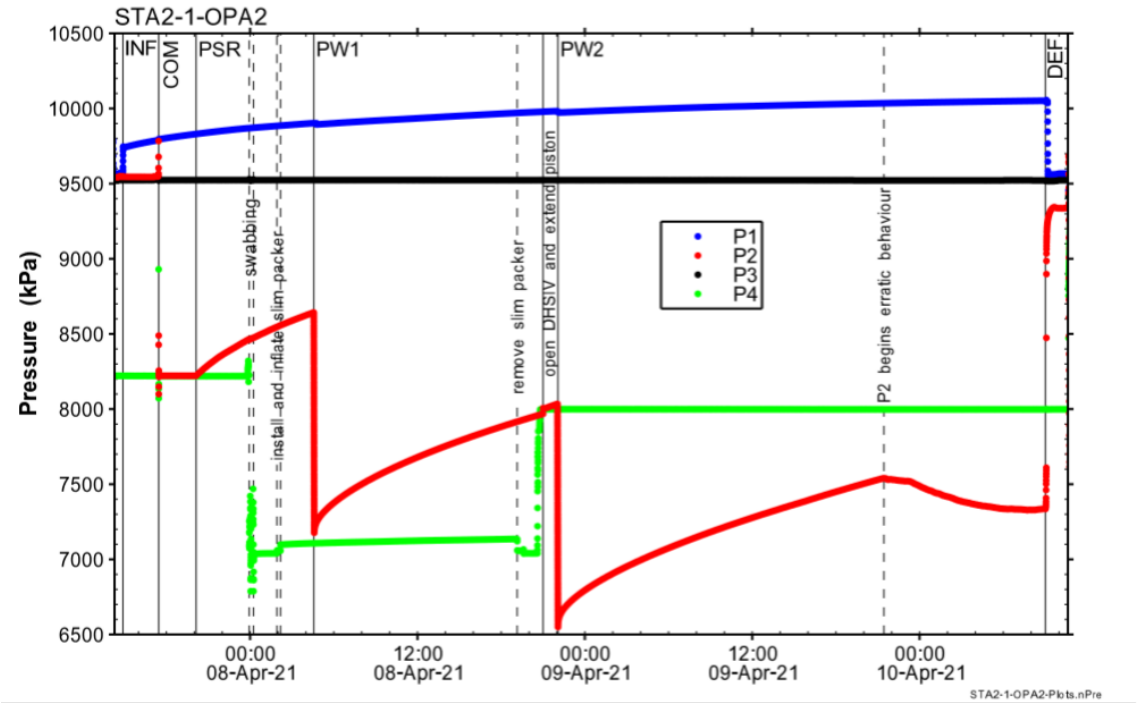

Fig. 4-14: Hydraulic packer test STA2-1-OPA2: Overview plot of pressure vs. time and date

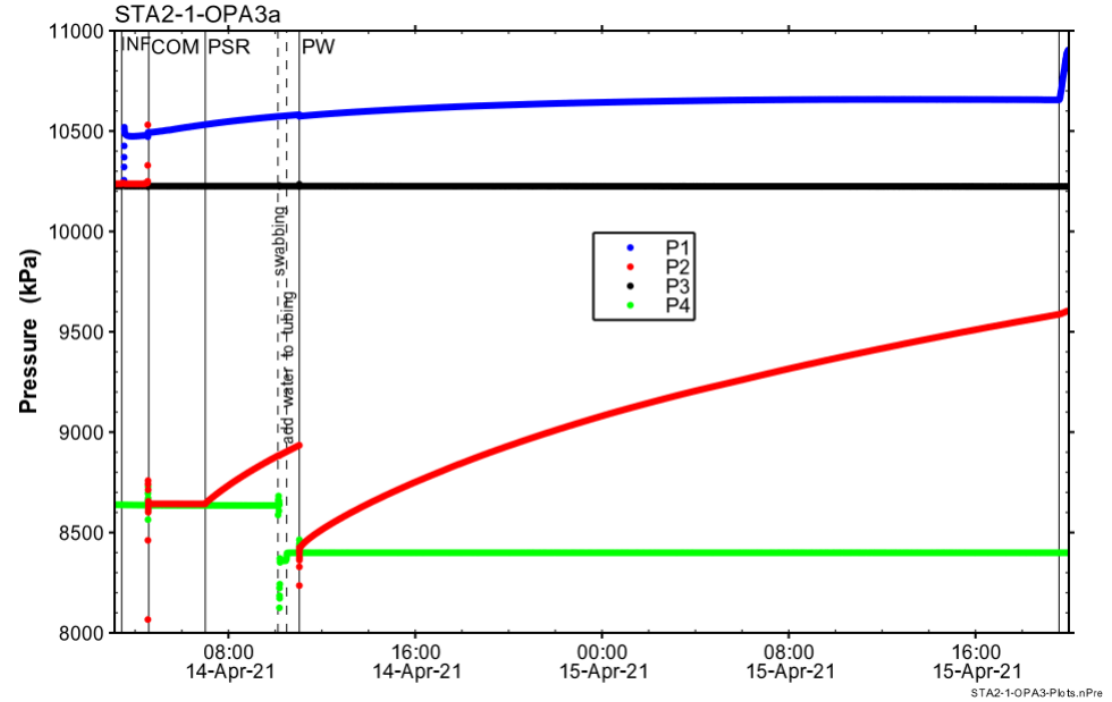

Fig. 4-15: Hydraulic packer test STA2-1-OPA3: Overview plot of pressure vs. time and date

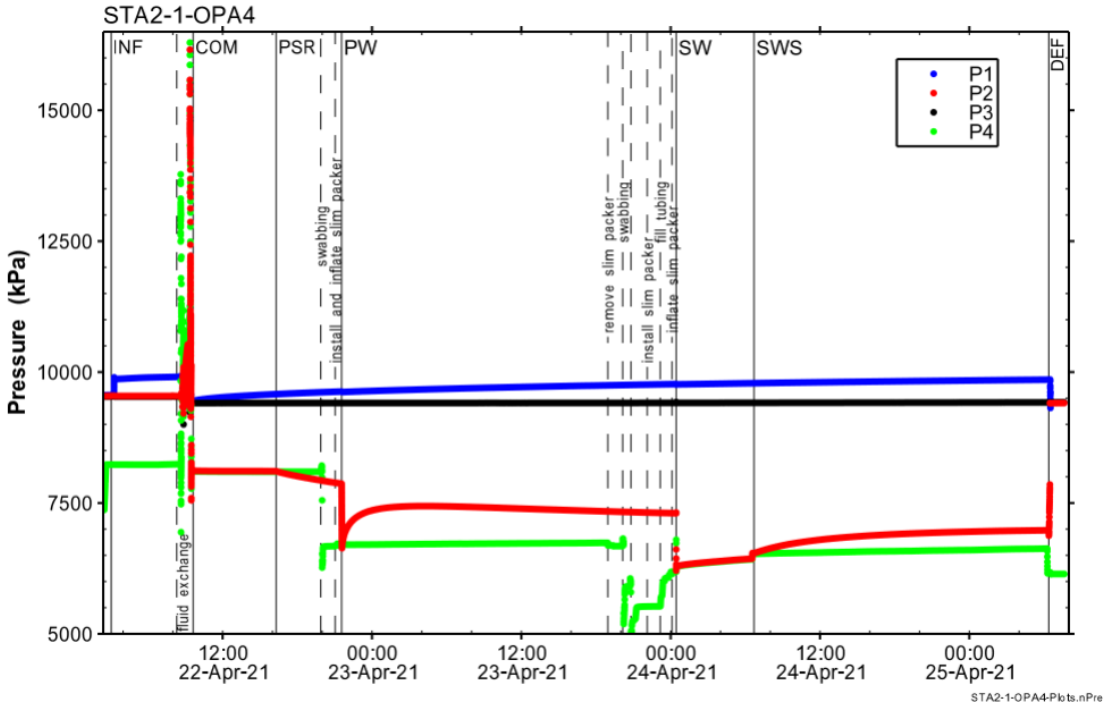

Fig. 4-16: Hydraulic packer test STA2-1-OPA4: Overview plot of pressure vs. time and date

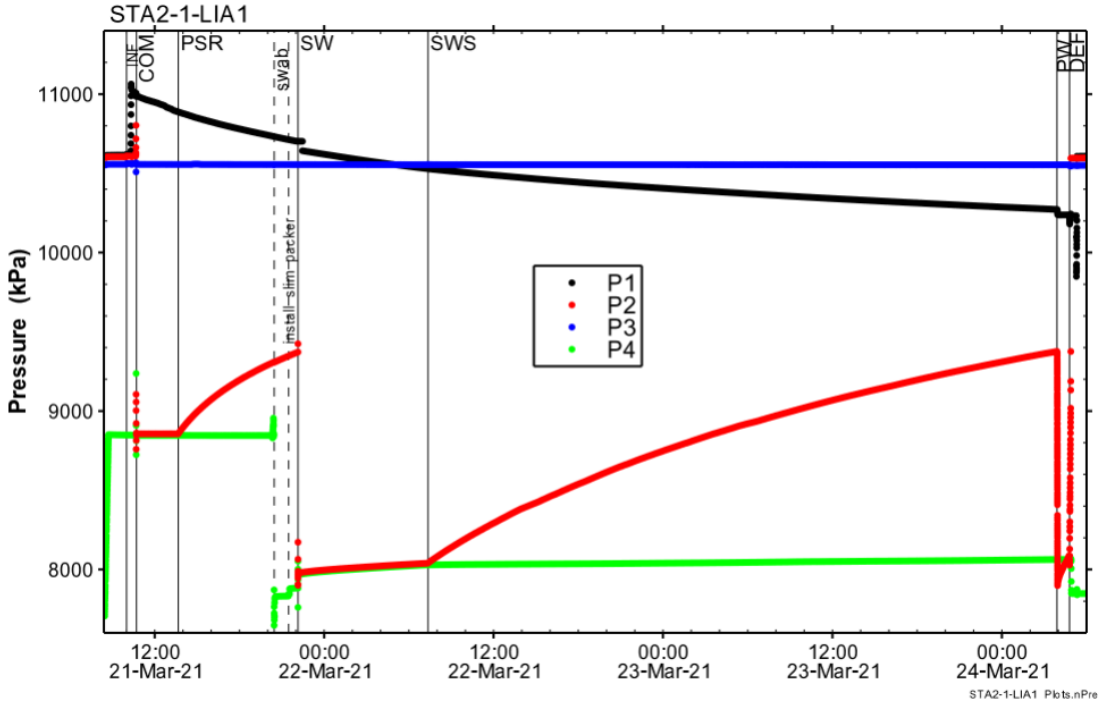

Fig. 4-17: Hydraulic packer test STA2-1-LIA1: Overview plot of pressure vs. time and date

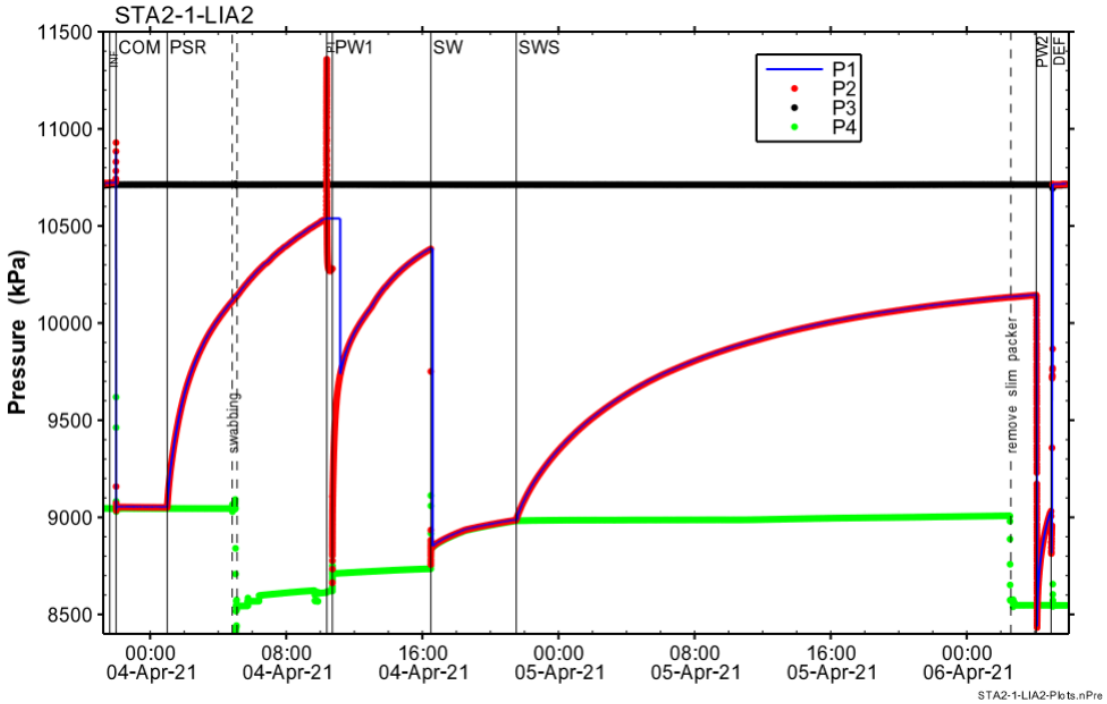

Fig. 4-18: Hydraulic packer test STA2-1-LIA2: Overview plot of pressure vs. time and date

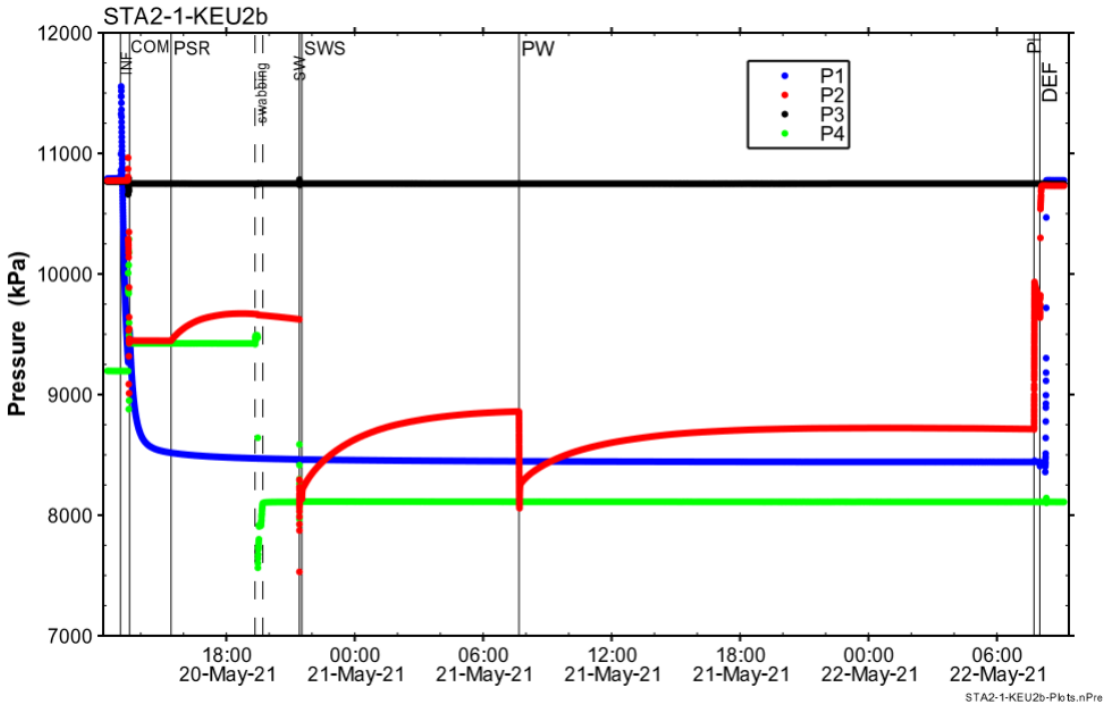

Fig. 4-19: Hydraulic packer test STA2-1-KEU2: Overview plot of pressure vs. time and date

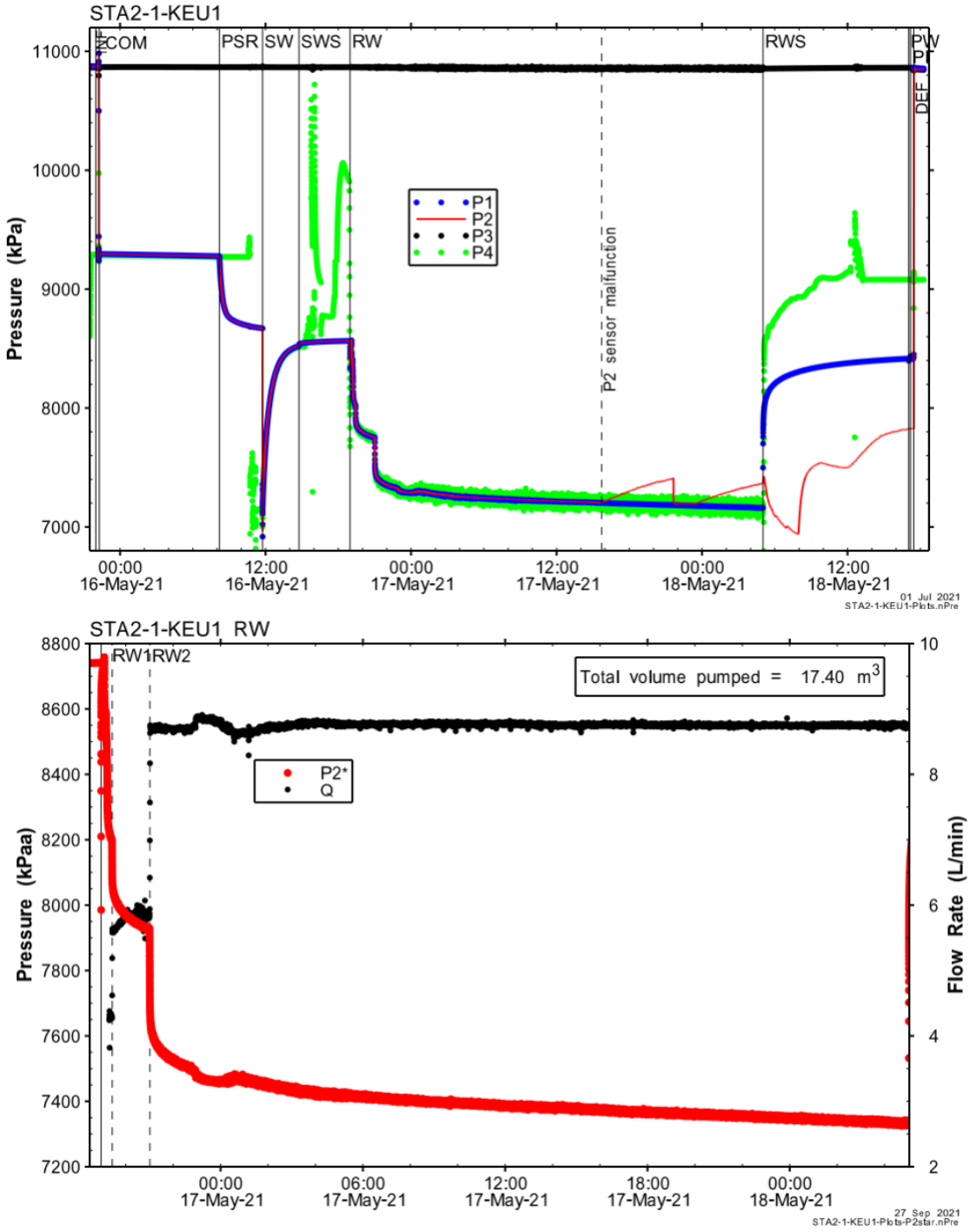

Fig. 4-20: Hydraulic packer test STA2-1-KEU1: Overview plot of pressure (top) and interval pressure (P2) and rate (Q) during the RW (bottom) vs. time and date

Note that the analysis used the P2* measurements (bottom) as erratic behaviour indicated a malfunction of the QSSP P2 gauge while the P1 gauge continued to show normal readings (top).

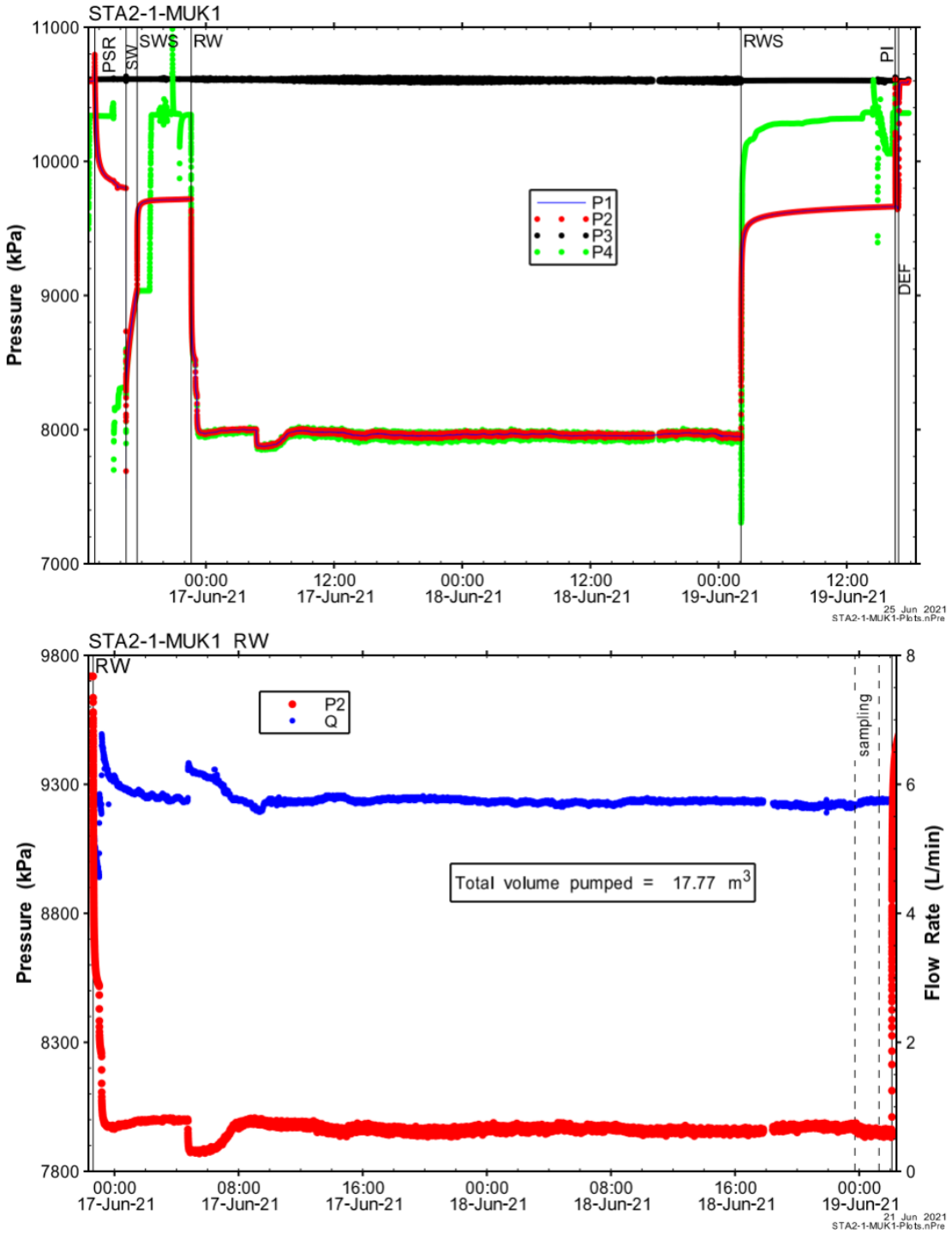

Fig. 4-21: Hydraulic packer test STA2-1-MUK1: Overview plot of pressure (top) and interval pressure (P2) and rate (Q) during the RW (bottom) vs. time and date

4.5 Details of selected tests

Two of the hydraulic packer tests are presented below in more detail: STA2-1-BDO1 and STA2-1-KEU1. STA2-1-BDO1 was performed in a combination of a slug withdrawal and a slug recovery test phase followed by a pulse withdrawal test phase to confirm the value of the test zone compressibility. The test illustrates an example of an analysis for formations with low to very low transmissivity. STA2-1-KEU1 illustrates an example of the test strategy for formations with medium to high transmissivity. The hydraulic test sequence consisted of a slug withdrawal and a slug recovery phase followed by a pumping phase and a subsequent pressure recovery phase.

The two test analysis examples are presented in this section in more detail. The results of the test analyses are provided in Section 4.6 together with the results of all other tests performed.

4.5.1 Hydraulic packer test STA2-1-BDO1

The hydraulic packer test STA2-1-BDO1 is an example of testing formations with low transmissivity using both an intermediate pressure history duration (464.6 h) and a short hydraulic test execution duration (49.7 h). For the analysis, the measurements of the QSSP P2 sensor were used at a depth of 778.78 m MD. Fig. 4-10 presents the P2 measurements.

4.5.1.1 Interval characterisation

The hydraulic test STA2-1-BDO1 was performed in double packer configuration. The entire interval was located within the Dogger Group («Brauner Dogger») and covered 3.75 m of the Wedelsandstein Formation, which consisted of: bioclastic limestone, silty claystone (calcareous) and bioclastic calcareous marl, 12.82 m of «Murchisonae-Oolith Formation» containing silty claystone and an alternation of limestone (iron-oolitic), bioclastic calcareous to argillaceous marl and 1.75 m of Opalinus Clay (*cf.* Dossier III). The main focus of this hydraulic test was the characterisation of the hydraulic properties of the «Murchisonae-Oolith Formation». The primary test objective was to obtain a reliable estimate of T (and K) for the formation based on the determination of the flow model. A secondary objective was to obtain an estimate of the hydraulic head (h_s) / static formation pressure (P_s) of the tested interval. Details of the interval and test duration are provided in Tab. 4-23.

Tab. 4-23: Hydraulic test STA2-1-BDO1: Information on the test interval

Test	**Depth**		**Length**	**Packer configuration**	**Hydraulic testing**		
	from [m MD]	to [m MD]	[m]		Start date	End date	Duration [h]
STA2-1-BDO1	783.10	801.42	18.32	Double	24.03.2021	26.03.2021	49.7

4.5.1.2 Test execution

Fig. 4-22 shows the system installation record as provided by the field test contractor. The equipment components are described in Section 4.2.

The hydraulic test tool including the heavy-duty double packer system and the piston pulse generator was installed in borehole STA2-1 on 24.03.2021. After testing in the Lias Group (STA2-1-LIA1), the HTT was repositioned in the borehole for the hydraulic test STA2-1-BDO1. The packers were seated in competent rock within the «Brauner Dogger» and the upper part of the Opalinus Clay. The entire borehole, including the test interval, was filled with potassium-silicate drilling mud during the STA2-1-BDO1 testing period. The test was started by inflating the bottom packer (INF1) followed by inflation of the top packer (INF2) using a 2:1 mixture of anti-freeze:water. The shut-in tool (SIT) was opened when the top packer began to isolate the interval volume.

The COM phase lasted 1 hour and 2 minutes which allowed some of the pressure and temperature transients caused by tool installation and packer inflation to dissipate before the SIT was again closed to initiate the PSR phase. The PSR phase lasted 8 hours and 41 minutes in order to allow the test interval pressure to establish a recovery trend after being isolated. Late in the PSR phase, the test tubing was swabbed to lower the pressure in the tubing (P4) below the pressure in the test interval (P2) so that a slug withdrawal (SW) test could be initiated by opening the SIT. A slim packer was installed in the test tubing with 4 mm inner diameter slim tubing to reduce the wellbore storage during the SW. The SIT was opened to initiate the SW that was terminated after 10 hours and 6 minutes by closing the SIT to initiate a slug withdrawal shut-in phase (SWS). The SWS phase lasted 27 hours and 5 minutes. After the SWS phase, a pulse withdrawal (PW) was initiated by retraction of a 250 ml piston inside the piston pulse generator housing. The PW lasted for a period of 1 hour and 48 minutes. The PW was conducted primarily to provide a measurement of test-zone compressibility. The subsequent deflation (DEF) of the packers was carried out with the SIT closed. The SIT remained closed for relocation of the HTT to the subsequent test interval STA2-1-BDO2.

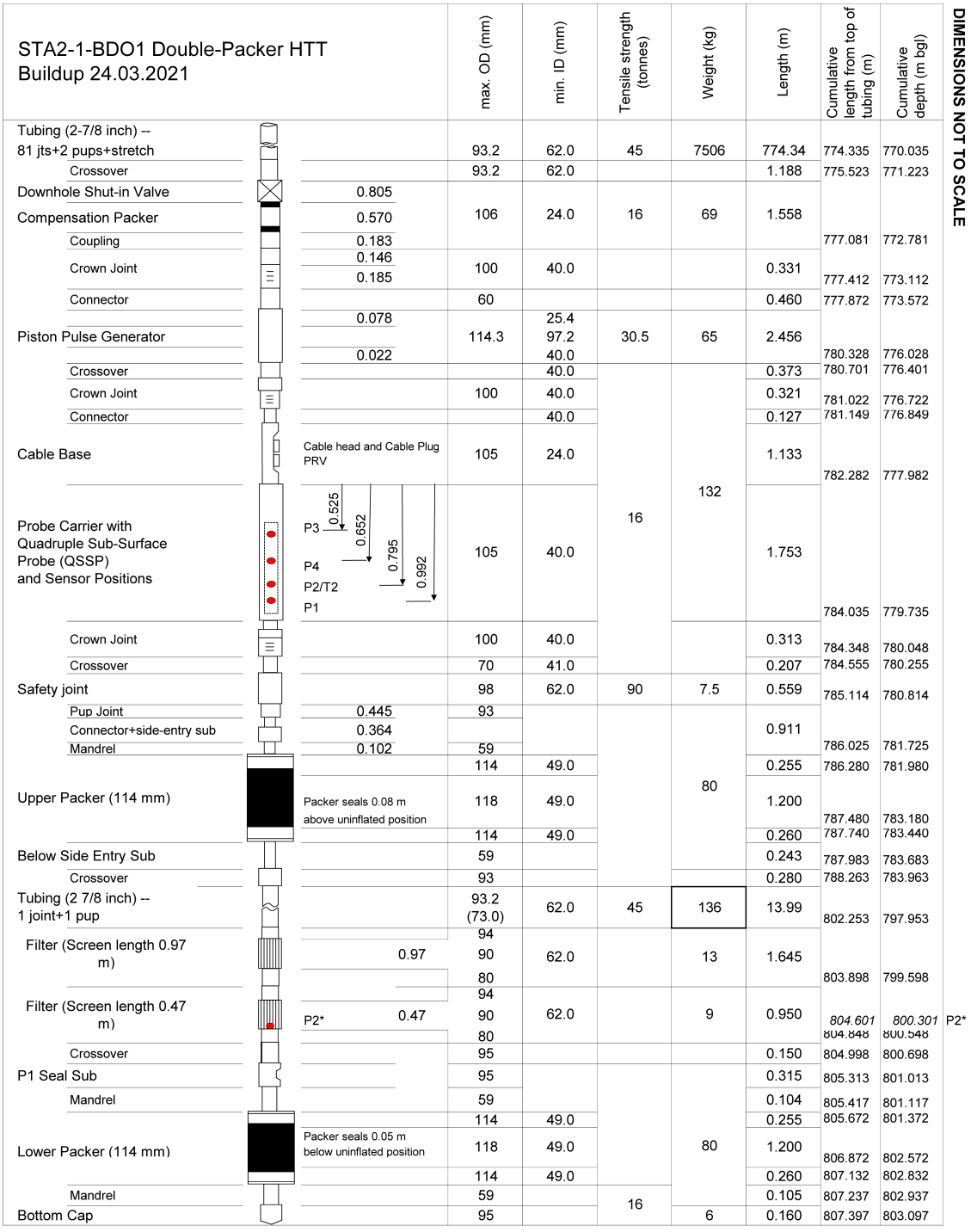

		max. OD (mm)	min. ID (mm)	Tensile strength (tonnes)	Weight (kg)	Length (m)	Cumulative length from top of tubing (m)	Cumulative depth (m bgl)
Tubing (2-7/8 inch) -- 81 jts+2 pups+stretch		93.2	62.0	45	7506	774.34	774.335	770.035
Crossover		93.2	62.0			1.188	775.523	771.223
Downhole Shut-in Valve	0.805							
Compensation Packer	0.570	106	24.0	16	69	1.558		
Coupling	0.183						777.081	772.781
Crown Joint	0.146 0.185	100	40.0			0.331	777.412	773.112
Connector		60				0.460	777.872	773.572
Piston Pulse Generator	0.078	114.3	25.4 97.2 40.0	30.5	65	2.456		
	0.022						780.328	776.028
Crossover			40.0			0.373	780.701	776.401
Crown Joint		100	40.0			0.321	781.022	776.722
Connector			40.0			0.127	781.149	776.849
Cable Base	Cable head and Cable Plug PRV	105	24.0			1.133	782.282	777.982
Probe Carrier with Quadruple Sub-Surface Probe (QSSP) and Sensor Positions	P3 0.525, P4 0.652, P2/T2 0.795, P1 0.992	105	40.0	16	132	1.753	784.035	779.735
Crown Joint		100	40.0			0.313	784.348	780.048
Crossover		70	41.0			0.207	784.555	780.255
Safety joint		98	62.0	90	7.5	0.559	785.114	780.814
Pup Joint	0.445	93						
Connector+side-entry sub	0.364					0.911		
Mandrel	0.102	59					786.025	781.725
Upper Packer (114 mm)	Packer seals 0.08 m above uninflated position	114 118 114	49.0 49.0 49.0		80	0.255 1.200 0.260	786.280 787.480 787.740	781.980 783.180 783.440
Below Side Entry Sub		59				0.243	787.983	783.683
Crossover		93				0.280	788.263	783.963
Tubing (2 7/8 inch) -- 1 joint+1 pup		93.2 (73.0)	62.0	45	136	13.99	802.253	797.953
Filter (Screen length 0.97 m)	0.97	94 90 80	62.0		13	1.645	803.898	799.598
Filter (Screen length 0.47 m)	P2* 0.47	94 90 80	62.0		9	0.950	*804.601* 804.848	*800.301* P2* 800.548
Crossover		95				0.150	804.998	800.698
P1 Seal Sub		95				0.315	805.313	801.013
Mandrel		59				0.104	805.417	801.117
Lower Packer (114 mm)	Packer seals 0.05 m below uninflated position	114 118 114	49.0 49.0 49.0		80	0.255 1.200 0.260	805.672 806.872 807.132	801.372 802.572 802.832
Mandrel		59		16		0.105	807.237	802.937
Bottom Cap		95			6	0.160	807.397	803.097

Fig. 4-22: Hydraulic test STA2-1-BDO1: Downhole equipment installation record with system layout as used in the field test

4.5.1.3 Analysis

Borehole pressure history

The borehole pressure history used for the analysis of the STA2-1-BDO1 tests is shown in Fig. B-1 (see Appendix B) and summarised in Tab. 4-24. The calculation of the mean interval fluid density using the measurement of the P2 pressure sensor (prior to packer inflation) gave a density of 1'199 kg m^{-3}. This value corresponds to the documented density of the drilling mud during drilling (1'200 kg m^{-3}; see Dossier I). For periods without a level measurement (e.g. during petrophysical logging), the mud level was assumed to be at the level of the drain pipe, approximately 1.9 m above ground level. This was due to the fact that for periods with no active mud circulation, the drillers generally kept the borehole full to this level. Therefore, the pressure measured by the P2 pressure sensor once the HTT had reached the test depth and the borehole was filled with drill mud was used for the history periods. This pressure value was also used for the STA2-1-LIA1 testing period when changes in the annulus fluid pressure were insignificant. During periods of coring, GEODATA monitored the mud circulation pressures using a pressure gauge mounted above the rig floor. These pressures were extrapolated to the depth of the P2 pressure sensor. During the petrophysical logging, no additional mud level measurements were documented. Hence, it was assumed that the mud level was at the level of the drain pipe. Once the HTT was at test depth and data acquisition began, the P2 pressure sensor measured pressure directly.

Tab. 4-24: Hydraulic test STA2-1-BDO1: Borehole pressure history

[1] Pressure at the P2 sensor level (778.78 m MD) was calculated from the history information, e.g. fluid level and density.

[2] Drilling through interval midpoint (792.26 m MD).

[3] Pressure measured when the borehole was filled with mud (e.g. when the P2 sensor arrived at test depth and before packer inflation).

Description	**Start date and time**	**Duration** [h]	**Pressure**[1] [kPa]	
		Total: 465.07	**Start**	**End**
Drilling[2]	05.03.2021 01:37	202.32	12'585	9'180 [3]
Pull out of hole (POOH) of coring string	13.03.2021 11:56	75.32	9'180 [3]	9'180 [3]
Petrophysical logging	16.03.2021 15:15	69.75	9'180 [3]	9'180 [3]
Run in hole (RIH) of HTT in double packer configuration	19.03.2021 13:00	45.38	9'180 [3]	9'180 [3]
STA2-1-LIA1	21.03.2021 10:23	66.40	9'180 [3]	9'180 [3]
Repositioning of HTT	24.03.2021 04:47	5.90	9'180 [3]	9'180 [3]
Start testing STA2-1-BDO1 (inflation of the second packer)	24.03.2021 10:41	-	9'180 [3]	-

Flow model evaluation

The hydraulic test sequence was analysed using a radial homogeneous flow model with a time-varying step-changing skin considering the analyses of the Ramey B diagnostic plots for the SW and PW phases and a log-log diagnostic plot for the SWS phase. Figs. B-2 and B-3 show the diagnostic plots of the SW and the PW phases, respectively, with pressures normalised to an assumed static formation pressure of 9'457 kPa. Fig. B-4 provides the log-log diagnostic plot of the SWS with a simple derivative. The derivatives do not provide indication of the presence of a negative skin but the existence of a skin cannot be generally ruled out, especially for the diagnostic of the PW due to the short duration of the test phase. Therefore, a traditional skin model was applied with a step change in the hydraulic conductivity per test phase in a small near-borehole area (K_s). This was supported by early simulations (e.g. during the quick-look analysis), which had shown an improved fit of the simulation to the early measurements using a homogeneous flow model for the formation (K) with a discrete skin on the borehole wall. The SWS phase pressure derivative shows that the response had left the wellbore storage (unit slope) by the end of the test (where the derivative (blue line) begins to deviate from the unit slope in Fig. B-4).

Analysis of the test sequence (SW-SWS-PW)

In the analysis, the temperature changes during all test phases were considered inside the test interval. For the temperature measurement within the test interval, the observation through the memory gauge (T2*) was considered. The parameter optimisation focused on the formation parameter static pressure (P_f) and hydraulic conductivity (K) as well as the thickness of the skin zone (t_s) and the skin hydraulic conductivity (K_s) for each test phase and their specific storage (S_{ss}). The value of the specific storage of the formation (S_s) was not optimised, it was fixed at the theoretical value of 1.4×10^{-6} m^{-1}. After some initial fitting, a perturbation analysis was performed using 2'000 optimisations. A fit discriminant of 1.16 was used to eliminate outliers and to build the base of the uncertainty range estimation. 293 perturbation optimisations were accepted as providing reasonable fits to the data. Figs. B-5 and B-6 present the distribution of the normalised objective function value over the matched formation parameters. Tab. 4-25 shows the best estimates and the resulting uncertainty ranges.

Tab. 4-25: Hydraulic test STA2-1-BDO1: Formation parameter estimation based on the perturbation analysis of the sequence SW-SWS-PW using a radial homogeneous flow model with a time-varying step-changing skin considering the borehole pressure history and temperature changes inside the test interval

[1] Fix theoretical parameter value.

[2] Static formation pressure at the depth of the P2 sensor (778.78 m MD).

SW-SWS-PW results	**K** [m s^{-1}]	**Ss** [1] [m^{-1}]	**P_f** [2] [kPa]
Best estimate	4.3×10^{-13}	1.4×10^{-6}	7'604
Uncertainty range	3.4×10^{-13} – 6.7×10^{-13}	-	7'578 – 7'655

All selected simulations provided lower normalised objective function values as defined by the fit discriminant. Figs. B-7 and B-8 show the Cartesian and Ramey B horsetail plots of the SW respectively, for these 293 simulations. Figs. B-9 and B-10 present the Cartesian and log-log horsetail plots of the SWS. Figs. B-11 and B-12 show the Cartesian and Ramey B horsetail plots of the PW respectively, for these 293 simulations.

Formation parameter estimates and associated uncertainty ranges

The best estimate and the uncertainty ranges for both the static formation pressure and the hydraulic conductivity were derived from the presented analysis of the tests sequence SW-SWS-PW. Further analyses to assess the effect of the borehole pressure history on the uncertainty of the results were not considered due to prior analysis results from other TBO boreholes. The influence of the borehole pressure history is always included in the analysis as described previously (see Tab. 4-24) using pressure records from existing measurements during coring and hydraulic testing. Previous analysis results (in both the BUL1-1 and MAR1-1 boreholes) showed no significant influence of small changes in mud density. The test zone compressibility was determined by a pressure change measured with the QSSP P2 sensor (Fig. B-13) and the associated volume change was clearly defined by the piston volume of the piston pulse generator. Inaccuracies in the determination of the wellbore storage and the associated volume change are thereby reduced to a minimum.

The value of the specific storage was kept at the theoretical value, as the storage properties cannot be reliably determined by a single bore test. However, the chosen parameter will slightly affect the estimation of the hydraulic conductivity and hydraulic head, as the estimates of these parameters are correlated due to the model used. Hence, this effect can be considered in the correct choice of perturbation parameter ranges.

The Jacobian plots (Fig. B-14 presents the longest test phase SWS) show that the sensitivity to K and P_f was still rising at the end of the test phase, indicating that the maximum sensitivity of these parameters was not reached. However, the quantile-normal plot of the residuals for the longest test phase (SWS phase; Fig. B-15) displays a highly normal distribution of residuals. Fig. B-16 presents the distribution of the residuals over time. The residuals are less than 1.3 kPa at early time of the SW and nearly zero during the second half of the SW phase. The SWS residuals are even smaller (less than 0.6 kPa). The PW residuals started at 2.5 kPa but are generally less than 1 kPa, with oscillatory behaviour. All of this information provides good evidence for a well-defined estimate of the hydraulic conductivity of the formation with only minor differences in the near-borehole area (estimated skin thickness of 0.11 m to 0.19 m).

For the STA2-1-BDO1 slug test which was performed with a slim tubing while thermal equilibration in the test tubing was still ongoing, thermal expansion of the fluid in the test tubing below the slim packer needs to be considered for estimating the uncertainty ranges. This process was observed before and after the slug phase (with a pressure increase during shut-in phases between 0.5 and 7 kPa/hour) and, therefore, must also have been occurring during the SW phase, contributing to an unknown portion of the observed slug recovery which cannot be handled by the numerical model used. By attributing too much slug recovery to formation flow, the simulations presumably overestimate the hydraulic conductivity (K). This additional flow does only exist during the slug phase. It does not affect the simulation in phases where the SIT is closed (SWS, PW). However, the pressure recovery of 95 kPa during the SW was well matched by the simulation (Fig. B-7). Furthermore, the subsequent test phases (SWS, PW) could be simulated with equally good quality (Figs. B-7 to B-12) relative to the slug phase (SW). The best estimate and especially the bandwidth of the hydraulic conductivity take into account the uncertainty during the slug phase by reducing the lower limit of the uncertainty range by a factor of three. Tab. 4-26 presents the results of the analysis of the formation parameters for STA2-1-BDO1. The hydraulic conductivity appears to be robustly defined with little uncertainty. The static formation pressure shows a narrow uncertainty range around hydrostatic conditions.

Tab. 4-26: Hydraulic test STA2-1-BDO1: Best estimates for the formation parameters and associated uncertainty ranges

[1] Static formation pressure at midpoint of test interval (792.26 m MD).

Results	**K** [m s^{-1}]	**P_S** [1] [kPa]
Best estimate	4×10^{-13}	7'763
Uncertainty range	$1 \times 10^{-13} – 7 \times 10^{-13}$	7'737 – 7'813

4.5.2 Hydraulic packer test STA2-1-KEU1

The hydraulic packer test STA2-1-KEU1 represents an example of testing in formations with medium to high transmissivity, a short pressure history duration (31.6 h) and a moderate hydraulic test duration (67.4 h). For the analysis, the P2* memory gauge measurements inside the test interval (953.06 m MD) were used.

4.5.2.1 Interval characterisation

The hydraulic test STA2-1-KEU1 was performed in single packer configuration. The entire interval was located in the Klettgau Formation of the Keuper Group. The test interval covered the layers of main interest in the Klettgau Formation, believed to be potentially conductive. The test interval included a small part of the Gruhalde Member, found above the Seebi Member (951.00 – 951.85 m MD) and contained mainly dolomitic marl. The Seebi Member (951.85 – 957.62 m MD) consisted of dolomitic marl (sandy) to dolostone (sandy to silty, argillaceous) and sandy dolostone. The Gruhalde Member found below the Seebi Member (957.62 – 959.06 m MD) contained an alternation of dolomitic marl and dolostone. The Gansingen Member (959.06 – 961.46 m MD) consisted of mostly dolostone and the Ergolz Member (961.46 – 969.87 m MD) included argillaceous marl, sandy marl and sandstone. Finally, a small part of the Bänkerjoch Formation (969.87 – 973.00 m MD) is made up of claystone containing anhydrite nodules (*cf.* Dossier III).

The primary test objectives were to obtain reliable estimates of the hydraulic transmissivity (T), the hydraulic conductivity (K), the freshwater hydraulic head (h_s) / static formation pressure (P_s) and to collect a water sample (if possible). A secondary objective was to derive a suitable flow model. Details of the interval and test duration are provided in Tab. 4-27.

Tab. 4-27: Hydraulic test STA2-1-KEU1: Test interval information

Test	**Depth**		**Length**	**Packer configuration**	**Hydraulic testing**		
	from [m MD]	to [m MD]	[m]		Start date	End date	Duration [h]
STA2-1-KEU1	951.00	973.00	22.00	Single	15.05.2021	18.05.2021	67.4

4.5.2.2 Test execution

Fig. 4-23 shows the system installation record as provided by the field test contractor. The equipment components are those described above (Section 4.2). The hydraulic test tool including the heavy-duty packer system and the piston pulse generator was installed in single packer configuration in borehole STA2-1 on 15.05.2021. The hydraulic test STA2-1-KEU1 was performed directly after reaching a depth of 973 m MD and pulling out of hole (POOH) the coring string. The test interval had been cored with potassium-silicate drilling mud and still contained this mud at the beginning of STA2-1-KEU1. The shut-in tool remained closed during the installation. The test was started by inflating the packer (INF) using a 2:1 mixture of anti-freeze:water. The packer was seated in competent rock within the Gruhalde Member of the Klettgau Formation. The stator for a Netzsch progressive cavity pump was installed in the tubing string at a depth of approximately 293 m MD.

By the time the packer began to isolate the interval volume, the SIT was opened. The COM phase lasted 9 hours and 53 minutes, after which the SIT was again closed to initiate the PSR phase. The PSR phase lasted 3 hours and 33 minutes. After the PSR phase, a slug withdrawal (SW) was initiated which lasted for 3 hours. At the end of the SW, the SIT was closed to initiate a slug-withdrawal shut-in phase (SWS). During the SWS phase, the rotor and sucker rods of the PCP were installed, the tubing was filled, and the PCP drive head was installed in preparation for the pumping phase (RW). The RW was initiated by turning on the PCP and then opening the SIT. The pumping rate was approximately 4.3 l min^{-1} for the first 7 minutes, after which it was increased to approximately 5.8 l min^{-1} and further increased to 8.7 l min^{-1} where it remained for 32 hours. In total the RW lasted 34 hours and 4 minutes before the subsequent pressure recovery (RWS) was initialised by closing the SIT. After 12 hours of pressure recovery, a pulse withdrawal phase of 8 minutes and a pulse injection phase of 12 minutes were performed using a 250 ml piston inside the PPG housing. Both pulse test phases were not used to estimate the wellbore storage because a noticeable recovery occurred even before the piston was fully retracted/extended, which was evident in the deviation from linearity of the pressure decline/rise. The subsequent deflation (DEF) of the packer was carried out with the SIT closed. After sufficient backflow of the packer fluid, the test system was removed from the borehole with a closed SIT.

During the pumping phase (RW), the geochemistry parameters were monitored beginning 11.9 hours after the start of the pumping, when the mud concentration in the produced fluid allowed for proper operation of the sensors. The sampling of produced formation water was completed at 04:00 on 18.05.2021, by which time a total of nearly 16.9 m^3 of water had been pumped. By the end of the RW an hour later, a total of 17.4 m^3 of water had been pumped when the RWS phase was started. The fluid density at the end of the RW phase was measured at 1'015 kg m^{-3}.

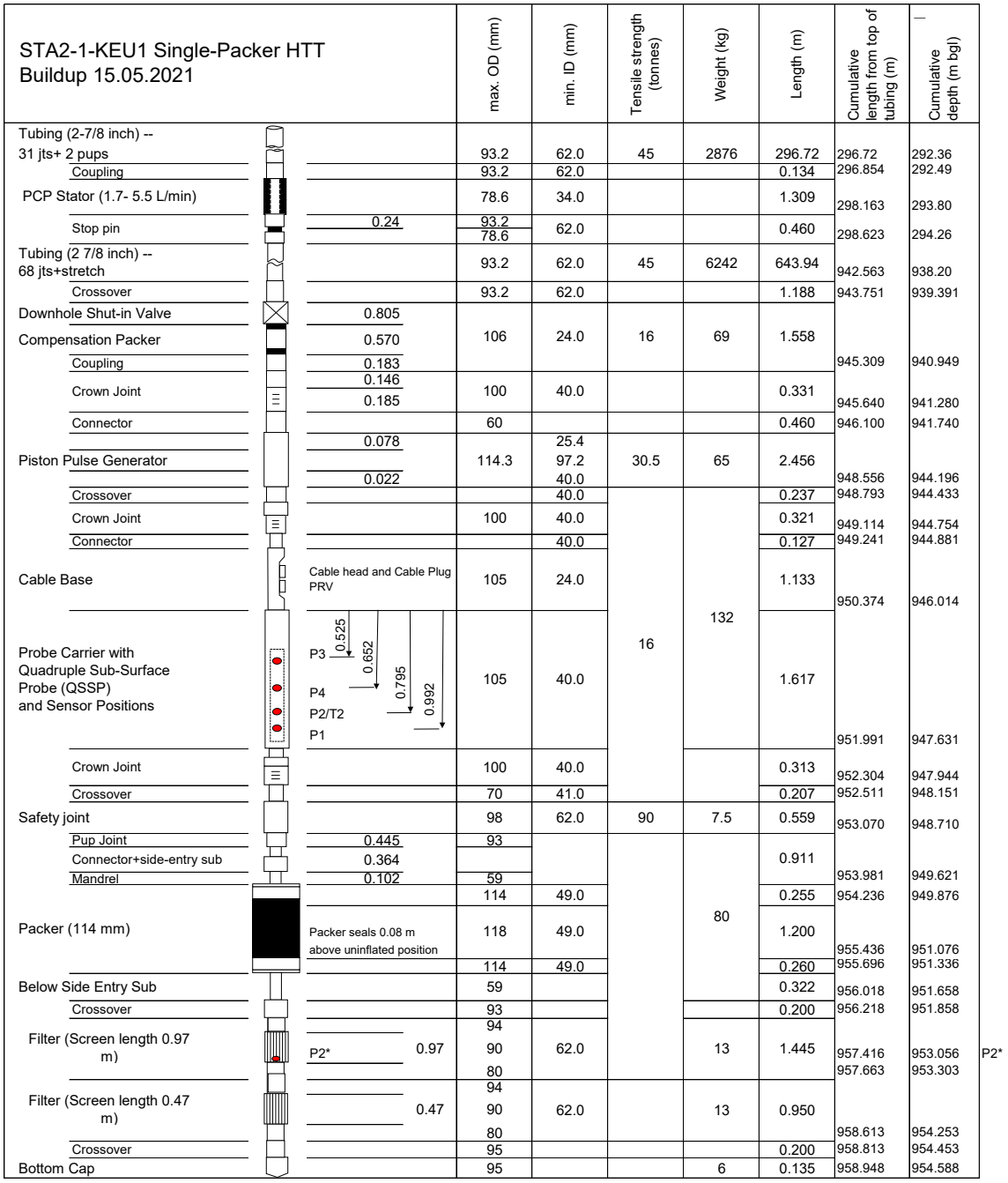

Fig. 4-23: Hydraulic test STA2-1-KEU1: Downhole equipment installation record with system layout as used in the field test

4.5.2.3 Analysis

Borehole pressure history

The borehole history used for the analysis of the STA2-1-KEU1 tests is shown in Fig. B-17 and summarised in Tab. 4-28. The calculation of the mean interval fluid density using the P2 pressure sensor measurement (prior to packer inflation) resulted in a density of 1'168 kg m^{-3}. This value corresponds well to the documented density of the drill mud during drilling (1'180 kg m^{-3}; see Dossier I). For periods without a level measurement, the mud level was assumed to be at the level of the drain pipe, approximately 1.9 m above ground level, because for periods with no active mud circulation (e.g. during POOH), the drillers generally kept the borehole full. During periods of coring, GEODATA monitored the mud circulation pressures using a pressure gauge mounted above the rig floor. These pressures were extrapolated to the depth of the memory gauge P2* transducer (953.06 m MD). Once the HTT arrived at the required test depth for hydraulic test STA2-1-KEU1, the P2* memory gauge pressure measurement could be used directly.

Tab. 4-28: Hydraulic test STA2-1-KEU1: Borehole pressure history

[1] Interval pressure (absolute) at P2* memory gauge level (953.06 m MD) measured or calculated from the history information, e.g. fluid level and density.

[2] Drilling through top of interval (951.00 m MD).

[3] Pressure measured when the borehole was filled with mud (e.g. when P2* arrived at test depth).

Description	**Start date and time**	**Duration** [h]	**Pressure**[1] [kPa]	
		Total: 41.18	**Start**	**End**
Drilling[2]	14.05.2021 04:47	19.68	12'111	11'051 [3]
Pull out of hole (POOH) of coring string	15.05.2021 00:30	5.00	11'051 [3]	11'051 [3]
Installation and run in hole (RIH) of HTT in single packer configuration	15.05.2021 05:30	16.50	11'051 [3]	11'051 [3]
Start testing STA2-1-KEU1	15.05.2021 22:00	-	11'051 [3]	-

Flow model evaluation

The evaluation of the flow model approach was based on the SW and RWS phases. Figs. B-18 and B-19 show the Ramey B diagnostic plot of the SW with pressures normalised to an assumed P_f value of 8'751 kPa and the log-log diagnostic plot of the RWS. In Fig. B-18 the absence of any inflection in the early-time derivative data in the Ramey B plot suggests that any skin that might have been present was positive, not negative. The log-log diagnostic plot of the RWS data (Fig. B-19) shows that the pressure derivative displays no period with a unit slope and stabilised rapidly, indicating infinite acting radial flow (IARF). The late-time derivative showed a small oscillation that might reflect some degree of heterogeneity in the formation, first a small decrease and then a small increase in the hydraulic conductivity as the radius of influence of the test expanded. The absence of an early-time unit slope that would reflect the wellbore storage and the absence of a hump in the derivative before stabilisation indicates the absence of any significant positive skin on the wellbore. However, a homogeneous flow model with a time-dependent discrete skin zone was used for the analysis in order to account for changes in the near surrounding of the borehole during the period of testing, especially pumping.

Analysis of the test sequence (SW-SWS)

In this analysis, the borehole history and the temperature change during test phases was considered inside the test interval. Fig. B-20 shows the development of the downhole temperature as measured by the memory gauge (T2*) and by the QSSP sensor T2 as well as the pressure of the P2 probe on the QSSP and the P2* memory gauge.

After the analysis of the slug phase (SW), the test sequence SW-SWS was analysed by a homogeneous model with test-phase-dependent skin hydraulic conductivity (K_s). The pressure measurements were matched while optimising the following: formation hydraulic conductivity (K) and the skin hydraulic conductivity during the slug and slug recovery phases K_s(SW) and K_s(SWS) respectively, the static formation pressure (P_f), the specific storage of the skin zone (S_{ss}) and the skin thickness (t_s). For the times of the borehole history, when the hydraulic gradient was directed out of the borehole, skin hydraulic conductivity was specified to be 1×10^{-13} m s^{-1} to keep drilling mud invasion in the formation low, in accordance with the observation of no mud losses during coring. The specific storage value of the formation was fixed to the theoretical value of 1.4×10^{-6} m^{-1}. A perturbation analysis of 750 optimisations was performed and all parameters showed clear minima for the optimised parameters. Figs. B-21 and B-22 illustrate this by showing the distribution of the normalised objective function value (normalised fit value) over the formation hydraulic conductivity and static formation pressure, respectively. For definition of the resultant parameter uncertainties, a fit discriminant of 1.07 was defined to isolate the observed minima of the objective function. This resulted in 479 optimisations that were accepted as providing reasonable matches on the recorded pressure measurements. Tab. 4-29 shows the resulting best estimates for the formation parameters and their ranges.

Tab. 4-29: Hydraulic test STA2-1-KEU1: Formation parameter estimation based on the perturbation analysis of test sequence SW-SWS using a radial homogenous flow model with time-dependent skin considering the borehole pressure history and temperature changes inside the test interval

[1] Fixed to the theoretical value in order to reduce the number of correlated fitting parameters.

[2] Static formation pressure (absolute) at depth of the P2* memory gauge (953.06 m MD).

SW-SWS results	**K** [m s^{-1}]	**Ss** [1] [m^{-1}]	**P_f** [2] [kPa]
Best estimate	5.7×10^{-8}	1.4×10^{-6}	8'752
Uncertainty range	4.9×10^{-8} – 5.9×10^{-8}	-	8'751 – 8'753

Figs. B-23 and B-24 show the 479 simulations that were used as the basis for determining the uncertainty ranges and whose normalised objective function values were lower than the defined value of the fit discriminant for the SW and SWS phases. Figs. B-25 and B-26 show the Ramey A and Ramey B horsetail plots, respectively, of the SW phase and Fig. B-27 presents the log-log horsetail plot of the SWS phase. Fig. B-28 shows that the static formation pressure is negatively correlated with the formation hydraulic conductivity, though in very narrow ranges.

Analysis of the sequence (RW-RWS)

In the analysis of the RW-RWS sequence, the borehole history and the temperature changes during test phases were considered inside the test interval. Fig. B-20 shows the development of the downhole temperature and pressure as measured by the memory gauge sensors inside the test

interval (T2* and P2*). Note that the analysis used the P2* measurements as erratic behaviour indicated a malfunction of the QSSP P2 gauge. The pressure measurements were matched while optimising the following parameters: the formation hydraulic conductivity (K), five different skin hydraulic conductivity values (one value for the history period including SW and SWS, two values during, and one value at the end of the pumping phase, and one value during the subsequent pressure recovery phase), the static formation pressure (P_f), the specific storage of the skin zone (S_{ss}) and the skin thickness (t_s). The five different skin hydraulic conductivities were included to capture the effect that drilling mud creates on a skin that changes with time (as the hydraulic gradient changes, especially the direction) and the effect of cleaning the formation while pumping. The specific storage value of the formation was fixed to the theoretical value of 1.4×10^{-6} m^{-1} and a perturbation analysis of 1'000 optimisations was performed.

Figs. B-29 and B-30 show the distribution of the normalised objective function values (normalised fit value) for the 950 optimisation results, with a normalised objective function value less than 2.4 over the hydraulic conductivity of the formation and static formation pressure, respectively. For the definition of the resulting parameter uncertainties, a fit discriminant of 1.02 was defined to isolate the observed minima of the objective function that resulted in 467 optimisations being considered as the basis for the estimation of the uncertainty ranges. Tab. 4-30 presents the resulting best estimates for the formation parameters and their uncertainty ranges which are in good agreement with the results from the SW-SWS analysis.

Tab. 4-30: Hydraulic test STA2-1-KEU1: Formation parameter estimation based on the perturbation analysis of test sequence RW-RWS using a radial homogenous flow model with time-dependent skin considering the borehole pressure history and temperature changes inside the test interval

[1] Fixed in order to reduce the number of correlated fitting parameters.

[2] Static formation pressure (absolute) at depth of P2* memory gauge (953.06 m MD).

RW-RWS results	**K** [m s^{-1}]	**Ss** [1] [m^{-1}]	**P_f** [2] [kPa]
Best estimate	5.84×10^{-8}	1.4×10^{-6}	8'704
Uncertainty range	5.84×10^{-8} – 5.85×10^{-8}	-	8'701 – 8'705

Figs. B-31 and B-32 show horsetail plots of the 467 simulations used as the basis for the determination of the uncertainty ranges, i.e. with lower normalised objective function values as defined by the fit discriminant, for the RW and the RWS phases. Fig. B-33 shows the log-log horsetail plot of the RWS phase.

Influence of the history period assumptions on the formation parameter estimates

For the presented analysis of the SW-SWS sequence, the skin hydraulic conductivity was fixed during the history, on the one hand to account for the observation of no mud losses during coring and, on the other hand, in order to reduce the number of free parameters needed in the optimisation process. To evaluate the effect of this assumption on the formation parameter estimates, two additional forward simulations of the slug and slug recovery sequence (SW-SWS) were performed using an upper and lower estimate for the hydraulic conductivity of the skin during the history times. A range of four orders of magnitude was studied for K_s(history) between 1×10^{-15} and 1×10^{-11} m s^{-1}. Figs. B-34 and B-35 show the simulated pressures using the best-fit parameter sets

from the SW-SWS analyses substituting different values for K_s(history). A visual inspection shows that fixing K_s(history) at a value of 1×10^{-13} m s^{-1} has no significant effect on the analysis results for the STA2-1-KEU1 tests.

Formation parameter estimates and associated uncertainty ranges

The influence of the borehole history was always included in the analyses of all tests. Variations in the borehole history were not simulated due to the availability of existing measurements during coring as well as the estimated formation transmissivity. Disturbances of the pressure field by a pressure history are of short duration in formations with medium to high transmissivity. The influence of the test zone compressibility on the test results was also very limited due to the estimated formation transmissivity. Therefore, a sampling analysis to account for inaccuracies in the determination of the wellbore storage was not required. As storage properties cannot be reliably determined from a single-borehole test, the specific storage value of the formation was fixed to the theoretical value. The uncertainties in the other formation parameters, due to the correlations between these parameters, were considered to be negligible.

The best estimates for the hydraulic properties represent the geometric mean for the formation hydraulic conductivity and the arithmetic mean for the static formation pressure of the best estimates from all simulations of STA2-1-KEU1. Tab. 4-31 shows the results. The uncertainty ranges represent the overall ranges from the analysis of all STA2-1-KEU1 test phases.

Tab. 4-31: Hydraulic test STA2-1-KEU1: Best estimates of the formation parameters and associated uncertainty ranges

[1] Static formation pressure at midpoint of test interval (962.00 m MD) assuming an interval fluid density of 1'015 kg m^{-3} (finally measured density of RW) for minimum value and best estimate, 1'180 kg m^{-3} for maximum value (drilling mud during SW-SWS) for the calculation.

Results	**K** [m s^{-1}]	**P_S** [1] [kPa]
Best estimate	6.0×10^{-8}	8'720
Uncertainty range	4.9×10^{-8} – 6.6×10^{-8}	8'686 – 8'752

The subsequent hydraulic test STA2-1-KEU2 was conducted in an interval starting at 941.50 m MD and extending to a depth of 962.04 m MD. Therefore, the test interval included the same lithological members of the Kettgau Formation as STA2-1-KEU1, excluding the main part of the Ergolz Member starting at 961.46 m MD. The Ergolz Member was described by the cores as an argillaceous marl (silty, dolomitic) between 961.46 m MD and 962.85 m MD. The deeper parts were characterised as sandy marl, underlain by sandstone and sandstone with siliciclastic rock (*cf.* Dossier III). The STA2-1-KEU2 lithological members represent a formation with low transmissivity and a best estimate of 6.5×10^{-12} m s^{-1} was calculated for the hydraulic conductivity that ranged between 7.0×10^{-13} m s^{-1} and 1.4×10^{-10} m s^{-1}. According to this result, the results of STA2-1-KEU1 can be attributed to the hydraulic properties of the Ergolz Member (*cf.* Dossier III). Tab. 4-32 shows the results of the hydraulic conductivity under the assumption that only the part of the Ergolz Member not included in the STA2-1-KEU2 interval (7.83 m) contributed to the high transmissivity estimated by the hydraulic test STA2-1-KEU1.

Tab. 4-32: Hydraulic test STA2-1-KEU1: Best estimates of the formation parameters and associated uncertainty ranges under the assumption that only the lower 7.83 m of the Ergolz Member contributed to the observed high transmissivity

[1] Static formation pressure at midpoint of test interval (962.00 m MD) assuming an interval fluid density of 1'015 kg m^{-3} (finally measured density of RW) for minimum value and best estimate, 1'180 kg m^{-3} for maximum value (drilling mud during SW-SWS) for the calculation.

Results	**K** [m s^{-1}]	**P_S** [1] [kPa]
Best estimate	1.7×10^{-7}	8'720
Uncertainty range	1.4×10^{-7} – 1.8×10^{-7}	8'686 – 8'752

4.6 Summary and discussion of hydraulic tests

4.6.1 Summary tables and plots

The results of the transmissivity and hydraulic conductivity estimates for all tested intervals are summarised in Tab. 4-33. The estimated freshwater hydraulic heads and static formation pressures are documented in Tab. 4-34. Both tables present the best estimates along with confidence ranges as determined by the field test contractor and are documented in the corresponding reports.

The permeabilities for all tested intervals are summarised in Tab. 4-35 and were calculated based on the hydraulic conductivities provided in Tab. 4-33. An assumed density of 1'000 kg m^{-3} and dynamic viscosity of 1×10^{-3} Pa s were used for the calculation of the hydraulic permeability values.

The hydraulic parameters T, K, P_S and h_S (in terms of m bgl and m asl) are illustrated with respect to the borehole depth (in m MD) and the geological profile in Figs. 4-24 to 4-28. The best estimates for these parameters are indicated by vertical lines within the corresponding interval position. The associated confidence ranges are shown as dashed rectangles, delimited vertically by the corresponding interval extent and laterally by the minimum and maximum values.

Tab. 4-33: Summary of hydraulic packer testing in borehole STA2-1: Transmissivity and hydraulic conductivity

[1] Based on the results presented by the field test contractor in the corresponding report.

[2] Tests STA2-1-OPA2 and STA2-1-OPA4 were performed in comparable test intervals. Due to artificially induced overpressures, test STA2-1-OPA4 did not provide representative hydraulic parameters.

Test interval details and hydraulic model							**Transmissivity and hydraulic conductivity**					
Test name	**Interval depth**				**Interval length**	**Hydraulic model**	**Best estimate[1]**		**Lowest estimate[1]**		**Highest estimate[1]**	
	From [m MD]	**To** [m MD]	**From** [m asl]	**To** [m asl]	[m]		**T** [$m^2 s^{-1}$]	**K** [$m s^{-1}$]	T_{min} [$m^2 s^{-1}$]	K_{min} [$m s^{-1}$]	T_{max} [$m^2 s^{-1}$]	K_{max} [$m s^{-1}$]
STA2-1-MAL1	473.50	542.67	-55.52	-124.69	69.17	radial-composite with time-varying step-change skin, time dependent c_{tz}	2×10^{-07}	3×10^{-09}	1×10^{-07}	2×10^{-09}	2×10^{-07}	3×10^{-09}
STA2-1-BDO3	744.68	763.00	-326.70	-345.02	18.32	homogeneous, time-varying step-change skin	6×10^{-14}	3×10^{-15}	3×10^{-14}	1×10^{-15}	3×10^{-13}	2×10^{-14}
STA2-1-BDO2	763.48	781.80	-345.50	-363.82	18.32	homogeneous, time-varying step-change skin	5×10^{-09}	3×10^{-10}	1×10^{-09}	7×10^{-11}	9×10^{-09}	5×10^{-10}
STA2-1-BDO1	783.10	801.42	-365.12	-383.44	18.32	homogeneous, time-varying step-change skin	8×10^{-12}	4×10^{-13}	2×10^{-12}	1×10^{-13}	1×10^{-11}	7×10^{-13}
STA2-1-OPA2[2]	822.00	839.11	-404.02	-421.13	17.11	homogeneous, time-varying skin	3×10^{-13}	2×10^{-14}	1×10^{-13}	1×10^{-14}	6×10^{-13}	3×10^{-14}
STA2-1-OPA4[2]	822.00	839.13	-404.02	-421.15	17.13	-	-	-	-	-	-	-
STA2-1-OPA1	881.50	899.82	-463.52	-481.84	18.32	homogeneous, time-varying step-change skin	5×10^{-13}	3×10^{-14}	3×10^{-13}	2×10^{-14}	8×10^{-13}	4×10^{-14}
STA2-1-OPA3	882.30	888.55	-464.32	-470.57	6.25	homogeneous, time-varying step-change skin	1×10^{-13}	2×10^{-14}	5×10^{-14}	9×10^{-15}	3×10^{-13}	4×10^{-14}
STA2-1-LIA1	904.00	922.32	-486.02	-504.34	18.32	homogeneous, time-varying step-change skin	2×10^{-12}	9×10^{-14}	1×10^{-12}	5×10^{-14}	3×10^{-12}	2×10^{-13}
STA2-1-LIA2	924.40	936.00	-506.42	-518.02	11.60	homogeneous, time-varying step-change skin	6×10^{-12}	5×10^{-13}	1×10^{-12}	1×10^{-13}	2×10^{-11}	1×10^{-12}
STA2-1-KEU2	941.50	962.04	-523.52	-544.06	20.54	homogeneous, time-varying step-change skin	1×10^{-10}	7×10^{-12}	1×10^{-11}	7×10^{-13}	3×10^{-09}	2×10^{-10}
STA2-1-KEU1	951.00	973.00	-533.02	-555.02	22.00	homogeneous, time-varying step-change skin	1×10^{-06}	6×10^{-08}	1×10^{-06}	4×10^{-08}	2×10^{-06}	7×10^{-08}
STA2-1-MUK1	1'058.80	1'117.00	-640.82	-699.02	58.20	radial composite, time-varying skin, linear changing K	2×10^{-06}	3×10^{-08}	1×10^{-06}	2×10^{-08}	4×10^{-06}	7×10^{-08}

Tab. 4-34: Summary of hydraulic packer testing in borehole STA2-1: Hydraulic head estimates

[1] Based on the results presented by the field test contractor in the corresponding report.

[2] Tests STA2-1-OPA2 and STA2-1-OPA4 were performed in comparable test intervals. Due to artificially induced overpressures, test STA2-1-OPA4 did not provide representative hydraulic parameters.

Test interval details and hydraulic model							**Hydraulic head** [m bgl]			**Hydraulic head** [m asl]			**Formation pressure**		
Test name	**Interval depth**				**Interval length**	**Hydraulic model**	**Best[1] h**	**Lowest[1] h_{min}**	**Highest[1] h_{max}**	**Best[1] h**	**Lowest[1] h_{min}**	**Highest[1] h_{max}**	**Best[1] P_S**	**Lowest[1] $P_{S\,min}$**	**Highest[1] $P_{S\,max}$**
	From [m MD]	**To** [m MD]	**From** [m asl]	**To** [m asl]	[m]		[m bgl]	[m bgl]	[m bgl]	[m asl]	[m asl]	[m asl]	[kPa]	[kPa]	[kPa]
STA2-1-MAL1	473.50	542.67	-55.52	-124.69	69.17	radial-composite with time-varying step-change skin, time dependent c_{tz}	50	53	45	368	365	373	4'497	4'464	4'543
STA2-1-BDO3	744.68	763.00	-326.70	-345.02	18.32	homogeneous, time-varying step-change skin	-239	-184	-315	657	602	733	9'741	9'196	10'486
STA2-1-BDO2	763.48	781.80	-345.50	-363.82	18.32	homogeneous, time-varying step-change skin	-128	-115	-148	546	533	566	8'835	8'708	9'029
STA2-1-BDO1	783.10	801.42	-365.12	-383.44	18.32	homogeneous, time-varying step-change skin	1	4	-4	417	414	422	7'763	7'737	7'813
STA2-1-OPA2[2]	822.00	839.11	-404.02	-421.13	17.11	homogeneous, time-varying skin	-487	-427	-561	905	845	979	12'925	12'338	13'648
STA2-1-OPA4[2]	822.00	839.13	-404.02	-421.15	17.13	-	-	-	-	-	-	-	-	-	-
STA2-1-OPA1	881.50	899.82	-463.52	-481.84	18.32	homogeneous, time-varying step-change skin	-532	-496	-550	950	914	968	13'952	13'599	14'137

Tab. 4-34: continued

[1] Based on the results presented by the field test contractor in the corresponding report.

Test interval details and hydraulic model							**Hydraulic head** [m bgl]			**Hydraulic head** [m asl]			**Formation pressure**		
Test name	**Interval depth**				**Interval length**	**Hydraulic model**	**Best[1] h**	**Lowest[1] h_{min}**	**Highest[1] h_{max}**	**Best[1] h**	**Lowest[1] h_{min}**	**Highest[1] h_{max}**	**Best[1] P_S**	**Lowest[1] $P_{S\,min}$**	**Highest[1] $P_{S\,max}$**
	From [m MD]	**To** [m MD]	**From** [m asl]	**To** [m asl]	[m]		[m bgl]	[m bgl]	[m bgl]	[m asl]	[m asl]	[m asl]	[kPa]	[kPa]	[kPa]
STA2-1-OPA3	882.30	888.55	-464.32	-470.57	6.25	homogeneous, time-varying step-change skin	-824	-503	-1'162	1242	921	1'580	16'767	13'620	20'086
STA2-1-LIA1	904.00	922.32	-486.02	-504.34	18.32	homogeneous, time-varying step-change skin	-227	-193	-279	645	611	697	11'184	10'848	11'693
STA2-1-LIA2	924.40	936.00	-506.42	-518.02	11.60	homogeneous, time-varying step-change skin	-128	-103	-141	546	521	559	10'384	10'136	10'505
STA2-1-KEU2	941.50	962.04	-523.52	-544.06	20.54	homogeneous, time-varying step-change skin	76	118	55	342	300	363	8'592	8'181	8'795
STA2-1-KEU1	951.00	973.00	-533.02	-555.02	22.00	homogeneous, time-varying step-change skin	73	77	70	345	341	348	8'720	8'686	8'752
STA2-1-MUK1	1'058.80	1'117.00	-640.82	-699.02	58.20	radial composite, time-varying skin, linear changing K	64	68	62	354	350	356	10'044	10'008	10'069

Tab. 4-35: Summary of hydraulic packer testing in borehole STA2-1: Permeability

[1] The calculation is based on the hydraulic conductivity provided by the field test contractor in the corresponding DR and standard conditions (density: 1'000 kg m^{-3}, dynamic viscosity: 1×10^{-3} Pa s).

[2] Based on the results presented by the field test contractor in the corresponding report.

[3] Tests STA2-1-OPA2 and STA2-1-OPA4 were performed in comparable test intervals. Due to artificially induced overpressures, test STA2-1-OPA4 did not provide representative hydraulic parameters.

Test interval details						**Permeability estimates**[1]		
Test name	**Interval depth**				**Interval length**	**Best**[2] **k**	**Lowest**[2] k_{min}	**Highest**[2] k_{max}
	From [m MD]	**To** [m MD]	**From** [m asl]	**To** [m asl]	[m]	[m^2]	[m^2]	[m^2]
STA2-1-MAL1	473.5	542.67	-55.52	-124.69	69.17	3×10^{-16}	2×10^{-16}	3×10^{-16}
STA2-1-BDO3	744.68	763	-326.7	-345.02	18.32	3×10^{-22}	1×10^{-22}	2×10^{-21}
STA2-1-BDO2	763.48	781.8	-345.5	-363.82	18.32	3×10^{-17}	7×10^{-18}	5×10^{-17}
STA2-1-BDO1	783.1	801.42	-365.12	-383.44	18.32	4×10^{-20}	1×10^{-20}	7×10^{-20}
STA2-1-OPA2 [3]	822	839.11	-404.02	-421.13	17.11	2×10^{-21}	1×10^{-21}	3×10^{-21}
STA2-1-OPA4 [3]	822	839.13	-404.02	-421.15	17.13	-	-	-
STA2-1-OPA1	881.5	899.82	-463.52	-481.84	18.32	3×10^{-21}	2×10^{-21}	4×10^{-21}
STA2-1-OPA3	882.3	888.55	-464.32	-470.57	6.25	2×10^{-21}	9×10^{-22}	4×10^{-21}
STA2-1-LIA1	904	922.32	-486.02	-504.34	18.32	1×10^{-20}	5×10^{-21}	2×10^{-20}
STA2-1-LIA2	924.4	936	-506.42	-518.02	11.6	5×10^{-20}	1×10^{-20}	1×10^{-19}
STA2-1-KEU2	941.5	962.04	-523.52	-544.06	20.54	7×10^{-19}	7×10^{-20}	2×10^{-17}
STA2-1-KEU1	951	973	-533.02	-555.02	22	6×10^{-15}	4×10^{-15}	7×10^{-15}
STA2-1-MUK1	1'058.8	1'117	-640.82	-699.02	58.2	3×10^{-15}	2×10^{-15}	7×10^{-15}

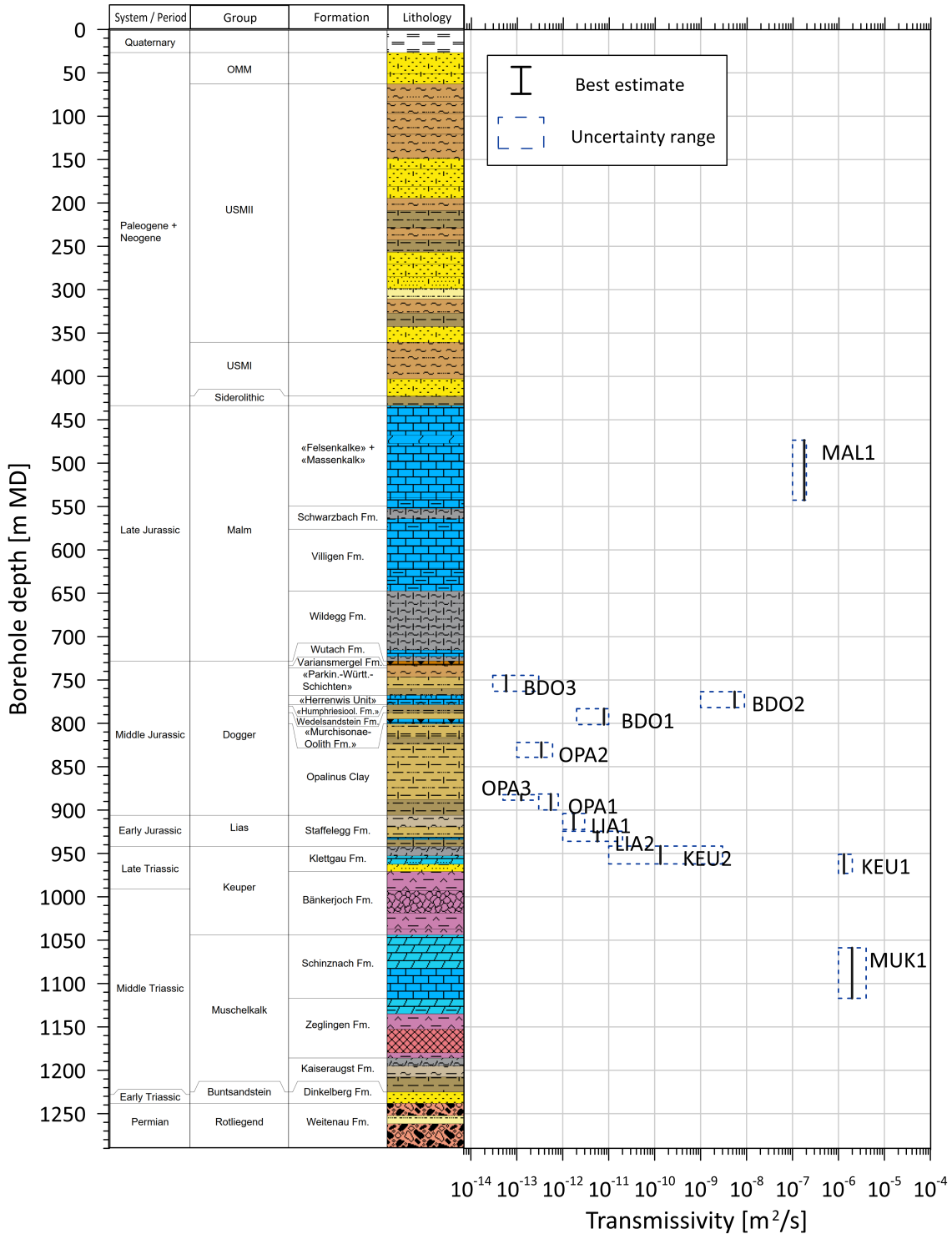

Fig. 4-24: Summary of hydraulic testing in borehole STA2-1: Formation transmissivity profile

Tests STA2-1-OPA2 and STA2-1-OPA4 were performed in comparable test intervals. Due to artificially induced overpressures, test STA2-1-OPA4 did not provide representative hydraulic parameters.

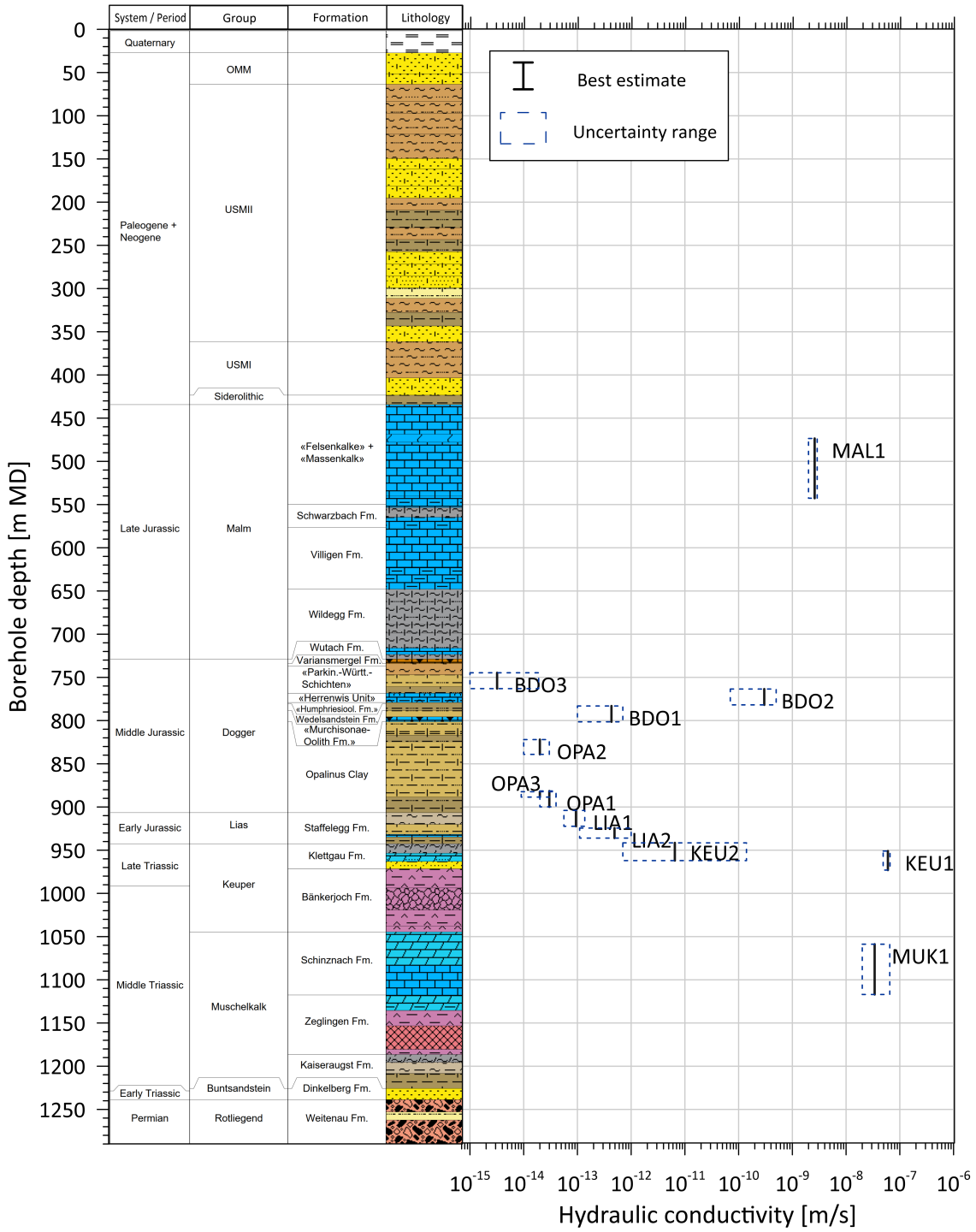

Fig. 4-25: Summary of hydraulic testing in borehole STA2-1: Formation hydraulic conductivity profile

Tests STA2-1-OPA2 and STA2-1-OPA4 were performed in comparable test intervals. Due to artificially induced overpressures, test STA2-1-OPA4 did not provide representative hydraulic parameters.

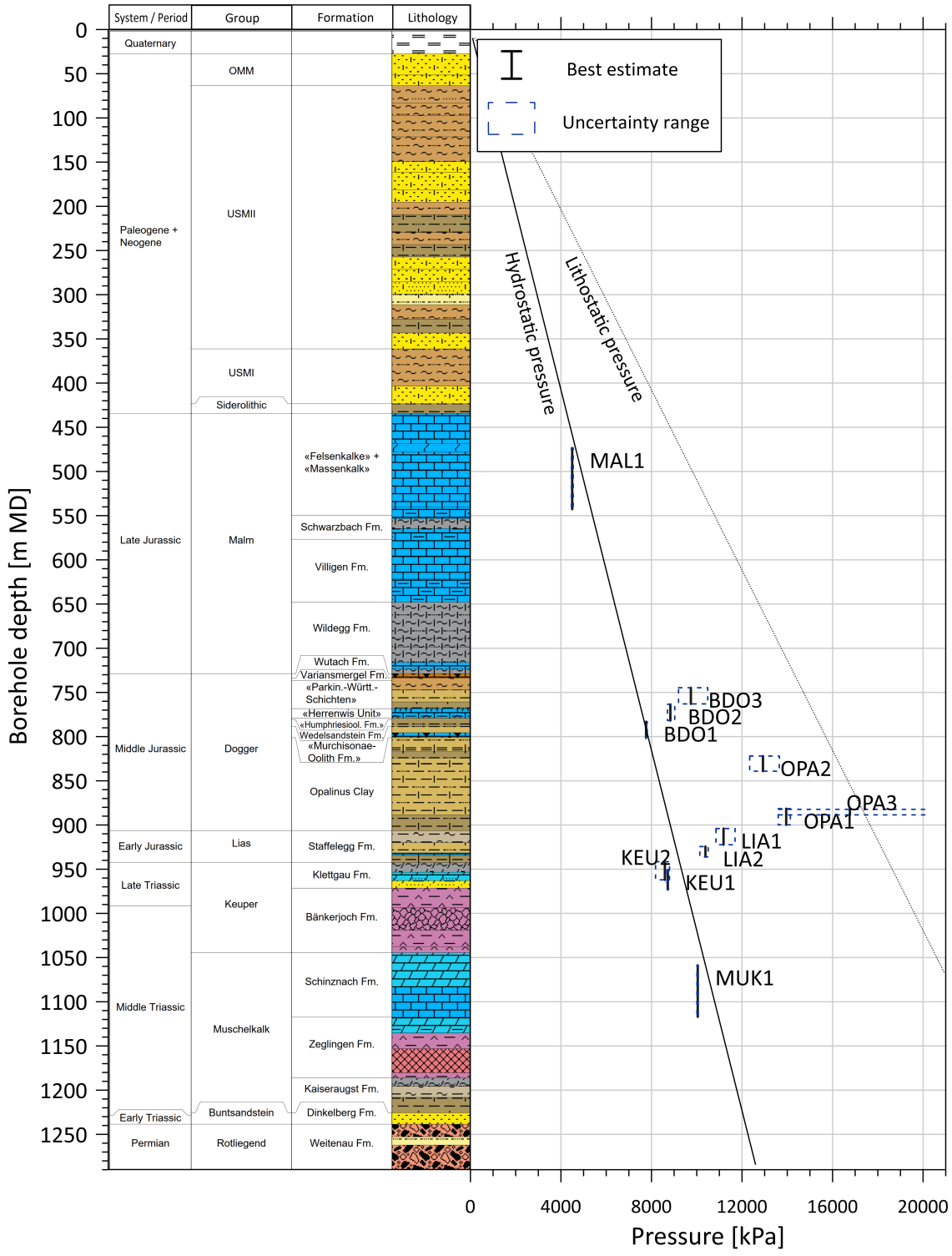

Fig. 4-26: Summary of hydraulic testing in borehole STA2-1: Static formation pressure profile

The lithostatic pressure is based on the assumption of a mean density of 2'000 kg m^{-3}.

Tests STA2-1-OPA2 and STA2-1-OPA4 were performed in comparable test intervals. Due to artificially induced overpressures, test STA2-1-OPA4 did not provide representative hydraulic parameters.

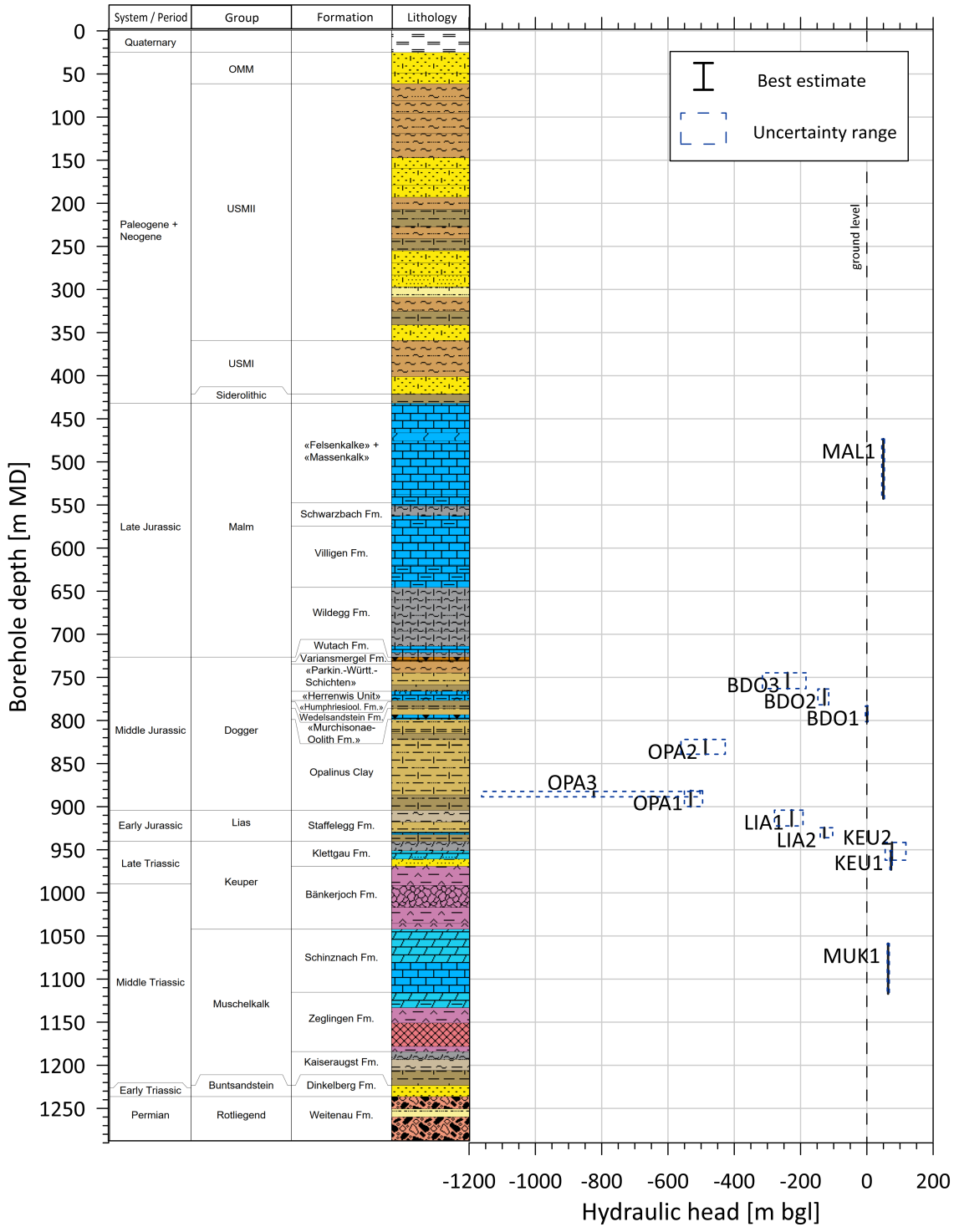

Fig. 4-27: Summary of hydraulic testing in borehole STA2-1: Formation hydraulic head profile (m bgl)

Tests STA2-1-OPA2 and STA2-1-OPA4 were performed in comparable test intervals. Due to artificially induced overpressures, test STA2-1-OPA4 did not provide representative hydraulic parameters.

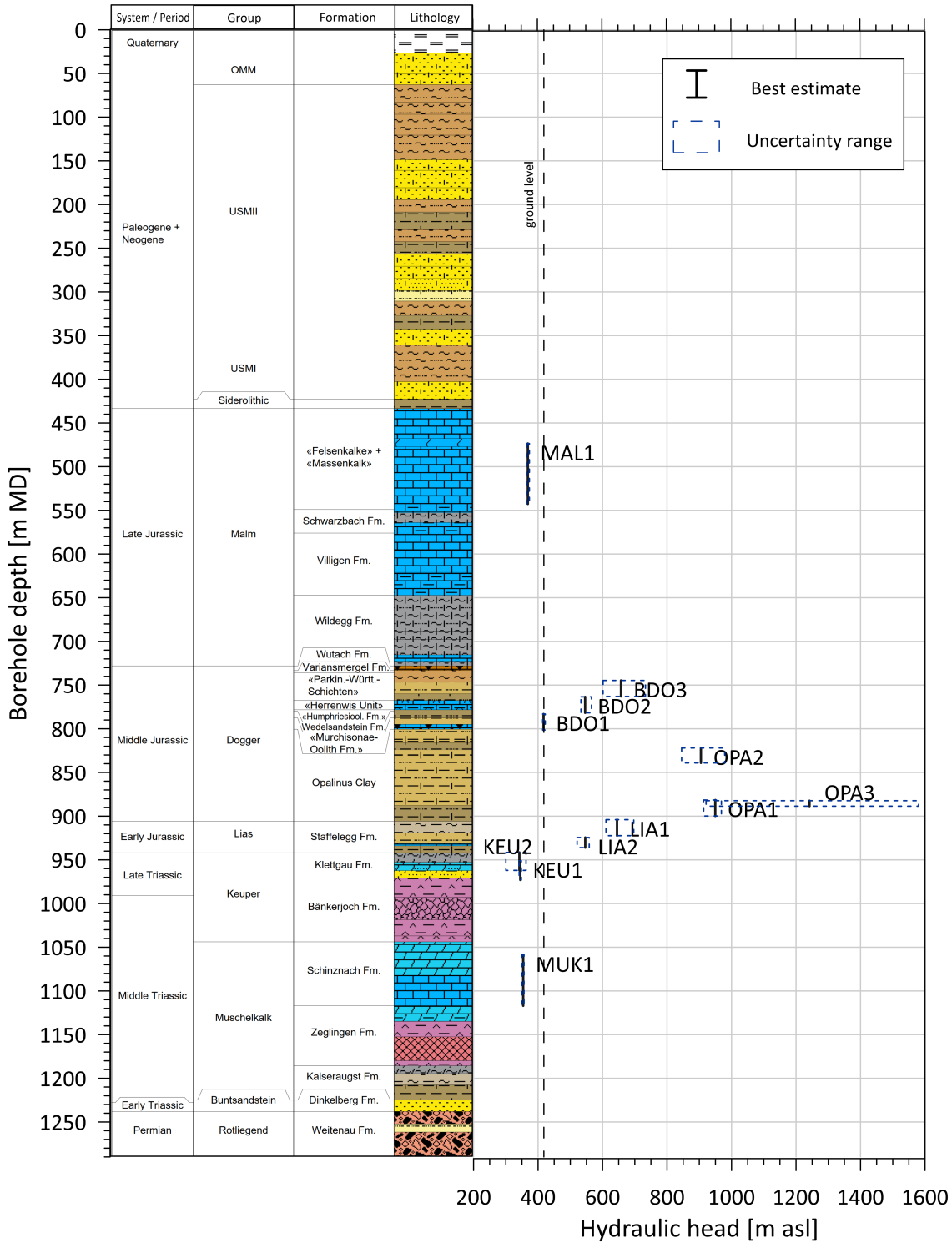

Fig. 4-28: Summary of hydraulic testing in borehole STA2-1: Formation hydraulic head profile (m asl)

Tests STA2-1-OPA2 and STA2-1-OPA4 were performed in comparable test intervals. Due to artificially induced overpressures, test STA2-1-OPA4 did not provide representative hydraulic parameters.

4.6.2 Discussion of data and test results

One hydraulic test focused on the «Felsenkalke» + «Massenkalk» as part of the Malm Group in borehole STA2-1 and took place after the fluid logging campaign (discussed in Chapter 3 above). As a result of the fluid logging campaign, the packer test interval was chosen to investigate the main inflow zones (between 475 – 500 m MD and 515 – 530 m MD) of the logged borehole section between 466 m MD and 670 m MD covering zones with abundant karst features, mostly filled with claystone (*cf.* Dossier III). The resulting best estimate of the transmissivity for the hydraulic test STA2-1-MAL1 (2.1×10^{-7} m^2 s^{-1}) confirms that the main inflow was captured by the hydraulic packer test. The packer test analysis results correspond well to the result of the analysis of the pump phase during fluid logging (transmissivity of approx. 8.9×10^{-8} m^2 s^{-1}) which were derived using a simple radially homogeneous analysis approach. The analysis of test STA2-1-MAL1 used a homogeneous flow model with time-varying skin producing clearly and narrowly defined estimates of the formation hydraulic properties which are considered more robust than the results of the fluid logging. The remaining uncertainty with respect to the estimates of the formation conductivity (not transmissivity) relates to the thickness of the formation really contributing to the hydraulic responses. While the interval tested spanned 69.17 m, the fluid logging that preceded the testing estimated five inflow zones of limited vertical extent. The hydraulic conductivity of the associated fractures must be higher than the average hydraulic conductivity estimated for the entire STA2-1-MAL1 test interval. Test STA2-1-MAL1 allowed for the successful production of a formation water sample.

The «Brauner Dogger» (Dogger Group excluding the Opalinus Clay) was studied by three hydraulic tests carried out during a series of hydraulic tests. The test STA2-1-BDO1 was performed after test STA2-1-LIA1 and was followed by tests STA2-1-BDO2 and STA2-1-BDO3. An analysis of STA2-1-BDO1 is presented in more detail in Section 4.5.1. The tests included slug and slug recovery phases as main test events which were analysed together with a preceding or following test phase (PSR or PW phase) as test sequence. The measurement results for all three test intervals were analysed using radial homogeneous flow models with a discrete time-dependent skin. Furthermore, a fracture flow model was established for STA2-1-BDO2 to test the fracture flow hypothesis from the flow diagnostics, but it did not provide reasonable agreement with the measurements. The best estimates for the hydraulic parameters illustrate large differences. For the interval STA2-1-BDO2, a best estimate of the formation hydraulic conductivity of 3×10^{-10} m s^{-1} was calculated. For intervals STA2-1-BDO1 and –BDO3, the calculated hydraulic conductivities were three and five orders of magnitude lower respectively. The uncertainty ranges were small and did not overlap. The differences in the best estimates for the hydraulic head also reflect the large differences inside the lithological group. The uncertainty is small for STA2-1-BDO1 and STA2-1-BDO2 based on the perturbation results, even if they differ greatly in value. For test STA2-1-BDO1 the estimated hydraulic head is close to ground level. The large uncertainty on the estimation of the hydraulic head for STA2-1-BDO3 seems to reflect the difficulties in the estimation of heads within low permeable formations, likely caused by a combination of factors, e.g. the duration of history vs. testing, or poroelastic effects. Taking the lithology of the tested intervals into account, the results for STA2-1-BDO2 may be attributed to the «Herrenwis Unit», a unit of approximately 11 m thickness found within the test interval (*cf.* Dossier III). The results of test STA2-1-BDO1 may be attributed to the «Murchisonae-Oolith Formation» and the interval STA2-1-BDO3 was entirely in the «Parkinsoni-Württembergica-Schichten».

The Opalinus Clay was tested within borehole STA2-1 using a total of four hydraulic tests. Test STA2-1-OPA1 consisted of a slug test followed by a slug recovery phase and a pulse test, STA2-1-OPA2 was performed as a sequence of two pulse tests. STA2-1-OPA3 consisted of one pulse test and was extended by the execution of a GTPT that is not part of this documentation. After the GTPT a second test sequence consisting of two pulse tests was performed. However, it

appeared that the test interval was not isolated during the second hydraulic test sequence. Therefore, no analysis of the second test sequence of STA2-1-OPA3 was performed. Test STA2-1-OPA4 was performed in a test interval at about the same depth as STA2-1-OPA2 and started with a fluid exchange over the upper packer using PEARSON water as the test fluid. However, during the fluid exchange the pressure inside the test interval increased significantly, so that an artificial opening (probably a hydraulic fracturing) of the formation could not be excluded preventing the derivation of representative hydraulic formation parameters. Tests STA2-1-OPA1, -OPA2 and -OPA3 were all analysed using radial homogeneous flow models with a discrete time-dependent skin and provided consistent best estimates of the formation hydraulic conductivity in the range of 2×10^{-14} m s^{-1} to 3×10^{-14} m s^{-1} with narrow uncertainty ranges between 9×10^{-15} m s^{-1} and 4×10^{-14} m s^{-1}. The estimates of the hydraulic head are not considered realistic due to the very long pressure history phases (468 – 1099 hours) in comparison to the short test durations (62 – 151 hours) and the physical processes that cannot be captured by the hydraulic modelling software used, e.g. poroelastic effects.

The Staffelegg Formation of the Lias Group was studied using two hydraulic tests, namely STA2-1-LIA1 and STA2-1-LIA2. STA2-1-LIA1 was the first hydraulic test performed after drilling of the corresponding borehole section stopped and the execution of a petrophysical logging campaign (218 hours after drilling through the interval midpoint). STA2-1-LIA2 was performed 523 hours after drilling through the midpoint of the test interval. The analysis of both intervals was based on a homogeneous flow model with a discrete time-dependent skin value, as no indication of the requirement for a more complex flow model could be observed. The best estimates and the uncertainty ranges of the transmissivity and consequently hydraulic conductivity, represent mainly the results of the perturbation analysis of the main undisturbed test phases, slug and slug recovery (SW-SWS) plus the PSR for STA2-1-LIA1 and slug-recovery and pulse withdrawal phase (SWS-PW) for STA2-1-LIA2 respectively. The best estimate of the hydraulic conductivity for the STA2-1-LIA2 interval is about 0.7 order of magnitude higher than the best estimate for the STA2-1-LIA1 with a small overlap in their uncertainty ranges. It is noted that the test interval STA2-1-LIA2 included limestone layers of the Beggingen Member of the Staffelegg Formation (see Tab. 4-22). As with the other tested formations of very low permeability, the estimated hydraulic heads are not considered realistic, most probably due to physical processes not captured by the hydraulic analysis model.

The Klettgau Formation of the Keuper Group was tested via hydraulic tests STA2-1-KEU1 and STA2-1-KEU2. For the analysis of these tests, a homogeneous flow model with a time-dependent skin was used. STA2-1-KEU1 is described in more detail in Section 4.5.2. The behaviour of the test fluid (potassium silicate) during the pressure history was implemented in the model using a separate skin value. In addition, the skin value during testing was separately handled for each test phase. The hydraulic test STA2-1-KEU2 was conducted in an interval starting at 941.50 m MD and extending to a depth of 962.04 m MD. Therefore, it covered the same lithological members of the Klettgau Formation as STA2-1-KEU1, excluding the main part of the Ergolz Member starting at 961.46 m MD. This suggests that the high transmissivity of the STA2-1-KEU1 interval (having a best estimate of 6.0×10^{-8} m s^{-1} for the hydraulic conductivity when considering the entire test interval) can be attributed to the part of Ergolz Member not included in the STA2-1-KEU2 interval, with a best estimate for the hydraulic conductivity of 1.7×10^{-7} m s^{-1}. STA2-1-KEU2 represents a formation with a much lower transmissivity, having a best estimate of 6.5×10^{-12} m s^{-1} for the hydraulic conductivity. However, the best estimate of the hydraulic head differs only by approx. 3 m between these two intervals. Whereas the STA2-1-KEU1 interval yielded a small uncertainty for the resulting estimate of the static formation pressure, STA2-1-KEU2 had a slightly higher associated uncertainty. Test STA2-1-KEU1 allowed for the successful production of a formation water sample.

One hydraulic test sequence was performed in the Schinznach Formation of the Muschelkalk Group. The test STA2-1-MUK1 was performed using a single packer configuration and it should be noted that no mud losses were observed before testing commenced. The test diagnostics indicated an inner (near borehole) zone of changing hydraulic conductivity over time, which was likely due to clean-up effects during pumping. A radial composite flow model with a linear decrease in the hydraulic conductivity was used to account for these changes in the hydraulic conductivity near the borehole as well as changes in the hydraulic conductivity with increasing radius of influence. An infinite acting radial flow (IARF) and the slight increase of the hydraulic conductivity with increasing distance from the borehole could be identified by the test phase diagnostics, especially for the shut-in phases RWS and SWS. The analysis was based on the simulation of the initial SW-SWS and the subsequent RW-RWS phases and yielded consistent results with a best estimate for the interval transmissivity of 2×10^{-6} m^2 s^{-1} which translates to a hydraulic conductivity of 3×10^{-8} m s^{-1} taking into account the entire thickness of the tested interval. The uncertainties in the results were evaluated based on two perturbation analyses and were mainly related to the assumption of isothermal conditions. The hydraulic conductivity and the hydraulic head of the formation were estimated within a small range of uncertainty and the collection of a groundwater sample was successful.

5 Summary

Borehole Stadel-2-1 (STA2-1) is the third exploratory borehole drilled in the TBO project in the siting region Nördlich Lägern.

A total of 13 hydraulic packer test sequences and one fluid logging campaign were performed in this borehole between February 2021 and June 2021. All hydraulic packer tests were performed in the cored borehole section using an HDDP packer system in single or double packer configuration (*cf.* Tab. 4-22). The test activities were performed in the following geological formations (*cf.* Dossier III):

- Malm Group with a focus on the «Felsenkalke» + «Massenkalk» including zones with abundant karst features, mostly filled with claystone (STA2-1-MAL1) following the realisation of a fluid logging (STA2-1-FL1-MAL)
- Dogger Group excluding Opalinus Clay («Brauner Dogger») within the «Parkinsoni-Württembergica-Schichten» (STA2-1-BDO3), the «Herrenwis Unit», «Humphriesioolith Formation» (STA2-1-BDO2), the Wedelsandstein Formation and the «Murchisonae-Oolith Formation» (STA2-1-BDO1)
- Dogger Group with a focus on the Opalinus Clay (STA2-1-OPA1, STA2-1-OPA2, STA2-1-OPA3 and STA2-1-OPA4)
- Lias Group with a focus on the Staffelegg Formation including the Gross Wolf, Rietheim, Grünschholz, Breitenmatt, Rickenbach and Frick Members (STA2-1-LIA1) respectively including the Frick, Beggingen and Schambelen Members (STA2-1-LIA2)
- Keuper Group with a focus on the Klettgau Formation including the Gruhalde, Seebi, Gansingen and the top part of the Ergolz Member (STA2-1-KEU2), respectively covering the Seebi, and Gansingen Members, the entire Ergolz Member and the first meters of Bänkerjoch Formation (STA2-1-KEU1)
- Muschelkalk Group with a focus on the Schinznach Formation including the Stamberg, Liedertswil, Leutschenberg and Kienberg Members (STA2-1-MUK1)

All hydraulic tests were supported by an on-site field analysis to optimise the test procedure. The pressures and rates measured during all tests are illustrated in Figs. 4-9 to 4-21. The main results and best estimates of the hydraulic formation parameters are presented in Tabs. 4-33 to 4-35 and Figs. 4-24 to 4-28. The fluid logging analysis (STA2-1-FL1-MAL; *cf.* Section 3.2) and two hydraulic test analyses (STA2-1-BDO1 and STA2-1-KEU1; *cf.* Sections 4.5.1 and 4.5.2) were selected for a detailed description in this report. Operational problems during test STA2-1-OPA4 did not allow for generation of a dataset in order to estimate representative formation parameters.

The best estimates and the uncertainty of the hydraulic conductivities and transmissivities lie in a reasonable range and are within the expected spectrum of values for the investigated formations (e.g. Nagra 2008, Nagra 2014a and b). However, it should be noted that the best estimates for the hydraulic conductivity in the Dogger Group excluding Opalinus Clay («Brauner Dogger») span over five orders of magnitude. The hydraulic conductivities in the Opalinus Clay were very low with narrow uncertainty ranges.

The extrapolated hydraulic heads are within an expected range (Luo et al. 2014) except for the hydraulic tests performed in the Dogger Group including the Opalinus Clay and the Lias Group, whereas the head estimate from test STA2-1-BDO1 is close to the head predicted by Luo et al.

(2014) for the «Brauner Dogger» (unit BD5). Due to inevitable, short-term borehole test conditions, the hydraulic heads estimated for STA2-1-BDO2, STA2-1-BDO3, STA2-1-OPA1, STA2-1-OPA2, STA2-1-OPA3, STA2-1-LIA1 and STA2-1-LIA2 appear to be affected by a large overestimation. They are considered as 'apparent' hydraulic heads.

General investigations concerning the physical explanation for the overestimation of the hydraulic head are continuing. The presented analysis considers the temperature effects in the test interval and the pressure induced effects resulting from the high-density drill mud during the entire time since drilling through the interval midpoint. Nagra will install long-term pressure monitoring systems in borehole STA3-1 and other selected boreholes to study these and further findings in detail.

6 References

Barker, J.A. (1988): A generalized radial flow model for hydraulic tests in fractured rock. Water Resour. Res. 24/10, 1796-1804.

Black, J., Holmes, D. & Brightman, M. (1987): Crosshole investigations – Hydrogeological results and interpretations. Nagra Technical Report NTB 87-37.

Bourdet, D., Ayoub, J.A. & Pirard, Y.M. (1989): Use of pressure derivative in well-test interpretation. Society of Petroleum Engineers, SPE Formation Evaluation, 293-302.

Detournay, E. & Cheng, A.H.-D. (1988): Poroelastic response of a borehole in a non-hydrostatic stress field. International Journal of Rock Mechanics and Mining Sciences & Geomechanics Abstracts 25/3, 171-182.

Doughty, C. & Tsang, C.F. (2005): Signatures in flowing fluid electric conductivity logs. Journal of Hydrology 310, 157-180.

Geofirma Engineering Ltd. & INTERA Inc. (2011): nSIGHTS Version 2.50 User Manual. INTERA Inc., Austin, TX, USA.

Grauls, D. (1999): Overpressures: Causal mechanisms, conventional and hydromechanical approaches. Oil & Gas Science and Technology – Rev. IFP 54, 667-678.

Horne, R.N. (1995): Modern Well Test Analysis: A Computer-Aided Approach. 2nd Edition. Petroway Inc., Palo Alto, CA, USA.

Horner, D.R. (1951): Pressure Buildup in Wells. Proceedings Third World Petroleum Congress 2, 503-523, The Hague, Netherlands. Reprinted 1967. Pressure Analysis Methods, AIME Reprint Series 9, 45-50. SPE.

Isler, A., Pasquier, F. & Huber, M. (1984): Geologische Karte der zentralen Nordschweiz 1:100'000. Herausgegeben von der Nagra und der Schweiz. Geol. Komm.

Jäggi, K. & Vogt, T. (2020): OPA: Sondierbohrung Benken, Langzeitbeobachtung 2019, Dokumentation der Messdaten. Nagra Arbeitsbericht NAB 20-05.

Lisjak, A., Garitte, B., Grasselli, G., Müller, H.R. & Vietor, T. (2015): The excavation of a circular tunnel in a bedded argillaceous rock (Opalinus Clay): Short-term rock mass response and FDEM numerical analysis. Tunnelling and Underground Space Technology 45, 227-248.

Lorenz, G.D. & Stopelli, E. (*in prep.*): Borehole STA2-1 (Stadel-2-1): Fluid sampling and analytical hydrochemical data report. Nagra Arbeitsbericht NAB 22-37.

Luo, J., Monningkoff, B. & Becker, J.K. (2014): Hydrogeological model Nördlich Lägern. Nagra Arbeitsbericht NAB 13-25.

Marschall, P., Croisé, J., Schlickenrieder, L., Boisson, J.Y., Vogel, P. & Yamamoto, S. (2003): Synthesis of hydrogeological investigations at the Mont Terri site (Phases 1 – 5). Mont Terri Technical Report TR 01-02. Mont Terri Project, Switzerland.

Nagra (1997): Hydrological investigations at Wellenberg: Hydraulic packer testing in boreholes SB4a/v and SB4a/s. Methods and field results. Nagra Technischer Bericht NTB 95-02.

Nagra (2001): Sondierbohrung Benken – Untersuchungsbericht. Nagra Technischer Bericht NTB 00-01.

Nagra (2008): Vorschlag geologischer Standortgebiet für das SMA- und das HAA-Lager – Geologische Grundlagen. Nagra Technischer Bericht. NTB 08-04.

Nagra (2014a): SGT Etappe 2: Vorschlag weiter zu untersuchender geologischer Standortgebiete mit zugehörigen Standortarealen für die Oberflächenanlage. Geologische Grundlagen. Dossier II: Sedimentologische und tektonische Verhältnisse. Nagra Technischer Bericht NTB 14-02.

Nagra (2014b): SGT Etappe 2: Vorschlag weiter zu untersuchender geologischer Standortgebiete mit zugehörigen Standortarealen für die Oberflächenanlage. Geologische Grundlagen. Dossier VI: Barriereneigenschaften der Wirt- und Rahmengesteine. Nagra Technischer Bericht NTB 14-02.

Pickens, J.F., Grisak, G.E., Avis, J.D., Belanger, D.W. & Thury, M. (1987): Analysis and interpretation of borehole hydraulic tests in deep boreholes: Principles, model development, and application. Water Resour. Res. 23/7, 1341-1375.

Pietsch, J. & Jordan, P. (2014): Digitales Höhenmodell Basis Quartär der Nordschweiz – Version 2013 (SGT E2) und ausgewählte Auswertungen. Nagra Arbeitsbericht NAB 14-02.

Ramey, H.J., Jr., Agarwal, R.G. & Martin, I. (1975): Analysis of 'Slug Test' or DST Flow Period Data. Journal of Canadian Petroleum Technology 14/3, 37-47.

Richards, D.J. (1981): Technical Manual on Radiometrics – Geophysical Field Manual for Technicians No. 2. South African Geophysical Association.

Tsang, C.F. & Hufschmied, P.A. (1998): Borehole fluid conductivity logging method for the determination of fracture inflow parameters. Nagra Technischer Bericht NTB 88-13.

Appendix A: Abbreviations, nomenclature and definitions

Tab. A-1: Lithostratigraphy abbreviations for test names in STA2-1

Lithostratigraphy	**Abbreviation**
Malm Group	MAL
Brauner Dogger (Dogger)	BDO
Opalinus Clay (Dogger)	OPA
Lias Group	LIA
Keuper Group	KEU
Muschelkalk Group	MUK

Tab. A-2: Test name definitions for hydraulic packer testing

Abbreviation	**Example**
Drill site abbreviation – lithostratigraphy abbreviation[1] + number of test	STA2-1-MUK1: First test interval in Muschelkalk aquifer in borehole STA2-1

[1] Based on the preliminary information

Tab. A-3: Test event abbreviations for hydraulic packer testing

Test phase	**Abbreviation**
Compliance phase	COM
Packer deflation phase	DEF
Filling of test tubing	FILL
Packer inflation phase	INF
Multi-rate pumping test with stepwise constant flow rates	MR
Pressure recovery after multi-rate pumping test (shut-in)	MRS
Pulse injection test	PI
Initial pressure recovery 'static pressure recovery' (SIT closed)	PSR
Pulse withdrawal test	PW
Pumping test with constant flow rate ('rate withdrawal test')	RW
Pressure recovery after pumping test with constant flow rate (shut-in)	RWS
Slug withdrawal test (flow phase)	SW
Slug withdrawal test – pressure recovery with closed SIT (shut-in)	SWS

Tab. A-4: Parameter definitions

Abbreviation / symbol	**Description**	**Unit**
c_{tz}	Test zone compressibility	1/Pa
C_i	Concentration (salinity) of one inflow i	g l^{-1}
EC_i	Electrical conductivity of one inflow i	µS cm^{-1}
g	Acceleration due to gravity (9.81)	m s^{-2}
h_s	Static hydraulic head (freshwater head) $h_s = z_{ref} - z_{int} + \left[\frac{P_f + \rho_{int}\, g\, (z_{int} - z_2) - P_{atm} - P_{offset}}{\rho_w\, g}\right]$	m asl
k	Intrinsic permeability	m^2
K	Hydraulic conductivity	m s^{-1}
K_{in}	Inner-zone hydraulic conductivity	m s^{-1}
K_{out}	Outer-zone hydraulic conductivity	m s^{-1}
K_s	Hydraulic conductivity of skin zone	m s^{-1}
n	Fractional flow dimension, e.g. Barker (1988)	-
P	Pressure (at QSSP-P2 level, if not otherwise specified)	Pa, kPa
P1	Pressure below bottom packer / interval P1 (downhole probe)	Pa, kPa
P2	Pressure in test interval (downhole probe)	Pa, kPa
P2*	(Absolute) pressure in test interval (memory gauge)	Pa, kPa, kPaa
P3	Pressure in annulus (above top packer, downhole probe)	Pa, kPa
P4	Pressure in test tubing above SIT (downhole probe)	Pa, kPa
P_{atm}	Atmospheric pressure	Pa, kPa
P_f	Static formation pressure (fitting parameter, at QSSP-P2 level, respectively P2* level)	Pa, kPa
P_{int}	Pressure at midpoint of test interval	Pa, kPa
P_{offset}	Offset of a pressure probe at atmospheric pressure	Pa, kPa
P_S	Static formation pressure (at midpoint of test interval if not specified otherwise)	Pa, kPa
$\Delta\ P_{packer}$	Interval packer pressure changes	bar
q	Flow rate	$m^3\ s^{-1}$
q_i	Flow rate of one inflow i	$m^3\ s^{-1}$
Q, Q_{tot}	Cumulative flow volume	m^3
r_d	Radius of discontinuity	m
r_s	Radius of the skin zone extension	m
$r_{w\ int}$	Borehole radius of the test interval	mm

Abbreviation / symbol	**Description**	**Unit**
ρ_{int}	Density of interval fluid	kg m^{-3}
ρ_w	Density of formation water (fluid)	kg m^{-3}
S	Storage	-
s	Skin factor	-
S_s	Specific storage	1/m
$S_{s\ in}$	Inner-zone specific storage	1/m
$S_{s\ out}$	Outer-zone specific storage	1/m
S_{ss}	Specific storage of skin zone	1/m
t_s	Thickness of the skin zone extension	m
T	Transmissivity	$m^2\ s^{-1}$
T_i	Transmissivity of one inflow i	$m^2\ s^{-1}$
t, dt	Time, elapsed time	s
T_{int}, T1, T2, T3, T4, T2*	Temperature in test interval, temperature triple probe (sensors 1, 2, 3 or 4 associated with specific transducer; sensor T2* associated with memory gauge)	°C
ΔV_{int}	Interval volume changes	mL
z_2	Depth of pressure sensor of test interval P2	m MD
z_{int}	Depth interval midpoint	m MD
z_{ref}	Reference point elevation	m asl

Tab. A-5: Non-parameter abbreviations

Abbreviation	**Description**	**Unit**
ΔP	Change in pressure	Pa, kPa
ΔV	Change in volume	m^3
1D	One dimensional	
2D	Two dimensional	
3D	Three dimensional	
AG	Aktiengesellschaft (company limited by shares "Ltd.")	
API	American Petroleum Institute	
BHPH	Borehole pressure history	
BOP	Blow out preventer	
STA2-1	Stadel-2 drill site, borehole 1	
cps	Counts per second	
CU	Copper	

Abbreviation	**Description**	**Unit**
DA	Detailed analysis	
DAS	Data acquisition system	
DR	Detailed report	
EU	External upset coupling	
EUE	External upset end	
FM	Flow model	
FS	Full scale	
GmbH	Gesellschaft mit beschränkter Haftung (company with limited liability)	
GTPT	Gas threshold pressure test	
HDDP	Heavy-duty double packer system	
HLW	High level waste	
HTT	Hydraulic test tool	
IARF	Infinite acting radial flow region	
ID	Inner diameter	
IPI	Inflatable Packers International, Perth, Australia	
IT	Information technology	
L/ILW	Low and intermediate level waste	
ln	Litre normal	ln
MAR1-1	Marthalen-1 drill site, borehole 1	
MD	Measured depth	m
MHF	Micro-hydraulic fracturing	
NBR	Nitrile butadiene rubber	
NDSA	Naphthalene disulfonate acid	
NL	Siting region Nördlich Lägern	
OD	Outer diameter	
PA1	Bottom packer of the hydraulic line of the HDDP	
PA2	Top packer of the hydraulic line of the HDDP	
PCP	Progressive cavity pump	
POOH	Pull out of hole	
PPG	Piston pulse generator	
PRV	Pressure release valve	
QC	Quality control	
QLA	Quick look analysis	
QLR	Quick look report	

Abbreviation	**Description**	**Unit**
QSSP	Quadruple sub-surface probe	
Rd	Reading	
RIH	Run in hole	
SIT	Shut-in tool	
SSE	Sum of squared errors	
TBO	Tiefbohrung(en) (German for deep borehole(s))	
TVD	True vertical depth	m
WS	Water sample	
WT	Water table	
WTW	Wissenschaftlich-technische Werkstätten GmbH	
ZH	Zürich	
ZNO	Siting region Zürich Nordost	

Appendix B: Analysis plots of the hydraulic packer tests STA2-1-BDO1 and STA2-1-KEU1

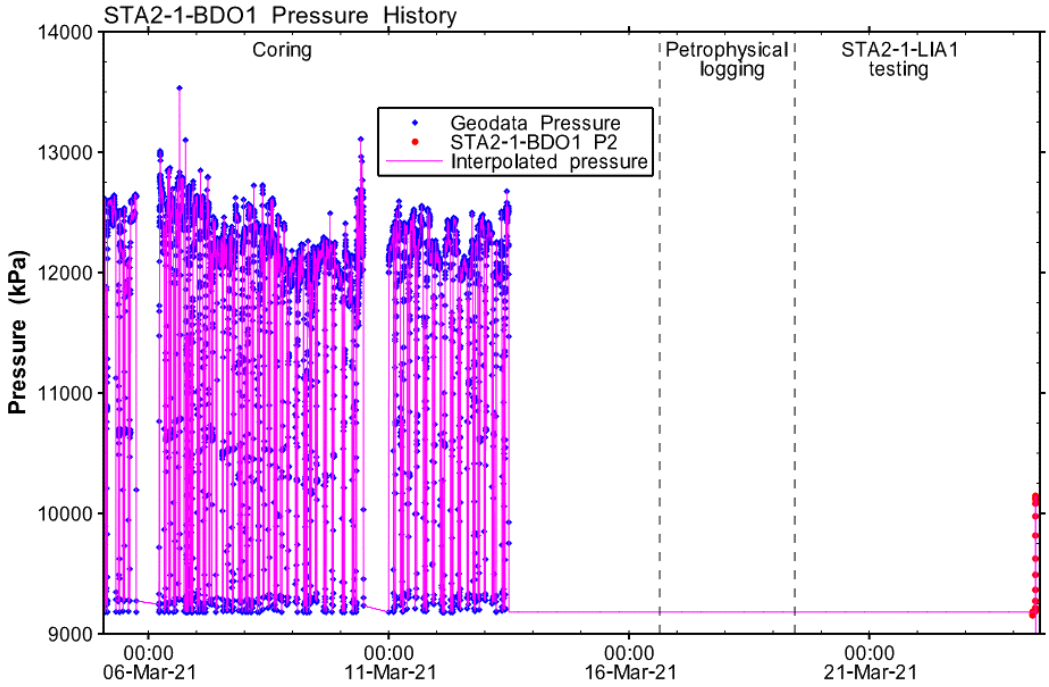

Fig. B-1: Hydraulic test STA2-1-BDO1: Entire record of the borehole pressure history used in the analysis

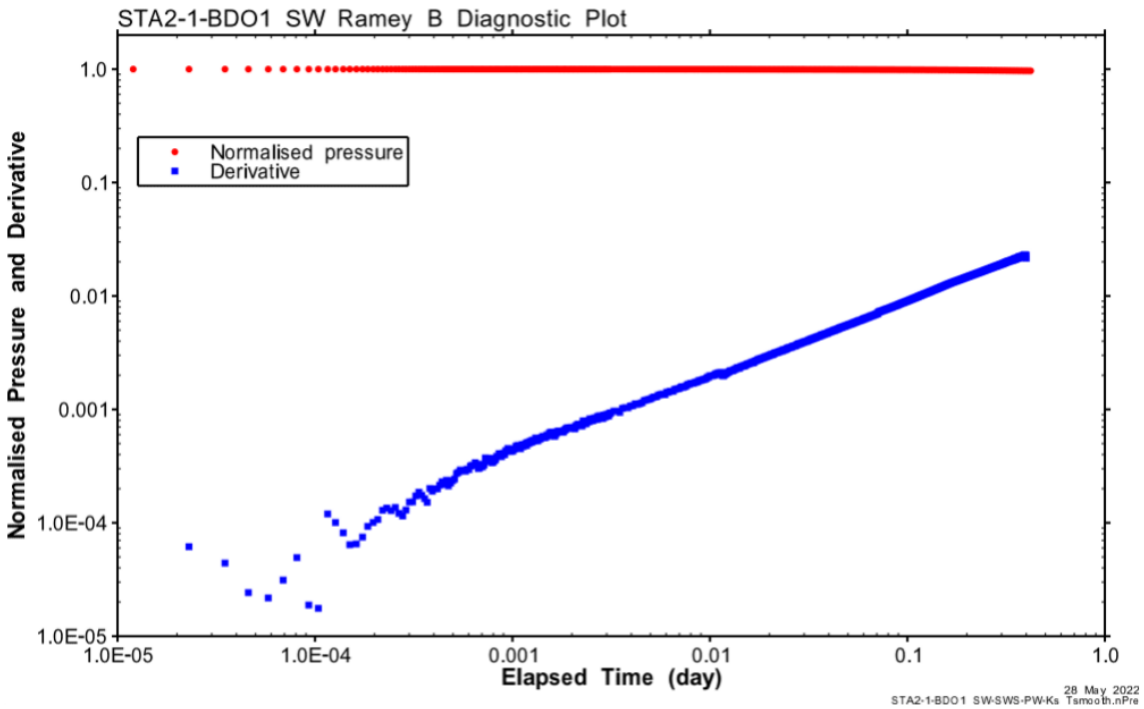

Fig. B-2: Hydraulic test STA2-1-BDO1: Ramey B diagnostic plot of the SW phase

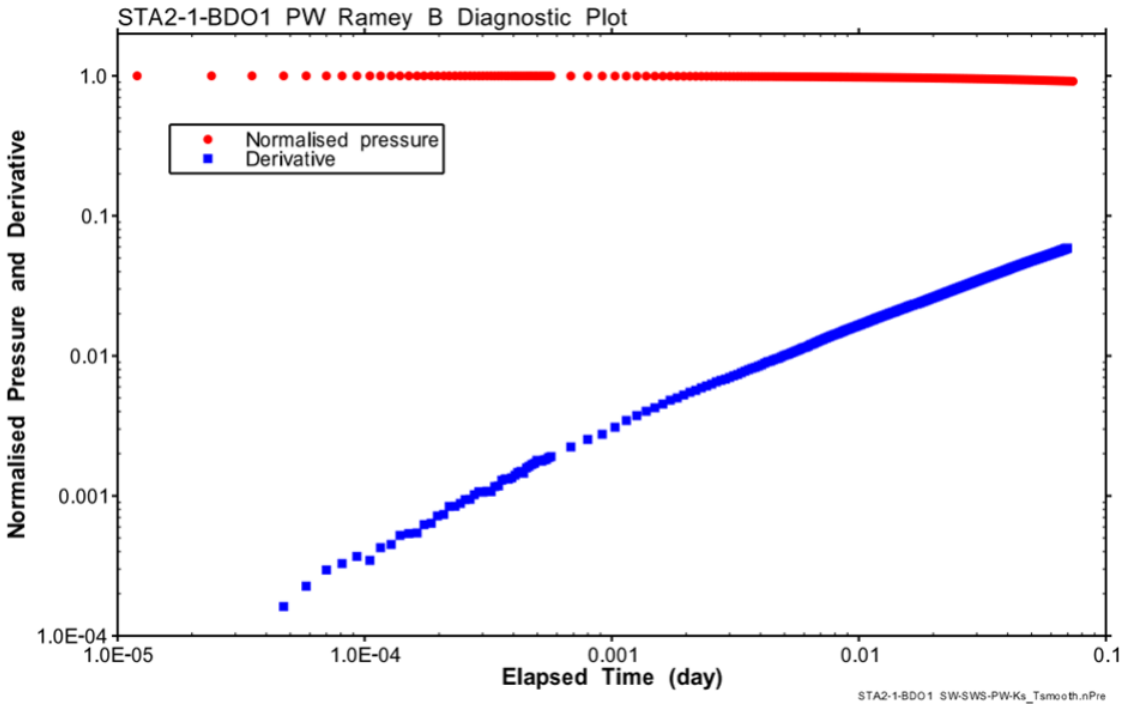

Fig. B-3: Hydraulic test STA2-1-BDO1: Ramey B diagnostic plot of the PW phase

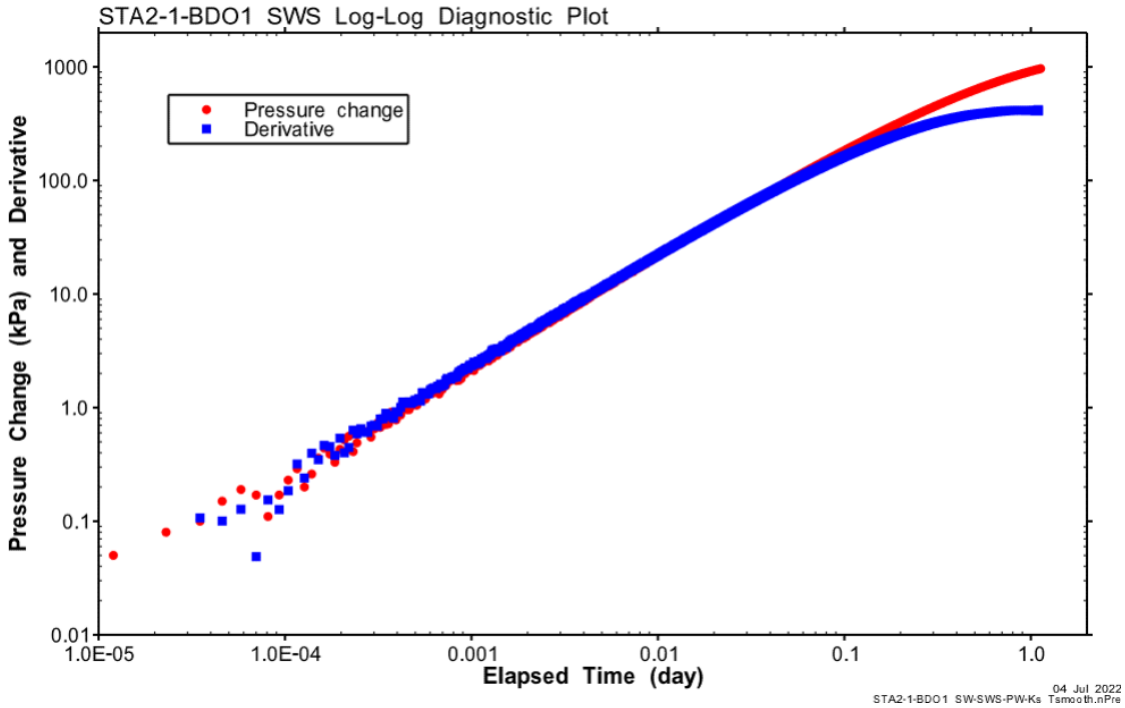

Fig. B-4: Hydraulic test STA2-1-BDO1: Log-log diagnostic plot of the SWS phase

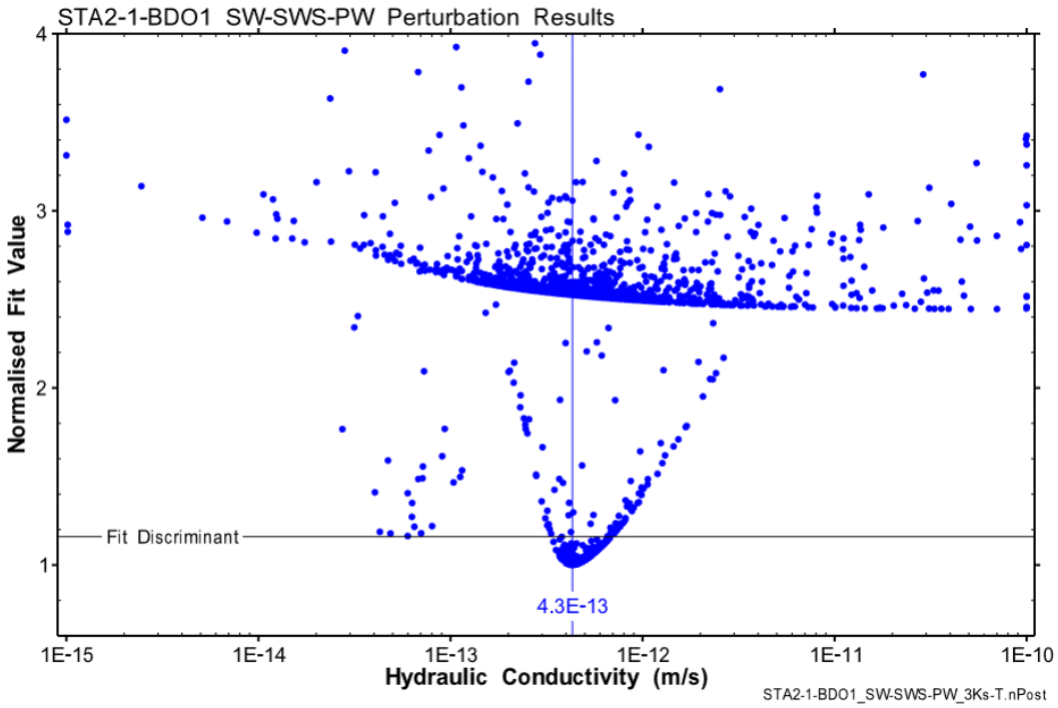

Fig. B-5: Hydraulic test STA2-1-BDO1: Distribution of the normalised objective function value over K for the numerical simulation of the SW-SWS-PW

1'946 / 2'000 results with a normalised objective function value less than 4.

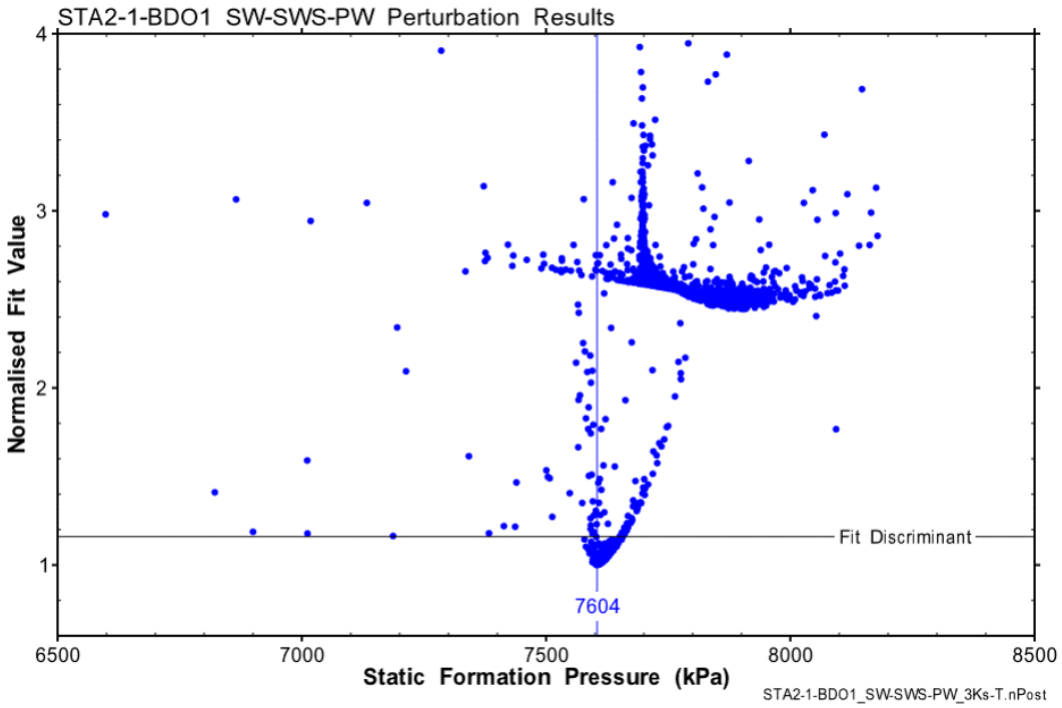

Fig. B-6: Hydraulic test STA2-1-BDO1: Distribution of the normalised objective function value over P_f for the numerical simulation of the SW-SWS-PW

1'946 / 2'000 results with a normalised objective function value less than 4.

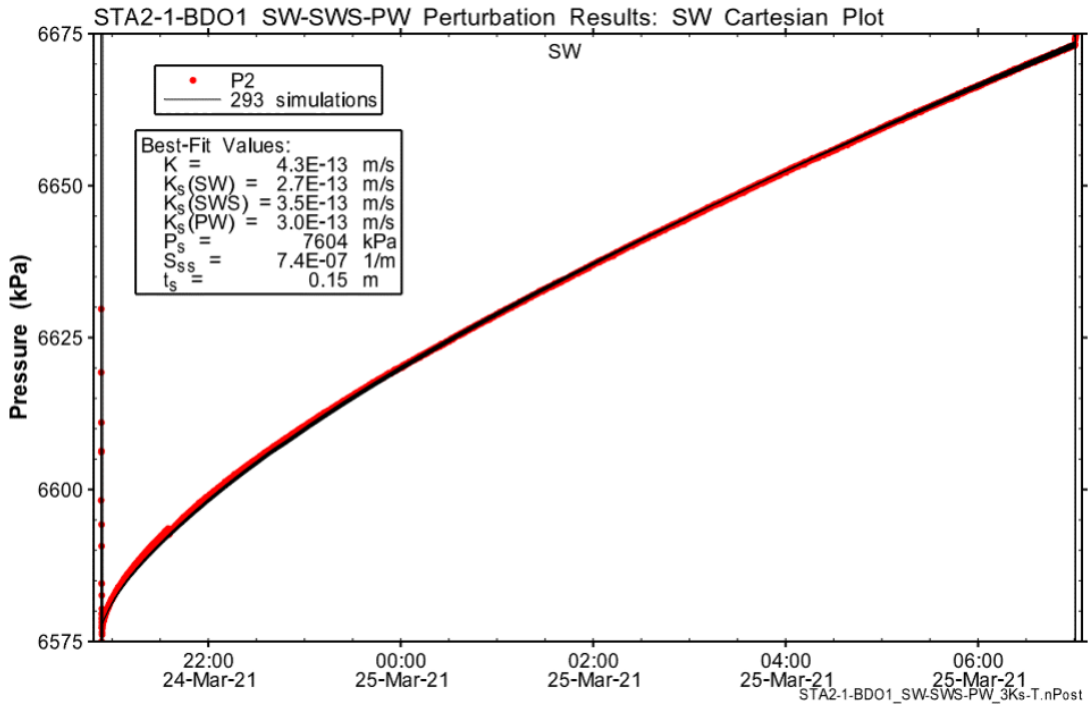

Fig. B-7: Hydraulic test STA2-1-BDO1: Cartesian horsetail plot of the perturbation simulations on the SW accepting the fit discriminant

293 / 2'000 results with a normalised objective function value less than 1.16.

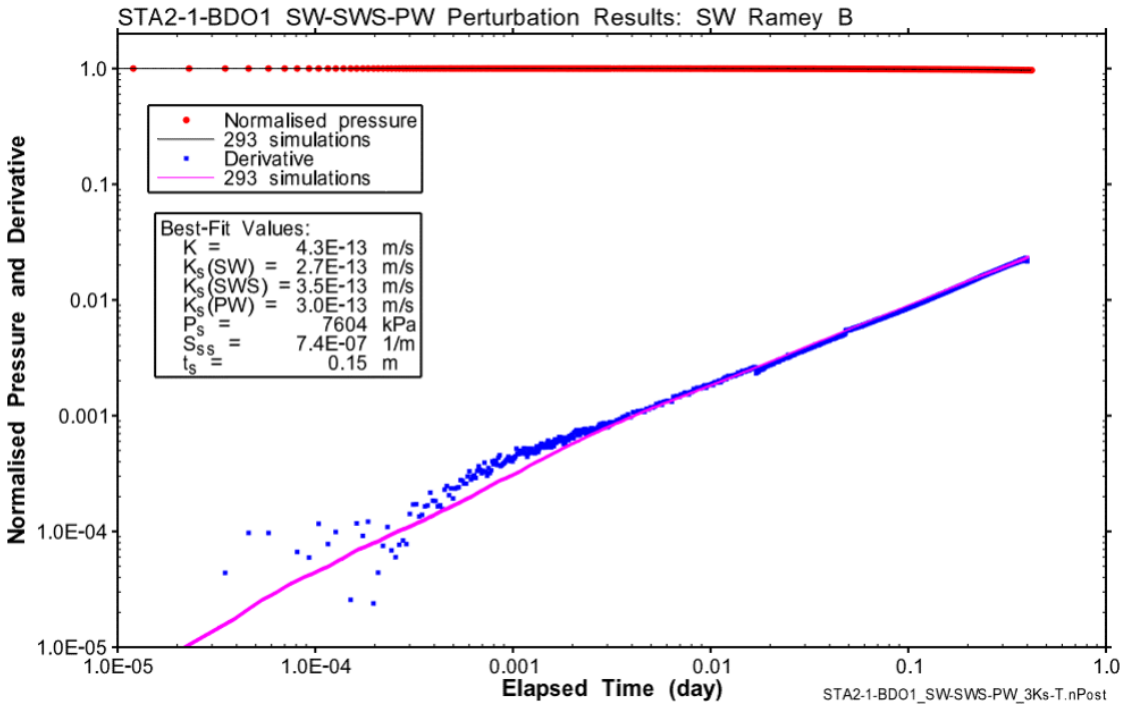

Fig. B-8: Hydraulic test STA2-1-BDO1: Ramey B horsetail plot of SW accepting the fit discriminant

293 / 2'000 results with a normalised objective function value less than 1.16.

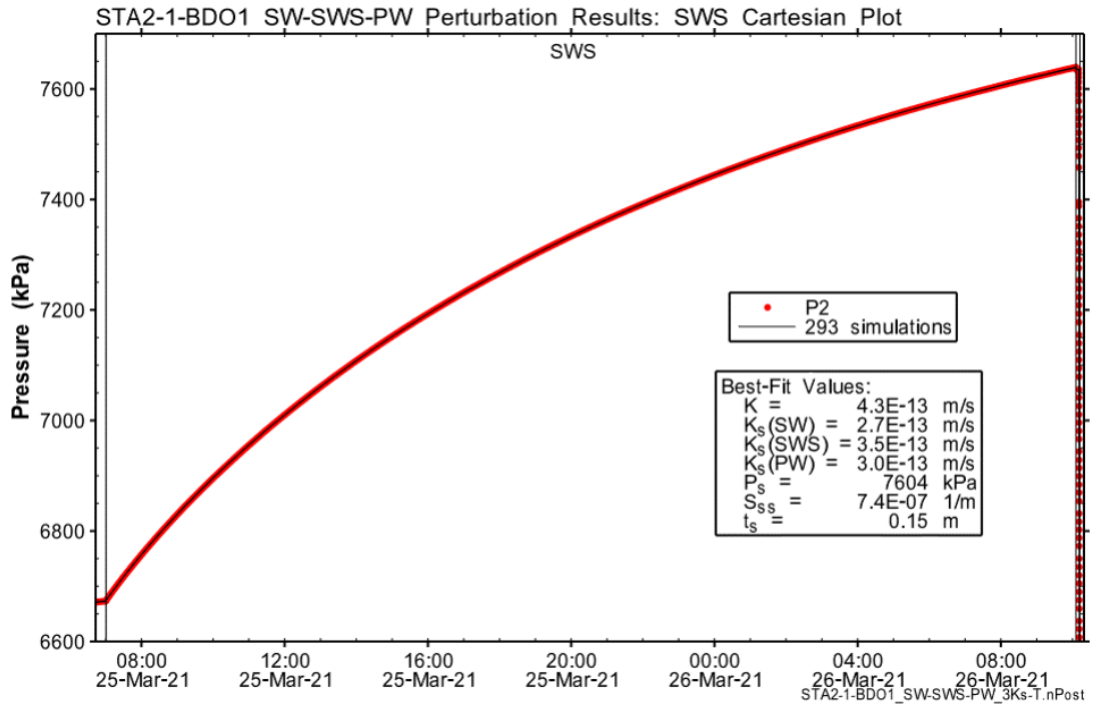

Fig. B-9: Hydraulic test STA2-1-BDO1: Cartesian horsetail plot of the perturbation simulations on SWS accepting the fit discriminant

293 / 2'000 results with a normalised objective function value less than 1.16.

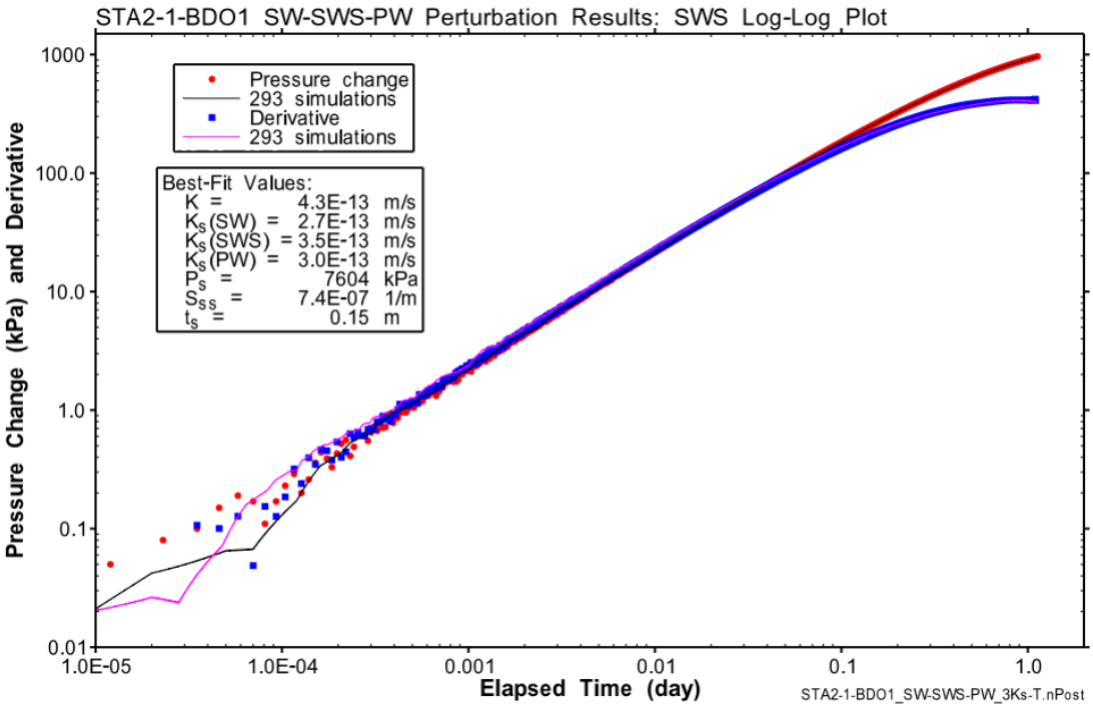

Fig. B-10: Hydraulic test STA2-1-BDO1: Log-log horsetail plot of SWS accepting the fit discriminant

293 / 2'000 results with a normalised objective function value less than 1.16.

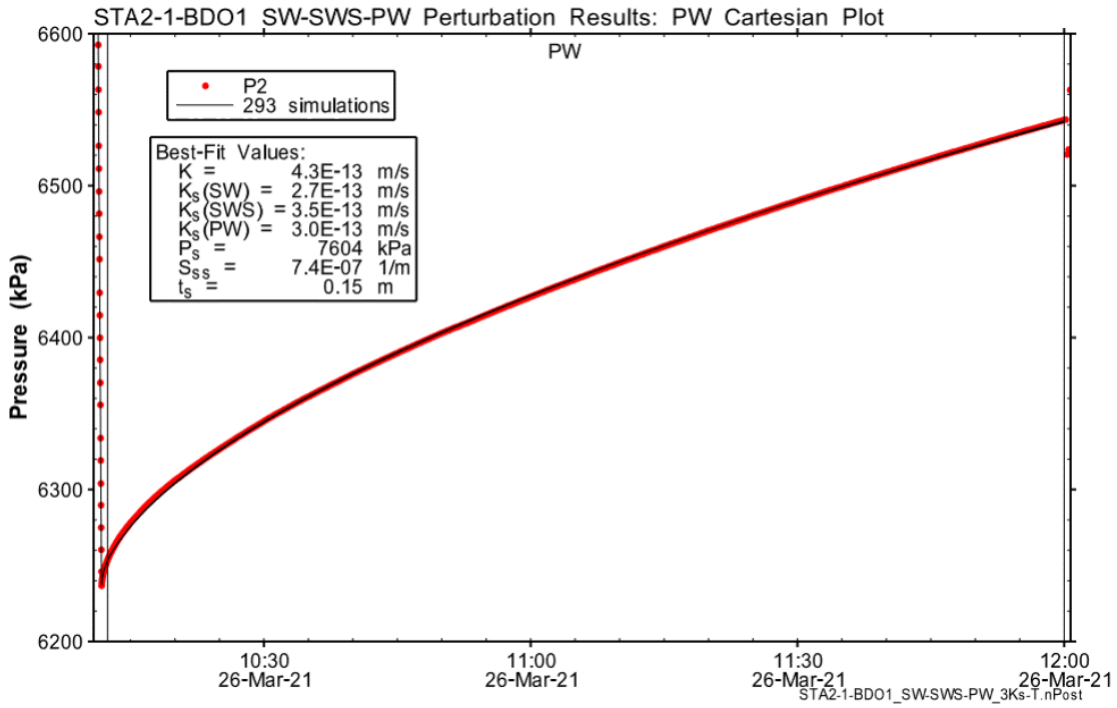

Fig. B-11: Hydraulic test STA2-1-BDO1: Cartesian horsetail plot of the perturbation simulations on the PW accepting the fit discriminant

293 / 2'000 results with a normalised objective function value less than 1.16.

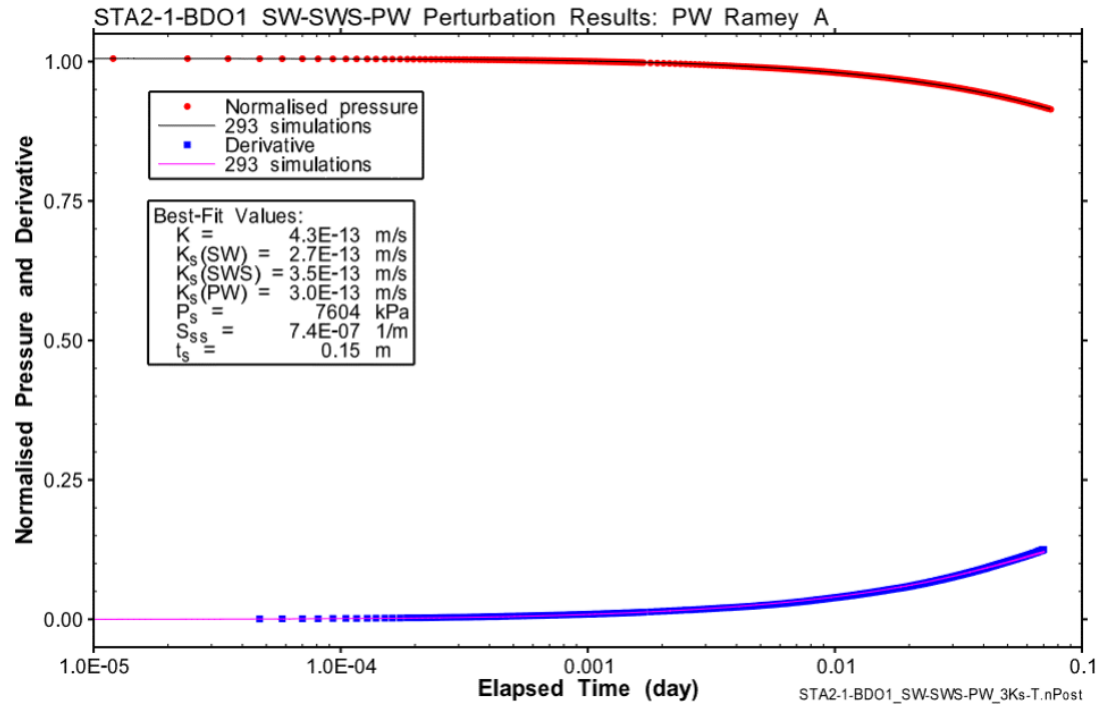

Fig. B-12: Hydraulic test STA2-1-BDO1: Ramey B horsetail plot of the PW accepting the fit discriminant

293 / 2'000 results with a normalised objective function value less than 1.16.

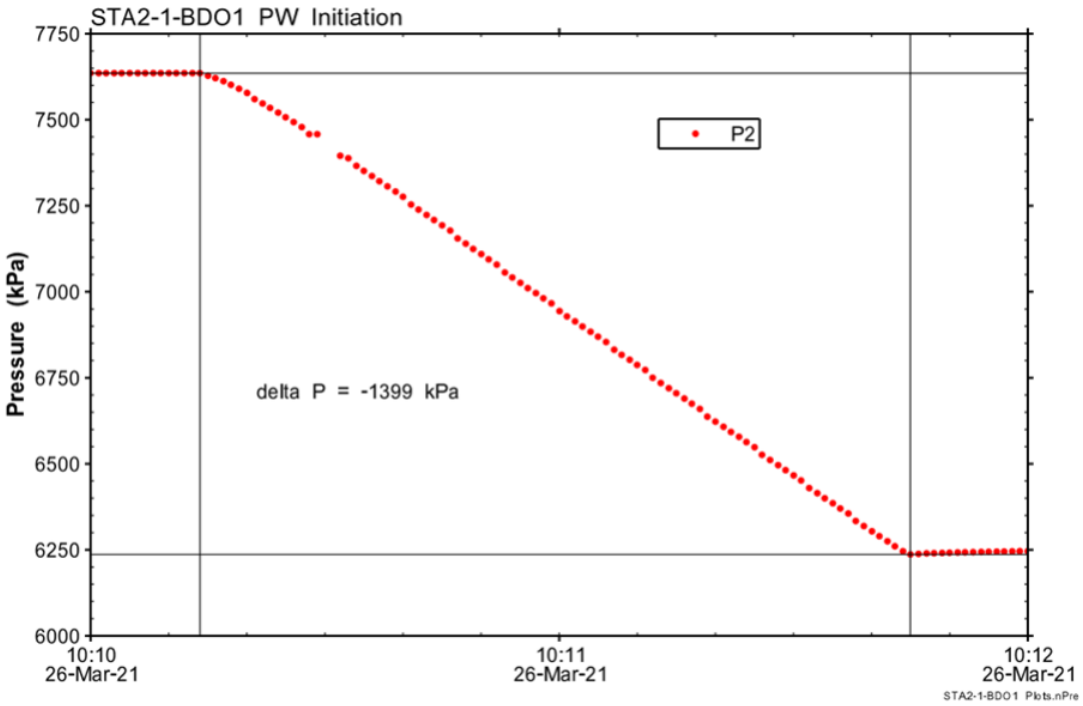

Fig. B-13: Hydraulic test STA2-1-BDO1: Interval pressure change during the initiation of the pulse withdrawal phase (PW)

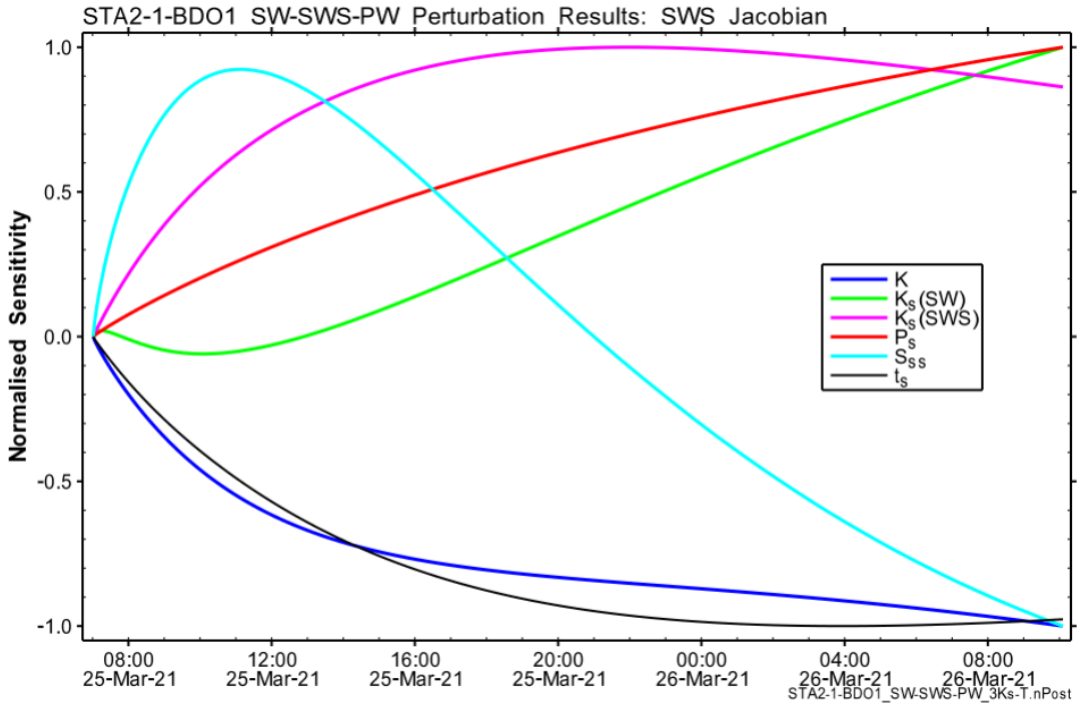

Fig. B-14: Hydraulic test STA2-1-BDO1: Jacobian plot of parameter sensitivities during the SWS

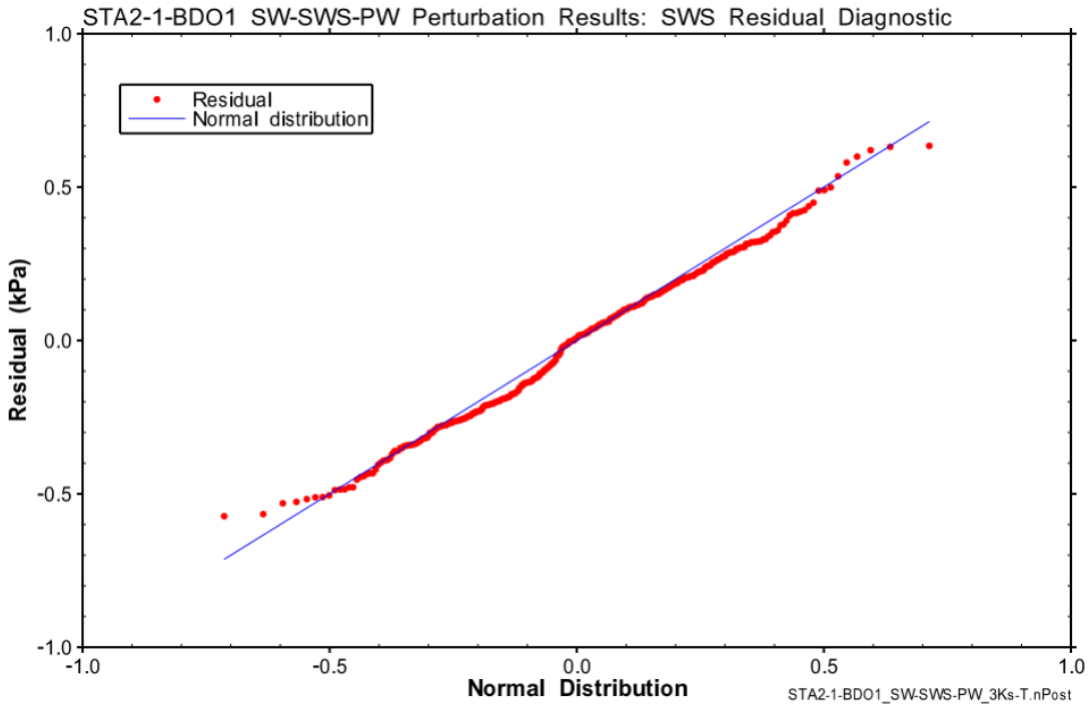

Fig. B-15: Hydraulic test STA2-1-BDO1: Quantile-normal plot of residuals from the best Cartesian fit to SWS data

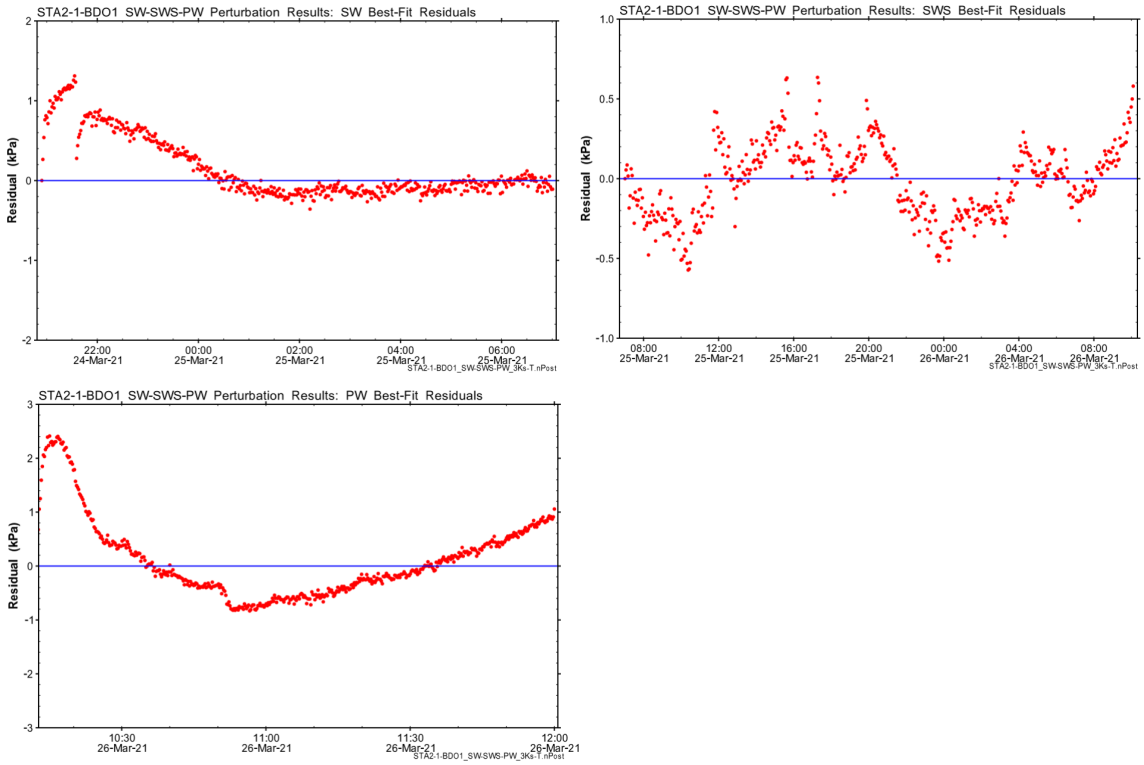

Fig. B-16: Hydraulic test STA2-1-BDO1: Residuals from the best Cartesian fit to SW (top left), SWS (top right) and PW data (bottom left)

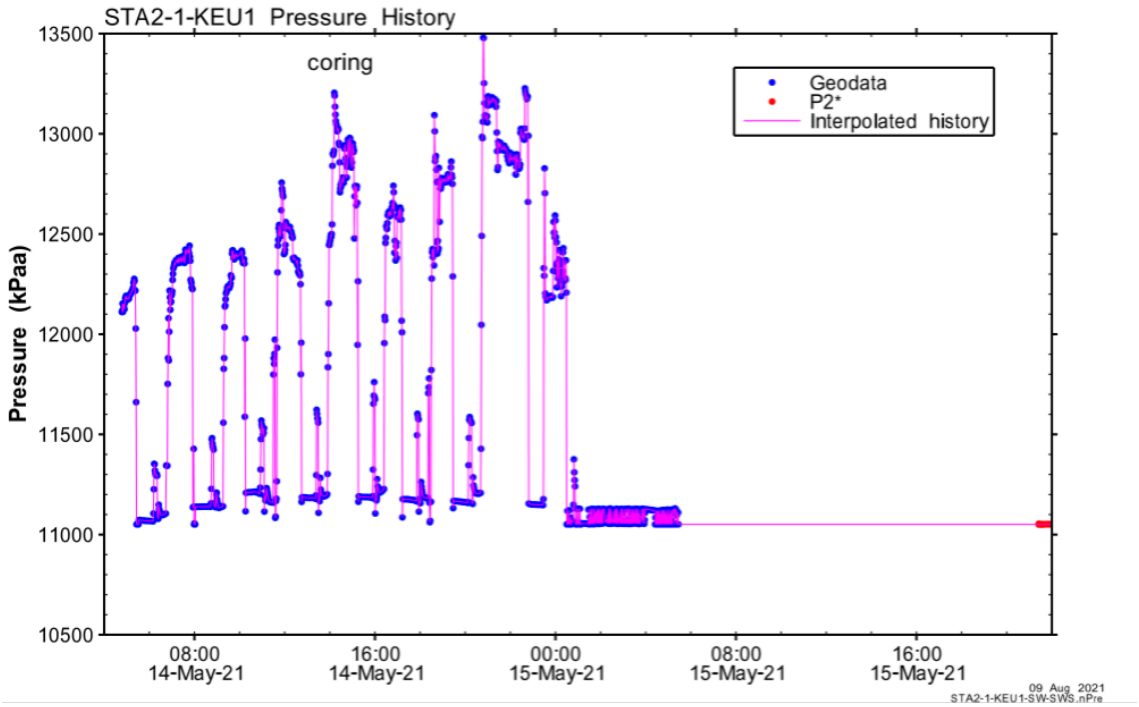

Fig. B-17: Hydraulic test STA2-1-KEU1: Entire record of the borehole pressure history used in the analysis

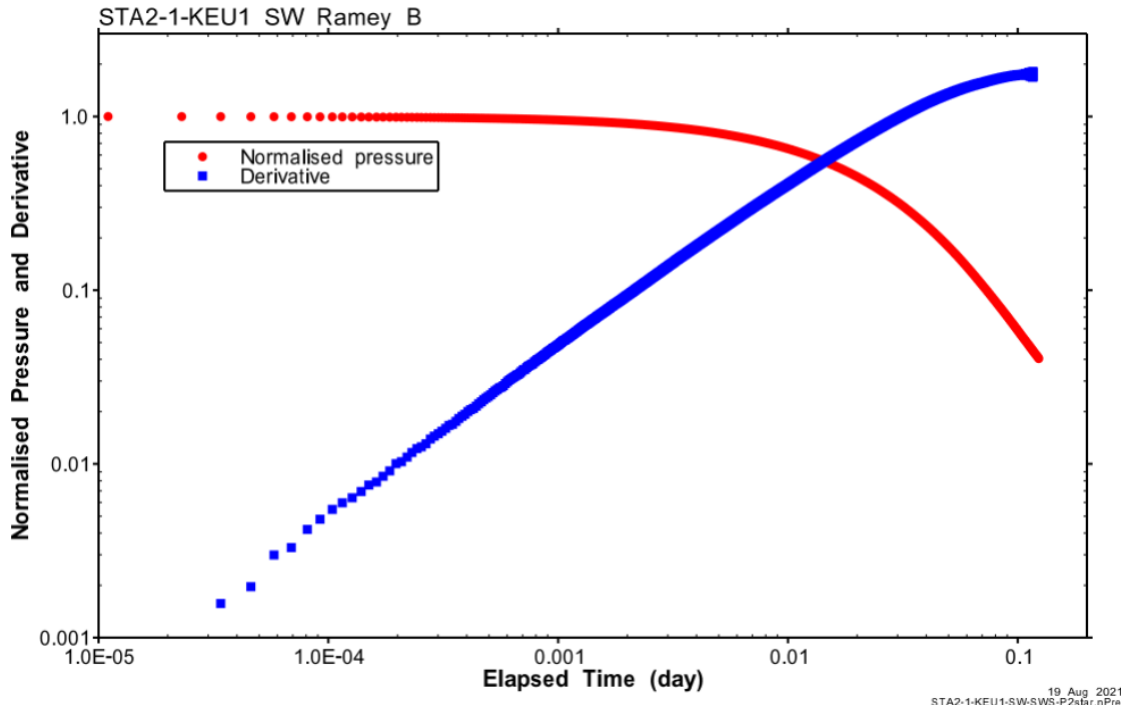

Fig. B-18: Hydraulic test STA2-1-KEU1: Ramey B diagnostic plot of the SW

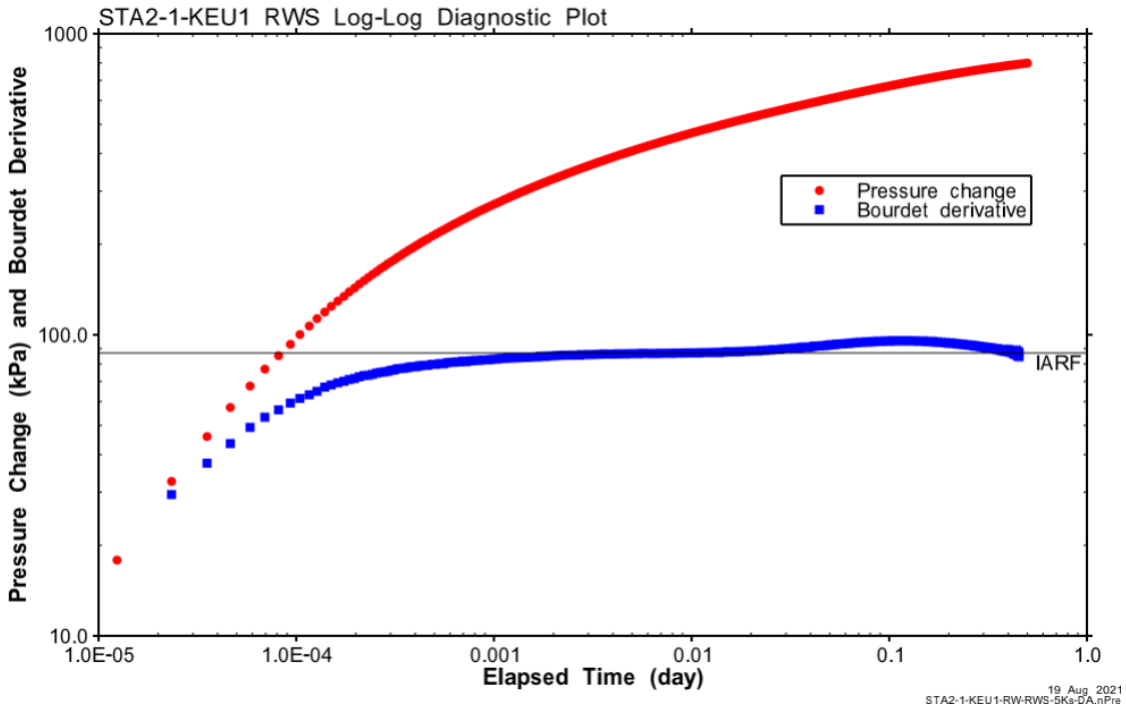

Fig. B-19: Hydraulic test STA2-1-KEU1: Log-log diagnostic plot of the RWS

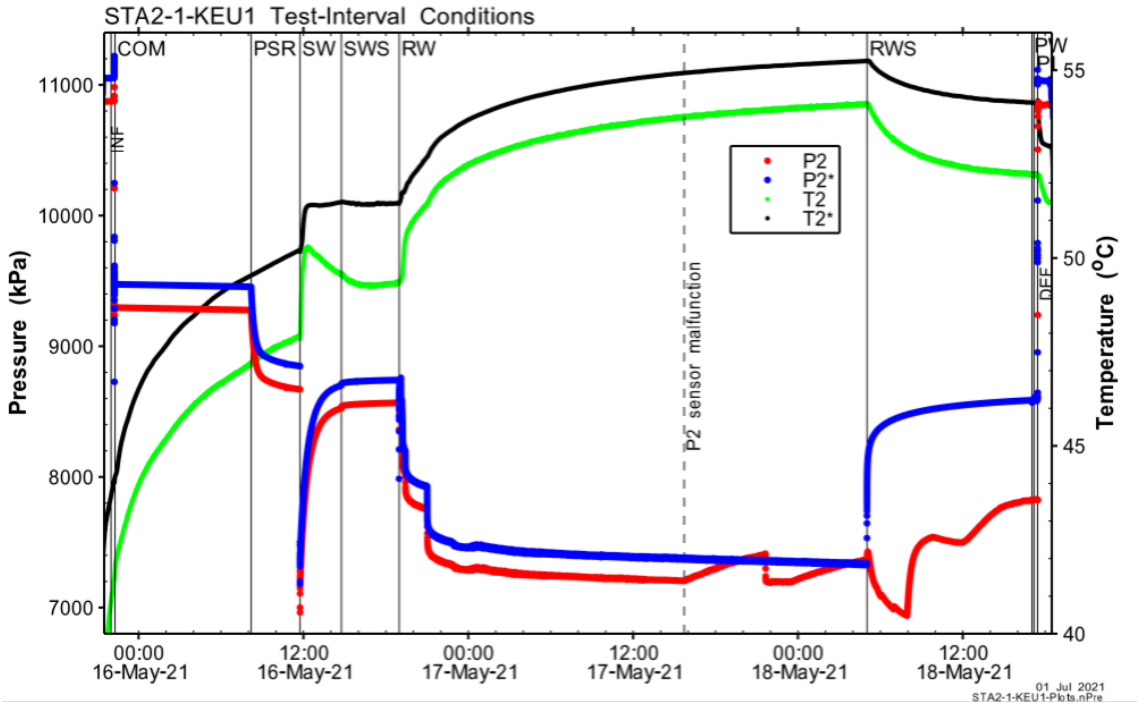

Fig. B-20: Hydraulic test STA2-1-KEU1: Comparison of QSSP measurement P2/T2 and the memory gauge P2*/T2* pressure and temperature measurements within the test interval

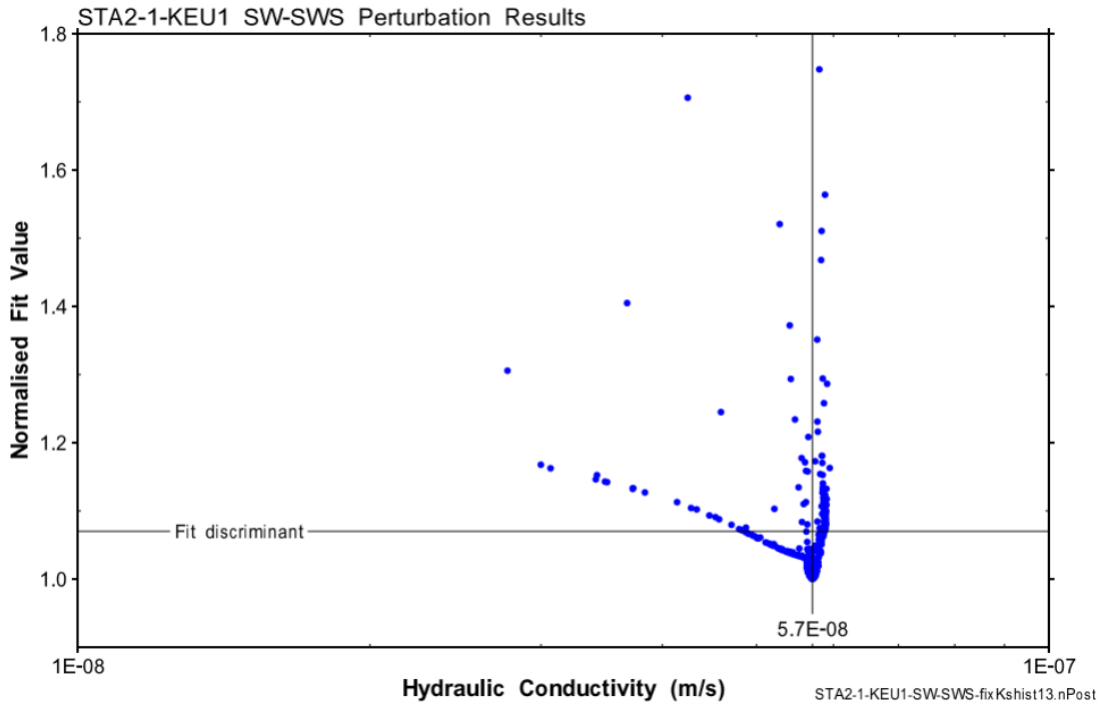

Fig. B-21: Hydraulic test STA2-1-KEU1: Distribution of the normalised objective function value (normalised fit value) over K for the numerical simulation of the SW-SWS

683 / 750 results with a normalised objective function value less than 1.8

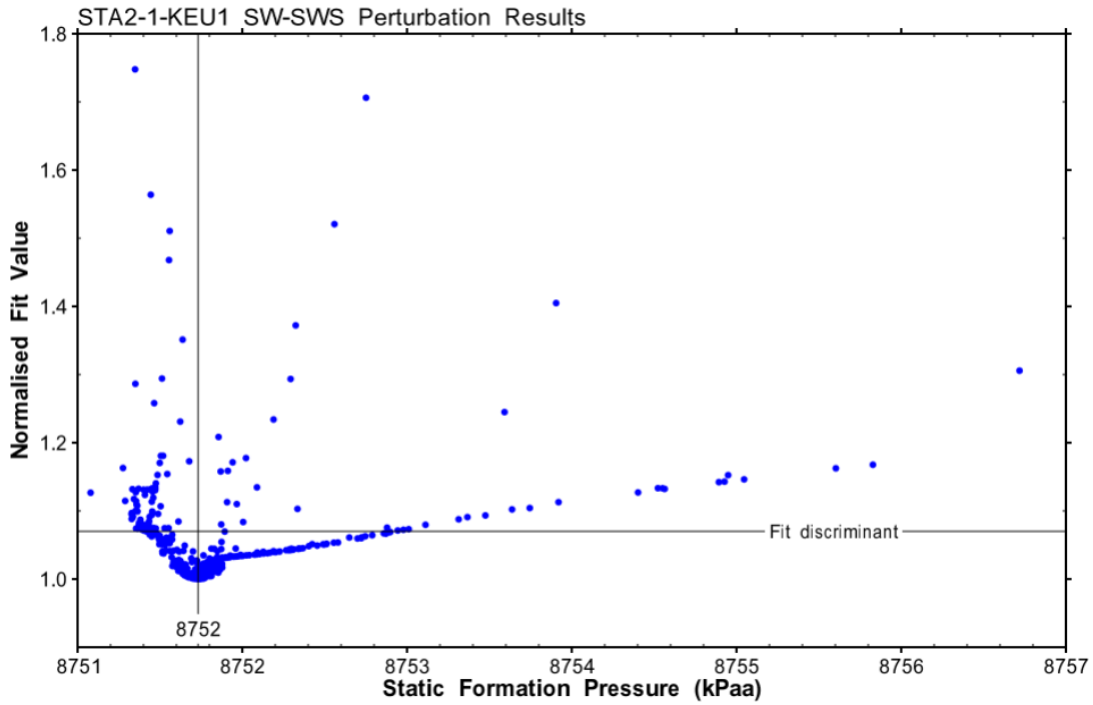

Fig. B-22: Hydraulic test STA2-1-KEU1: Distribution of the normalised objective function value (normalised fit value) over P_f for the numerical simulation of the SW-SWS

683 / 750 results with a normalised objective function value less than 1.8.

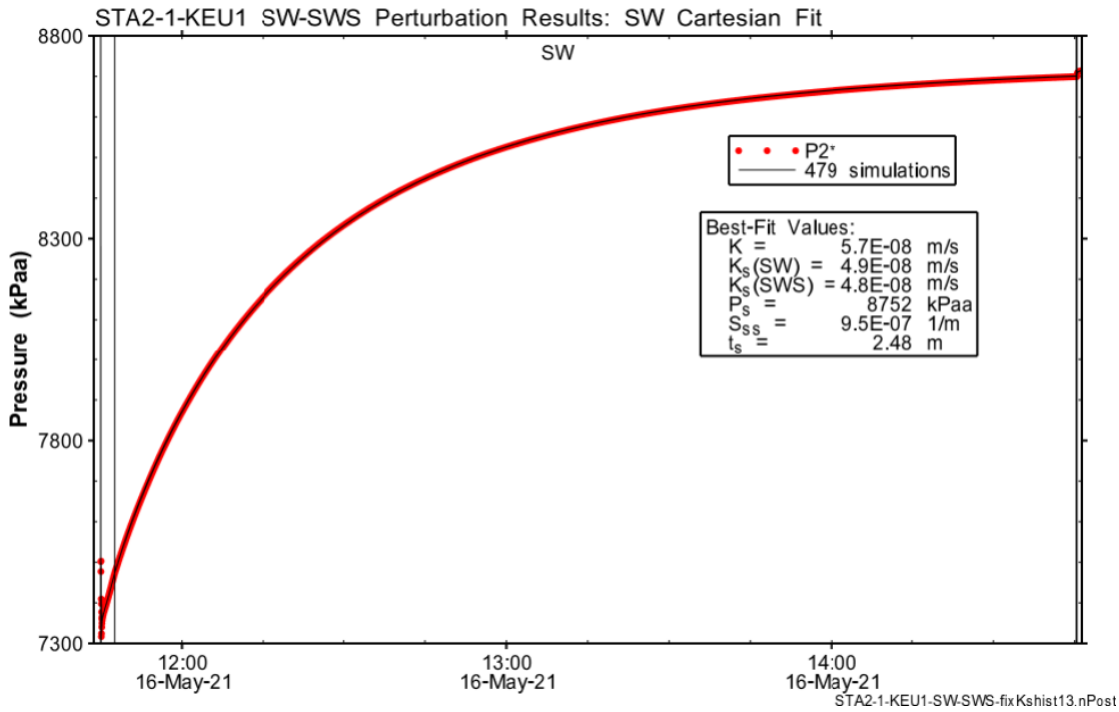

Fig. B-23: Hydraulic test STA2-1-KEU1: Cartesian horsetail plot of the perturbation simulations of the SW on the SW-SWS accepting the fit discriminant

479 / 750 results with a normalised objective function value less than 1.07.

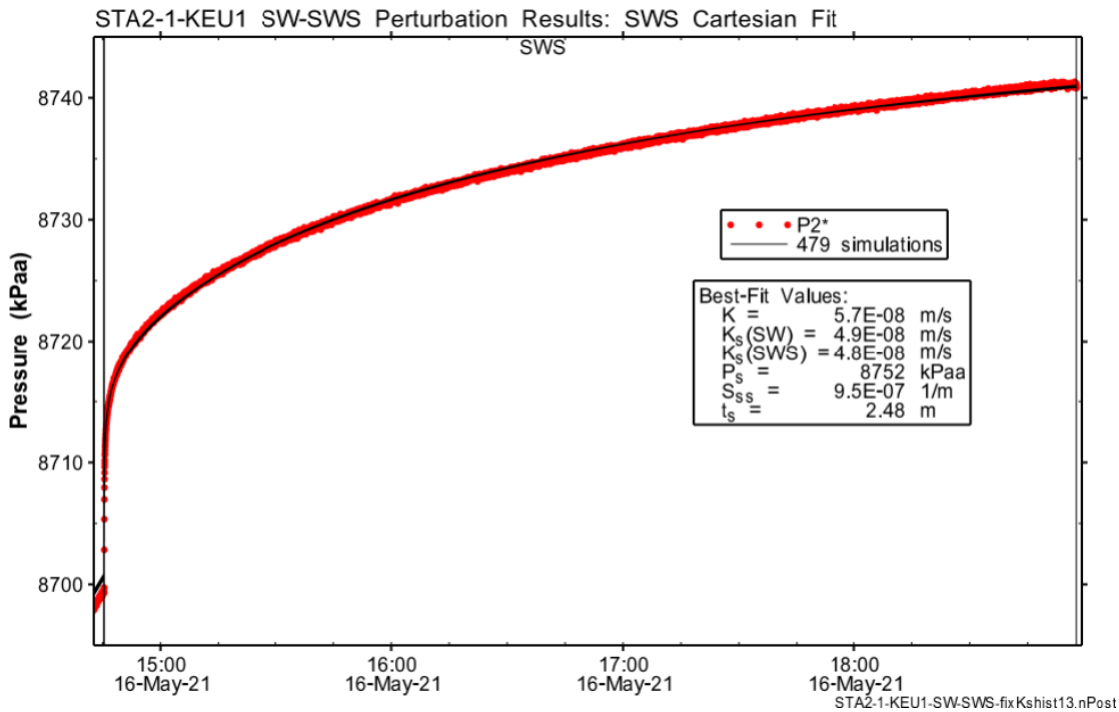

Fig. B-24: Hydraulic test STA2-1-KEU1: Cartesian horsetail plot of the perturbation simulations of the SWS on the SW-SWS accepting the fit discriminant

479 / 750 results with a normalised objective function value less than 1.07.

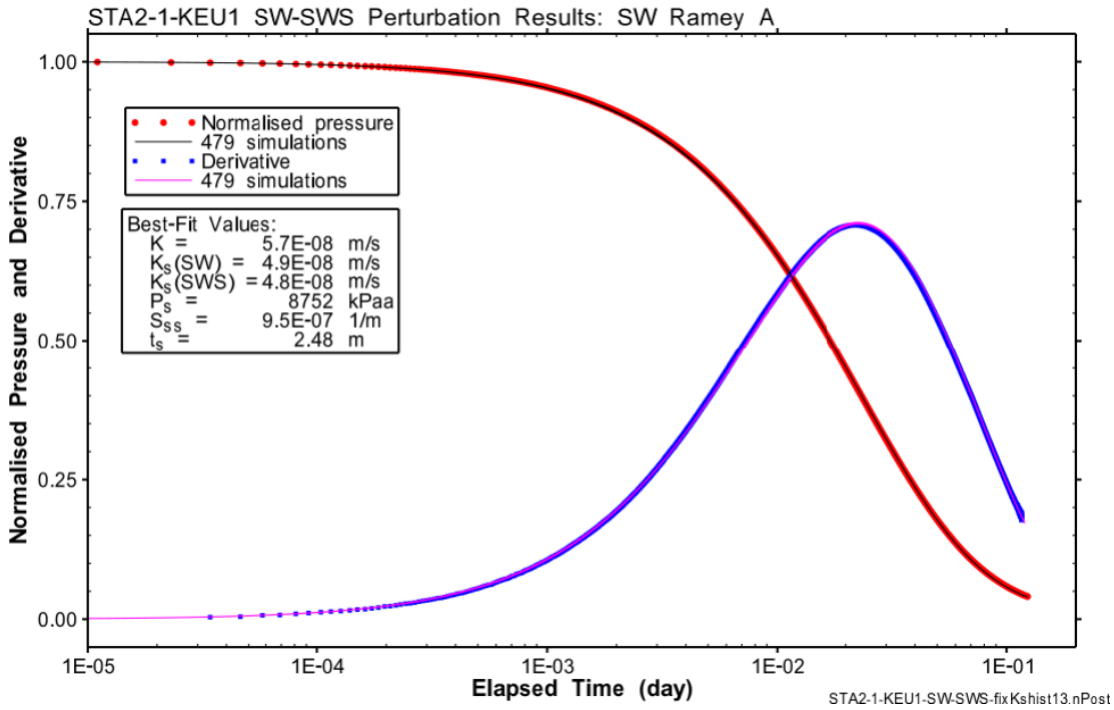

Fig. B-25: Hydraulic test STA2-1-KEU1: Ramey A horsetail plot of the SW of the SW-SWS simulations accepting the fit discriminant

479 / 750 results with a normalised objective function value less than 1.07.

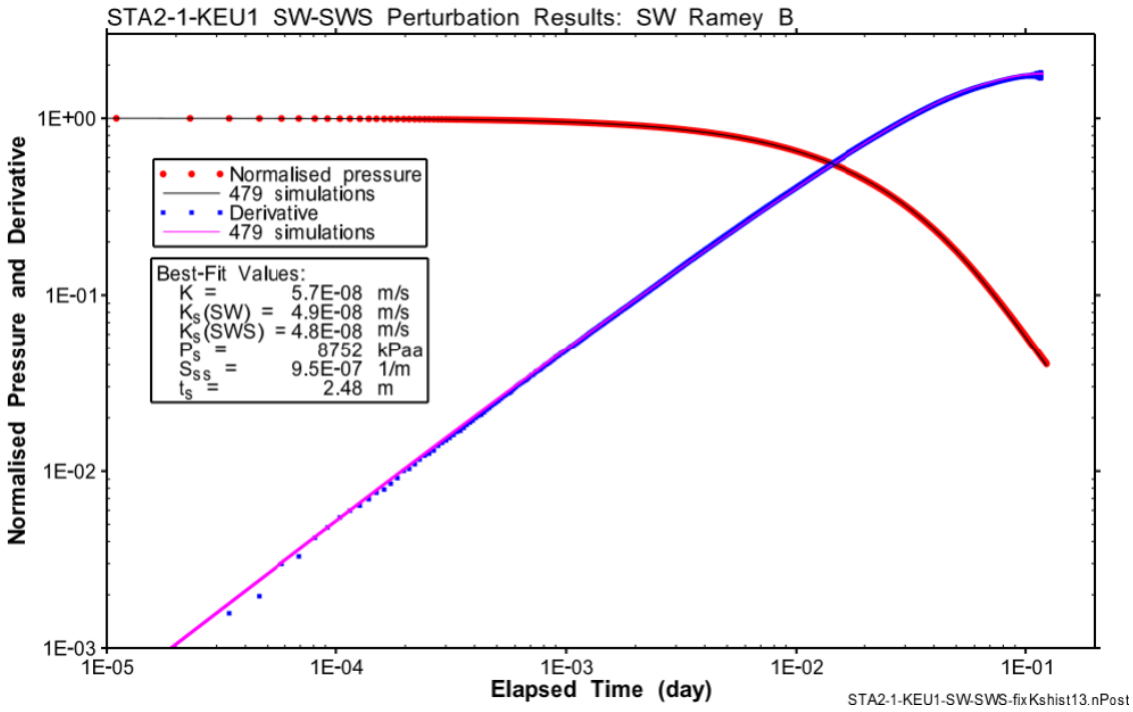

Fig. B-26: Hydraulic test STA2-1-KEU1: Ramey B horsetail plot of the SW of the SW-SWS simulations accepting the fit discriminant

479 / 750 results with a normalised objective function value less than 1.07.

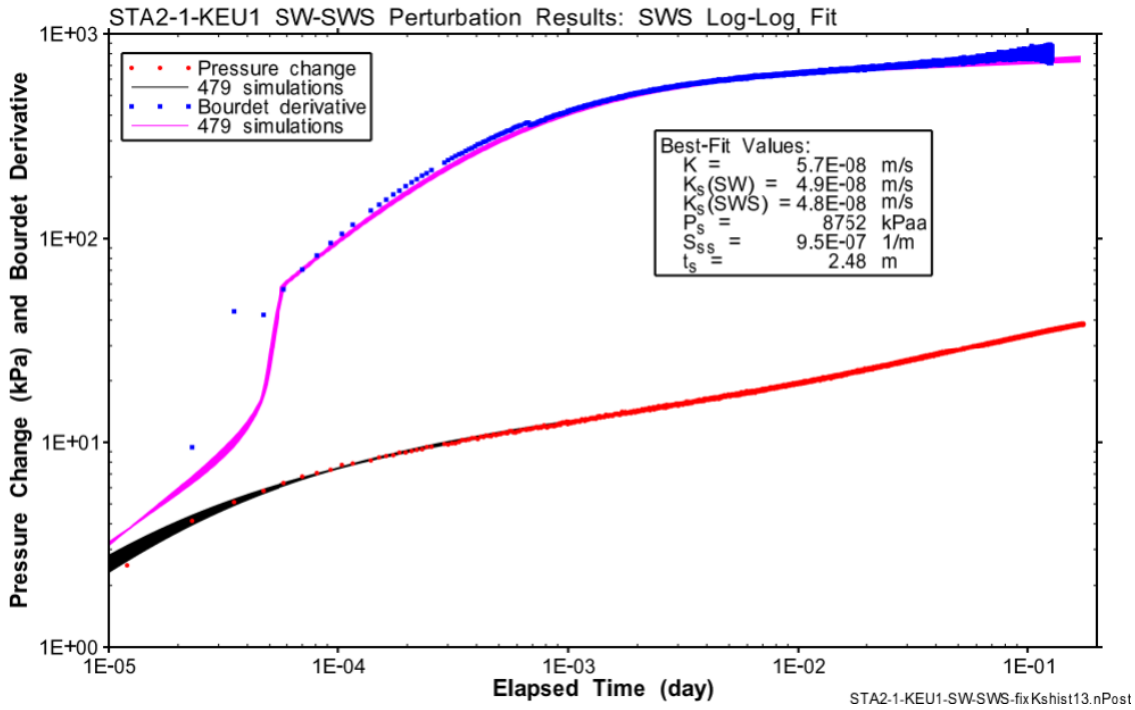

Fig. B-27: Hydraulic test STA2-1-KEU1: Log-log horsetail plot of the SWS of the SW-SWS simulations accepting the fit discriminant

479 / 750 results with a normalised objective function value less than 1.07.

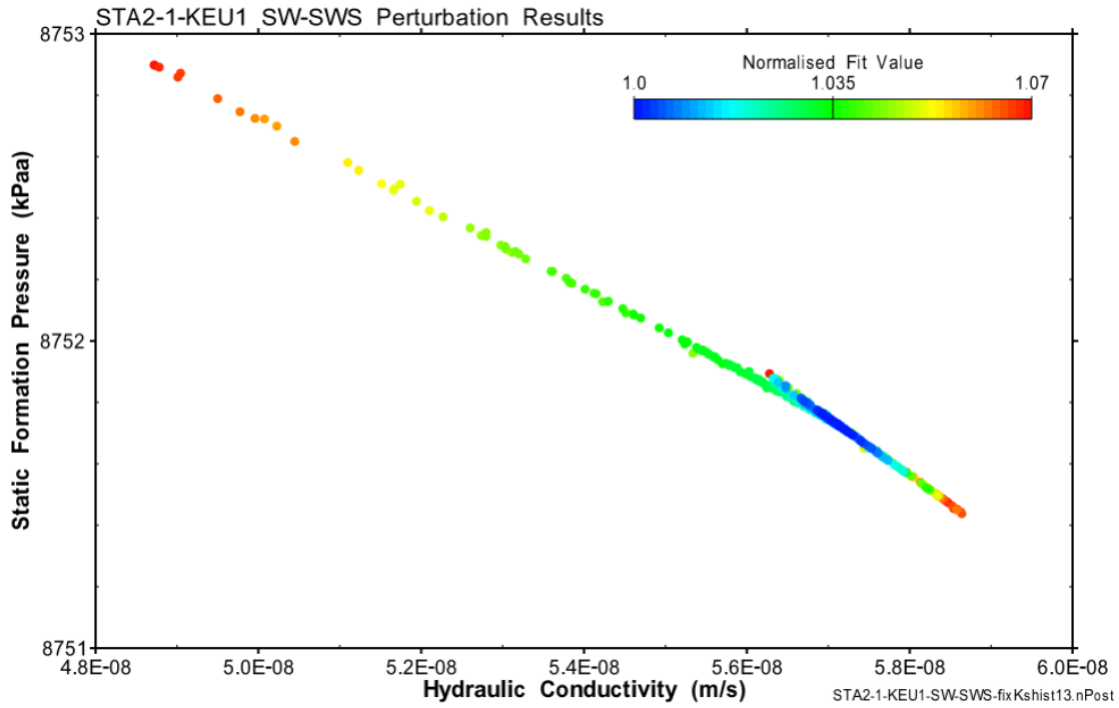

Fig. B-28: Hydraulic test STA2-1-KEU1: Scatter plot hydraulic conductivity – static formation pressure correlation of the SW-SWS perturbation

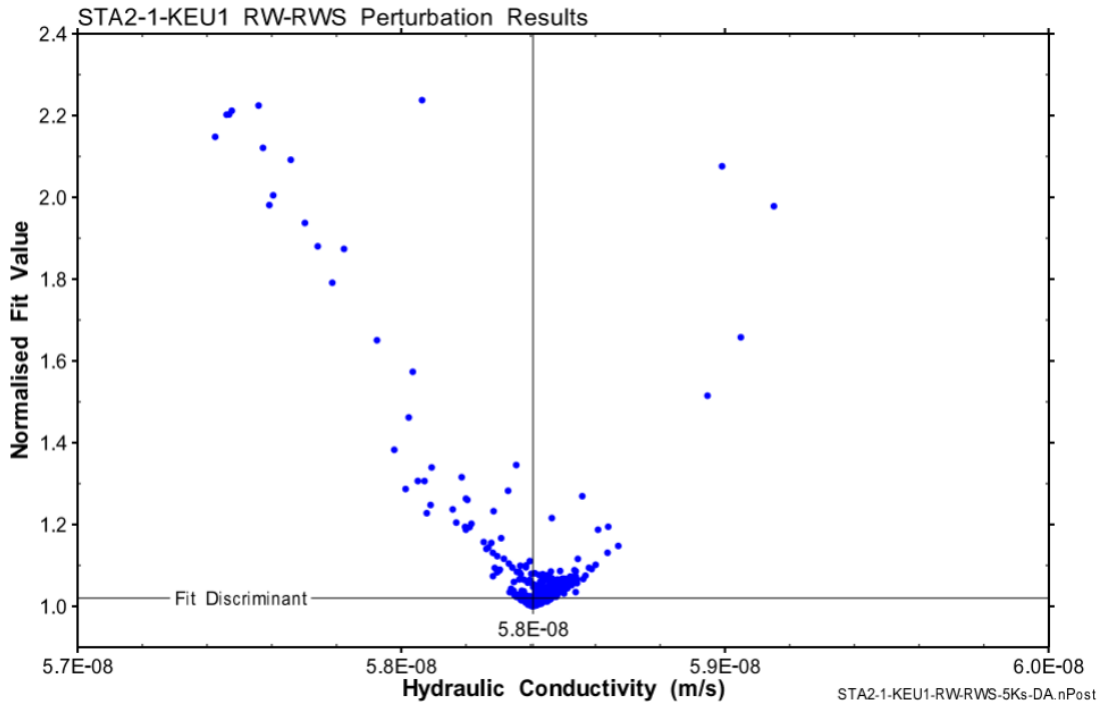

Fig. B-29: Hydraulic test STA2-1-KEU1: Distribution of the normalised objective function value (normalised fit value) over K for the numerical simulation of the RW-RWS

950 / 1'000 results with a normalised objective function value less than 2.4

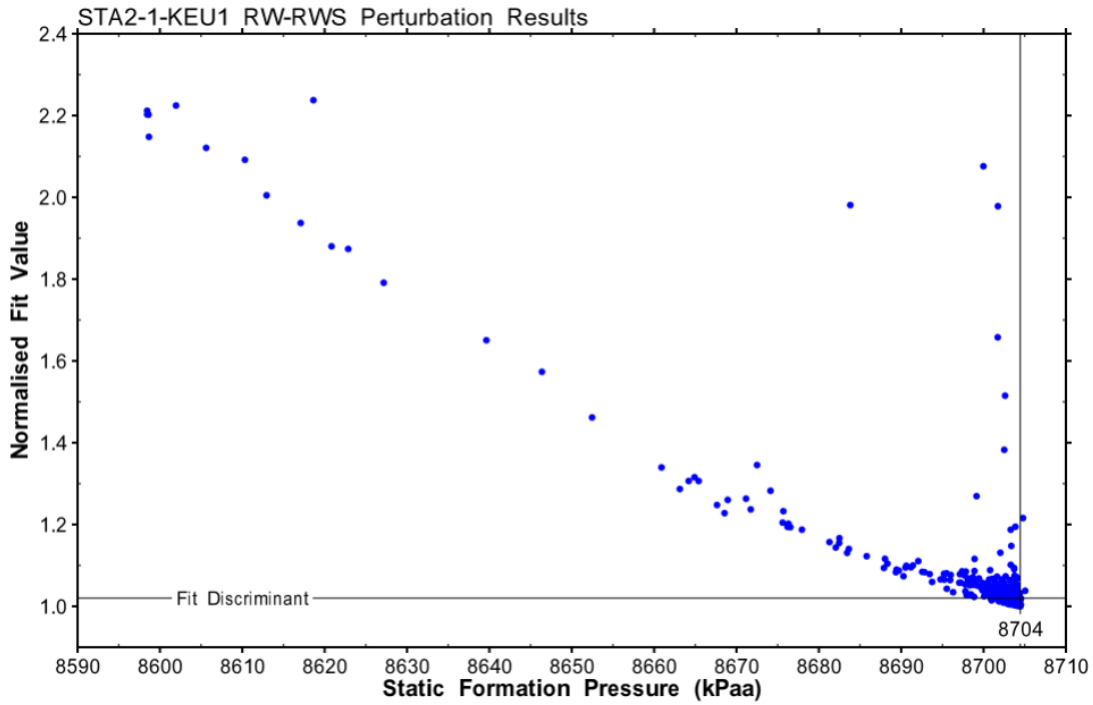

Fig. B-30: Hydraulic test STA2-1-KEU1: Distribution of the normalised objective function value (normalised fit value) over P_f for the numerical simulation of the RW-RWS

950 / 1'000 results with a normalised objective function value less than 2.4

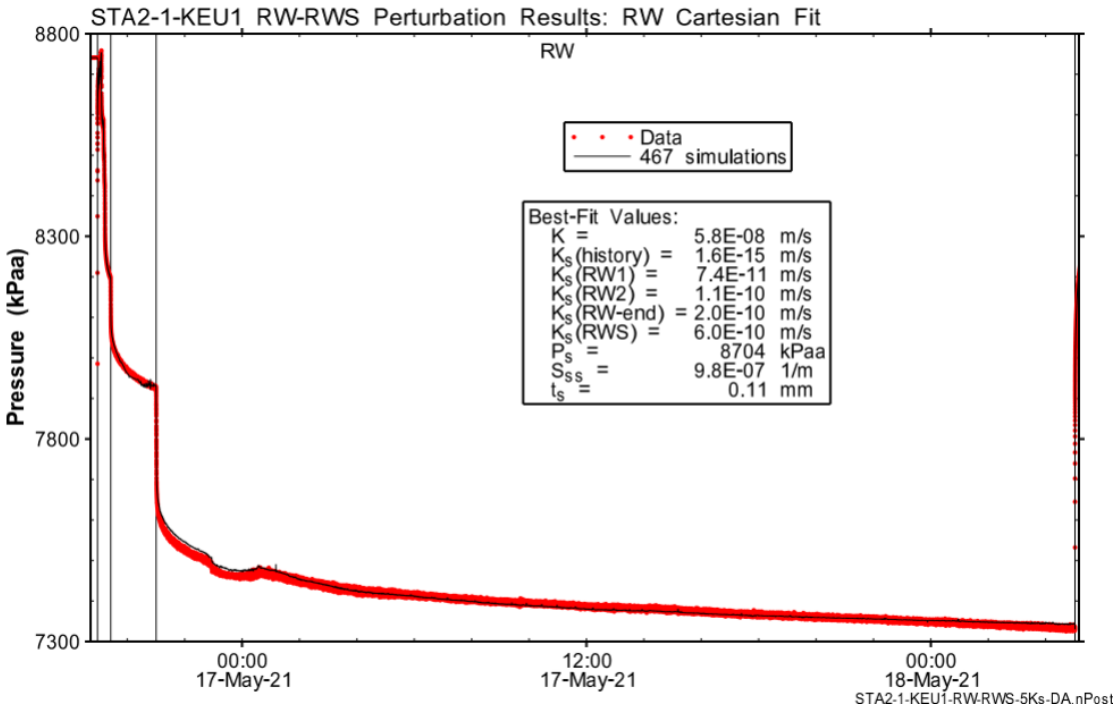

Fig. B-31: Hydraulic test STA2-1-KEU1: Cartesian horsetail plot of the perturbation simulations of the RW on the RW-RWS accepting the fit discriminant

467 / 1'000 results with a normalised objective function value less than 1.02.

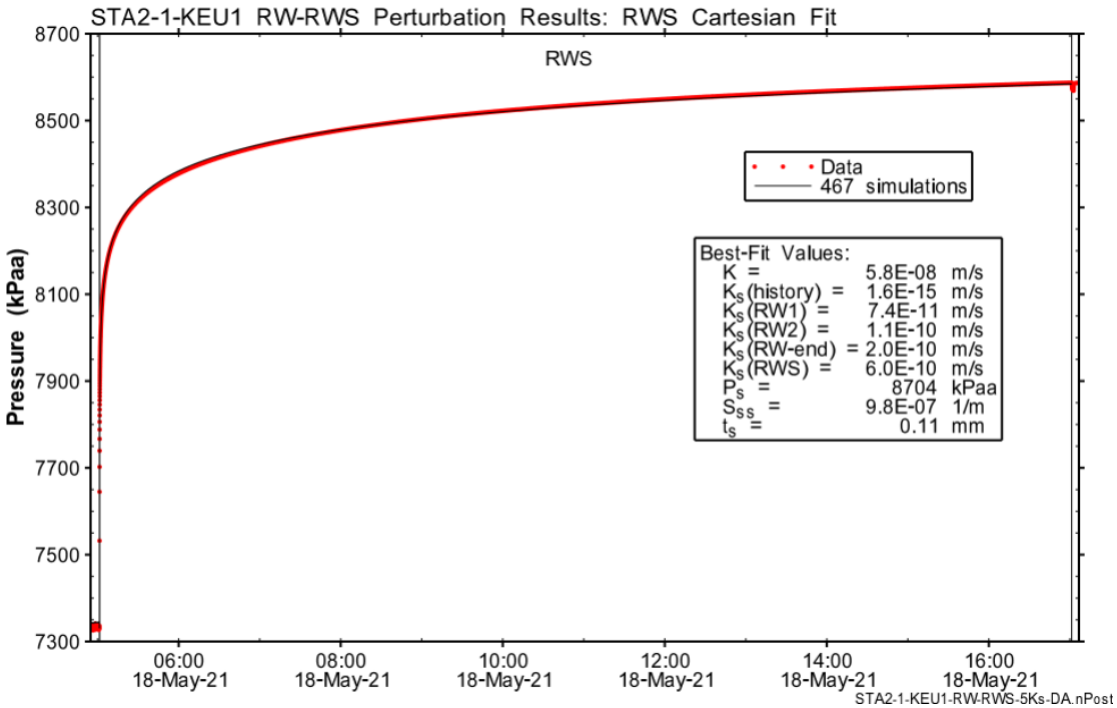

Fig. B-32: Hydraulic test STA2-1-KEU1: Cartesian horsetail plot of the perturbation simulations of the RWS on the RW-RWS accepting the fit discriminant

467 / 1'000 results with a normalised objective function value less than 1.02.

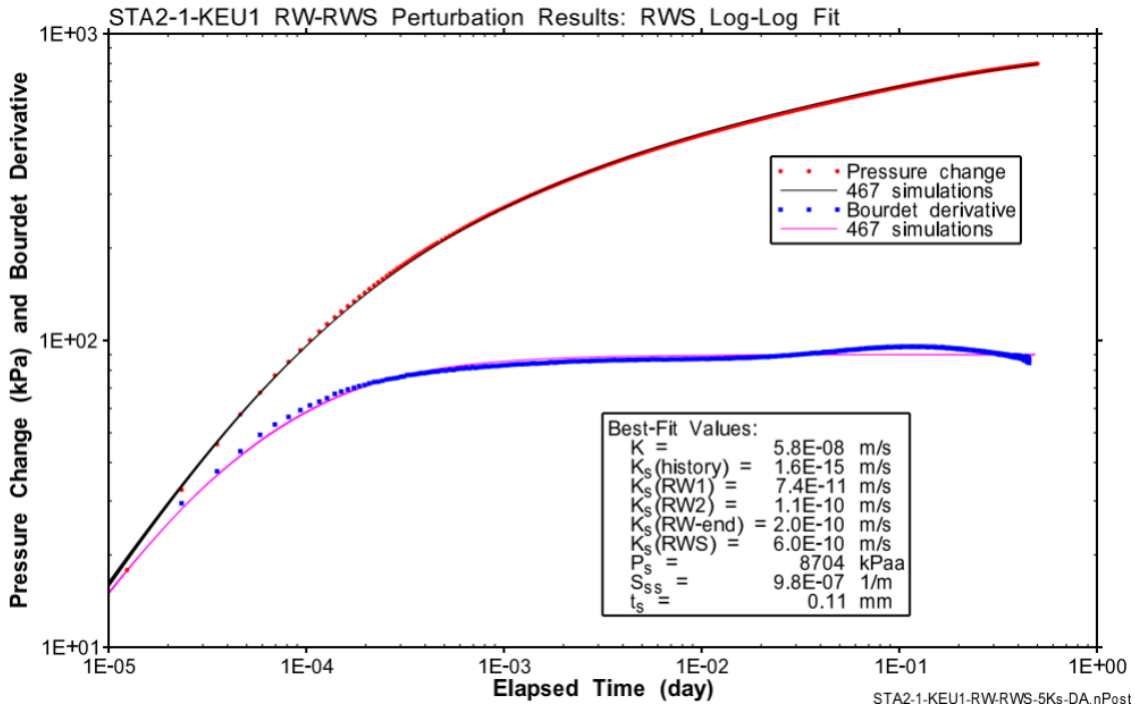

Fig. B-33: Hydraulic test STA2-1-KEU1: Log-log horsetail plot of RWS of the RW-RWS simulations accepting the fit discriminant

467 / 1'000 results with a normalised objective function value less than 1.02.

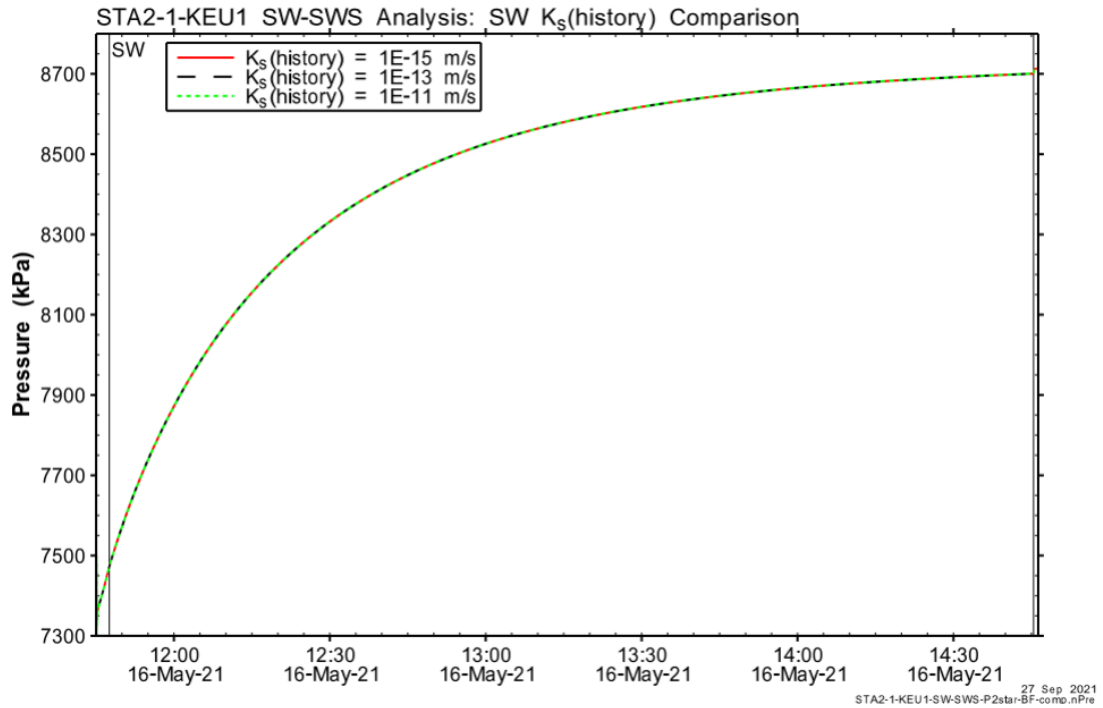

Fig. B-34: Hydraulic test STA2-1-KEU1: SW phase of simulations of the SW-SWS with different values of K_s(history)

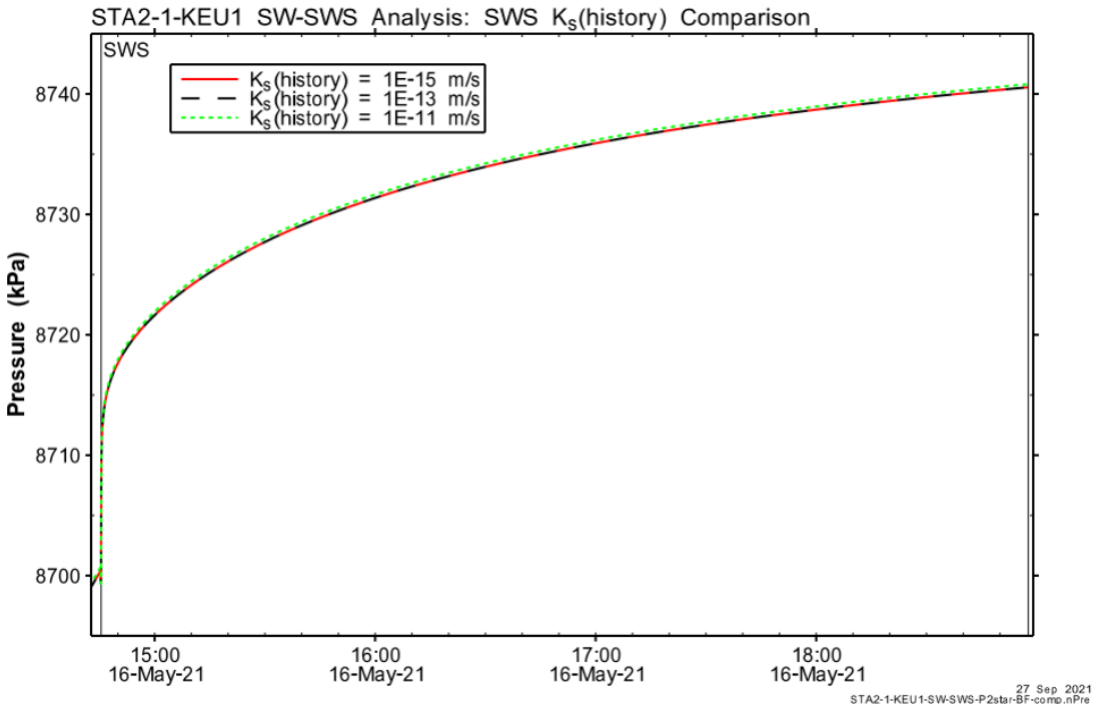

Fig. B-35: Hydraulic test STA2-1-KEU1: SWS phase of simulations of the SW-SWS with different values of K_s(history)